PRESSURELESS SINTERING OF MULLITE-ZrO_2 PARTICULATE COMPOSITES AND THEIR PROPERTIES

A Thesis Submitted
in Partial Fulfilment of the Requirements
for the Degree of

DOCTOR OF PHILOSOPHY

by

NAGESWAR KAPURI

to the

MATERIALS SCIENCE PROGRAMME
INDIAN INSTITUTE OF TECHNOLOGY KANPUR
MARCH, 1995

MSP-1995- N- KAP PRE

A121703

Dedicated

to

My Parents

CERTIFICATE

It is certified that the work contained in the thesis entitled "Pressureless Sintering of Mullite-ZrO_2 Particulate composites and Their Properties" by Mr. Nageswar Kapuri has been carried out under our supervision and that this work has not been submitted elsewhere for a degree.
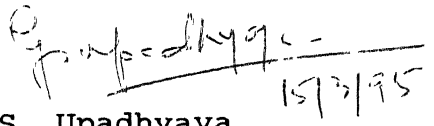
K. N. Rai

Professor

Materials Science Programme,

and Materials and Metallurgical

Engineering

Indian Institute of Technology

Kanpur

G. S. Upadhyaya

15/3/95

Professor

Materials and Metallurgical

Engineering

Indian Institute of Technolog

Kanpur

ACKNOWLEDGEMENTS

I take this opportunity to express my deepest sense of gratitude to Dr. G. S. Upadhyaya, Professor, Materials and Metallurgical Engineering, and Dr. K. N. Rai, Professor, Materials science Programme and Materials & Metallurgical Engineering for their constant guidance and encouragement throughout the course of this work.

I like to thank Mr. S. C. Soni, Mr. R. K. Prasad, Mr. O. P. Malviya, Mr. B. Sharma, Mr. B. K. Jain, Mr. Umasankar, Mr. P. K. Pal for their extensive help throughout the work. I also thank my labmates i.e Mr. D. Banerjee, Mr. P. K. Bagdi for their cooperation and encouragement. Special thanks are due to also Mr. M.R.R.I. Shamsi, Mr. S. Bhattacharya The blessings of my parent and moral support of my brothers and sisters are highly appreciated.

Finally I thank Mr. Yash Pal for his neat typing.

March, 1995   Nageswar Kapuri

LIST OF PUBLICATIONS:

1. SEM Studies of Mullite-ZrO_2 Particulate Composites, Practical Metallography (in Press).

2. Sintering of Mullite Based Particulate Composites Containing ZrO_2, Journal of Materials Science (Communicated).

3. Sintered Mullite-ZrO_2 Composites Prepared Through Different Routes, Interceram (Communicated).

CONTENTS

LIST OF FIGURES

LIST OF TABLES

SYNOPSIS

Mullite ceramic has been extensively used in different structural and electrical applications due to its high melting point, low thermal expansion coefficient, high creep resistance, chemical inertness, enhanced flexural strength at high temperature and good dielectric constant. In the present investigation, mullite was therefore selected as a matrix material to utilize these good structural properties. Incorporation of second phase, mainly ZrO_2, was made to improve the relatively low fracture toughness of mullite alongwith mechanical properties.

Mullite-ZrO_2 composites can be prepared through different routes, namely sol-gel; reaction sintering; premix milling, compaction and sintering. In the present study, composites were prepared by the process of premix milling/compaction/sintering route, due to its low capital investment for the production of technical grade materials. Two different types of easily available mullite powders namely fused (MC) and sol-gel (MP-20 & MP-40) have been selected. Again in the sol-gel mullites, two different stoichiometries Al_2O_3/SiO_2 = 1.5 (MP-20) and 1.51 (MP-40)] were considered to study relative compositional fluctuation in mullite matrix. ZrO_2 powders were also used in its straight and MgO/MgO-Y_2O_3 modified forms. Reaction sintering of zircon and Al_2O_3, so as to obtain mullite-ZrO_2 composites, was also studied to have a comparative study of these composites with mechanically milled mullite-ZrO_2 ones.

Mullite powders with 0 to 25 vol% ZrO_2 and its modified versions were separately wet ball milled for 3 hours. Rectangular pellets of the premixed powders, measuring 25 mm x 8 mm x 2.5 mm were compacted in a uniaxial hydraulic press at a pressure ranging from 300-350 MPa in order to impart sufficient green strength. These compacts (>55% relative density) were sintered in a super kanthal resistance heated muffle furnace at 1650°C and 1700°C for 1 hour in ambient atmosphere. The sintered densities were measured with the help of a mercury densometer.

Transverse rupture strength (TRS) of the as sintered samples were measured under three point bending load. Fracture toughness (K_{IC}) was measured according to single edge-notch bend (SENB) method. Three main aspects of SEM studies namely (i) microstructure, (ii) EDX dot mappings of zirconium and (iii) fractography were covered. X-ray diffractometry was used for estimating the fractional tetragonal and monoclinic ZrO_2 present in the as sintered samples. Dielectric constant (k') values were measured at one MHz frequency. Thermal shock resistance was measured by quenching the heated specimens in a water bath kept at room temperature.

Lowest sintered porosity (5%) was observed for MP-40 (sol-gel) mullite, sintered at 1700°C, while MC mullite (fused) showed highest sintered porosity (26%) at either sintering temperatures. TRS and K_{IC} values increased with the increase in sintering temperature. These values were highest for MP-20 mullite. Microstructure of fused mullite consisted of elongated matrix grains, whereas sol-gel mullites showed equiaxed grains.

The fracture mode was intergrannular in nature for all compositions. Dielectric constant values increased with the increase in sintering temperature. High Al_2O_3 containing mullite showed higher thermal shock resistance than lower Al_2O_3 containing ones.

Full reaction sintering of mullite-ZrO_2 composites occurred at $1700^{\circ}C$ with 8% total sintered porosity so as to give a composition of mullite ~ 25 vol% ZrO_2. The sintered properties of this particular composite increased with the increase in sintering temperature with the exception for K_{IC} which remained same at either sintering temperatures. However, the sintered properties of sol-gel mullite based composites, containing equivalent vol% ZrO_2, were higher than the reaction sintered ones.

Densification of MC mullite based composites increased with the increase in vol% additives and sintering temperature. The increased densification was in the order of $ZrO_2 \longrightarrow ZrO_2$ - MgO $\longrightarrow ZrO_2$-MgO-Y_2O_3 additives in the composites. However, this trend was not observed for MP-20 mullite based composites. Densification for sol-gel mullite based composites remained almost same with the increase in vol% additives, whereas a decreasing trend was observed for MP-40 mullite based ones, sintered at $1700^{\circ}C$.

TRS of MC mullite based composites increased marginally with the increase in vol% additive and sintering temperature. However, sol-gel mullite based composites, showed maxima at particular vol% additive, with exception for MP-40 mullite composites sintered at $1650^{\circ}C$ where TRS continuously increased with the

increase in vol% additive. K_{IC} of all the composites showed an increasing trend with the increase in vol% additives irrespective of the type of mullite powders. MP-20 mullite based composites showed highest mechanical properties.

Fracture mode of mullite-ZrO_2 composites were mainly intergrannular in nature. Microstructure consisted of elongated (for MC based composites) or equiaxed mullite grains (for sol-gel based ones) with homogeneously distributed ZrO_2 particles. The ZrO_2 particle size increased with the increase in vol% additives. Matrix grain size increased with the increase in sintering temperature.

Fractional tetragonal ZrO_2 values deceased with the increase in vol% additive and sintering temperature. Retention of this phase increased in the order of $ZrO_2 \longrightarrow ZrO_2$ -MgO $\longrightarrow$ ZrO_2-MgO-Y_2O_3 additives in the composites.

Dielectric constant values increased with the increase in vol% additive and sintering temperature. Different types of mullites and ZrO_2 powders showed very little effect on thermal shock resistance which increased with the increase in sintering temperature.

Mullite and its composites were found to sinter mainly through solid-state sintering. However, small amount of extraneous liquid phase due to the presence of oxide impurities led to the enhanced sinterability of the composites. This extraneous liquid phase promoted the formation of elongated mullite grains which was predominant in MC mullite based composites.

Stress induced transformation toughening appeared to be the main strengthening mechanisms for these composites apart from the dispersion strengthening effect. ZrO_2 particle coarsening led to the decrease in TRS values. However, microcrack toughening was mainly responsible for the increased K_{IC} values with the increase in vol% additive. Formation of mullite-ZrO_2 solid-solution at the grain boundaries was proposed to contribute to the K_{IC} values. Larger mullite grain size and higher sintered porosity led to the lower values of mechanical properties for MC mullite based composites than the sol-gel mullite based ones.

Dielectric constant (k') of mullite and its composites showed a direct relation with the sintered density, such that an increase in sintered density led to the increased dielectric constant values. As a result MC mullite based composites exhibited lower k' values than sol-gel based ones.

CHAPTER I
LITERATURE REVIEW

I.1   INTRODUCTION

Mullite is an alumino-silicate material extensively used in the traditional refractory applications. It is the only stable crystalline phase in the Al_2O_3-SiO_2 system under normal atmospheric pressure. It has a chemical composition range from $3Al_2O_3 \cdot 2SiO_2$ to approximately $2Al_2O_3 \cdot SiO_2$ and crystallizes in the orthorhombic system, most commonly in the form of elongated needle shaped crystals, the exception being when it is sintered in the absence of a liquid phase. Mullite is one of the most common phases found in industrial ceramic products. However, it is rare in nature, the most important place of occurrence being the Isle of Mull, Scotland. Synthetic mullite with controlled microstructure and properties is extensively used in various structural and electrical applications because of its high melting point, low thermal expansion, creep resistance, chemical inertness, slightly increased flexural strength at high temperature and good dielectric properties.

Mullite is a brittle material and possesses low fracture toughness. Further improvement in the mechanical properties can be however achieved by developing mullite based composites. The major advantage in composites is that their properties can be specifically engineered via microstructural modifications. To a large extent, the type, size, shape, volume fraction, distribution and interfacial characteristics of the matrix and other phases dictate the microstructure and properties of the composites. A detailed review of the mullite and mullite matrix composites has

been made in the following sections.

I.2 MULLITE

I.2.1   Preparation

Considerable efforts have been directed towards the preparation of high purity mullite ($3Al_2O_3.2SiO_2$) for its potential use in different structural and electrical applications. The major preparation methods are through precipitation of alkoxide, wet chemical mixing, sol-gel route and reaction sintering/reaction bonding routes.

Alkoxide Method :

The synthesis of mixed alkoxide (aluminium tris isopropoxide and silicon tetrakis isopropoxide) was reported by Mazdiyasni and Brown [1]. Aluminium isopropoxide was prepared by the process reported by Adkins [2]. Al foil of 99.999+% purity was reacted with excess isopropyl alcohol using a small amount of $HgCl_2$ (10^{-4} mol/mol of metal) as a catalyst as per following reaction:

$$Al + 3C_3H_7OH \xrightarrow[82^\circ C]{HgCl_2} Al(OC_3H_7)_3 + \frac{3}{2}H_2\uparrow$$
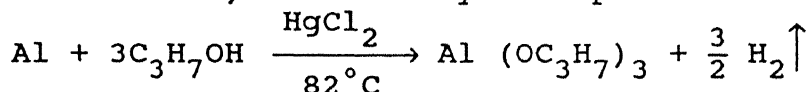
Silicon tetrakis isopropoxide was prepared by the methods of Bradley et al. [3] according to following reaction:

$$SiCl_4 + 4C_3H_7OH \xrightarrow[82^\circ C]{} Si(OC_3H_7)_4 + 4HCl\uparrow$$
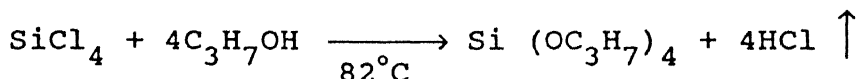
The hydroxyl aluminosilicate was prepared by slowly adding stoichiometric mixed alkoxides solution to ammoniated triply distilled deionized water according to the reaction:

$$6Al(OC_3H_7)_3 + 2Si(OC_3H_7)_4 + xH_2O \xrightarrow{H_2O+NH_3}$$
$$3Al_3Si(OH)_{13}.xH_2O + 26\ C_3H_7OH$$
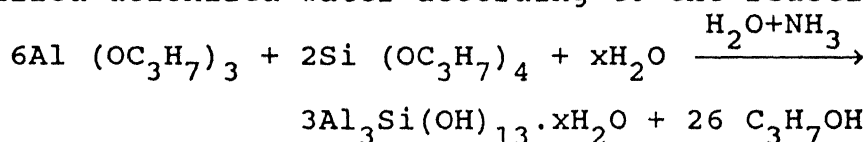
The resulting hydroxyl aluminosilicate was repeatedly washed and dried at 60°C in vacuum to get mullite, according to the following

$$2Al_3Si(OH)_{13} \xrightarrow[60°C]{Vacuum} 3Al_2O_3 \cdot 2SiO_2 + 13H_2O$$
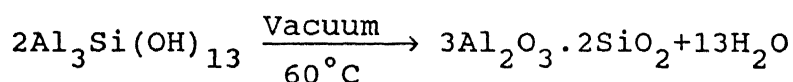
The as prepared oxide was found to be amorphous and had a surface area of $\simeq 550$ m^2/g ± 10%. They showed very fine needle like crystallites. On calcination at 600°C surface area of the particles reduced to 280 m^2/g ±10%, which was attributed to nucleation and growth of the finer particles to larger networks of needlelike crystallites. This retention of needlelike morphology at higher temperatures, in absence of liquid phase, was reported to be contrary to the findings of other investigators [4,5]. DTA observation showed no endothermic or exothermic reactions from room temperature to 1200°C, other than dehydration peak occurring from 50 to 200°C. The authors [[1] reported this phenomenon as the clear evidence of formation of mullite at the time of preparation, as evidenced by the needlelike morphology of the as prepared powders. After X-ray studies the material was found to be amorphous upto 435°C. At temperatures greater than 435°C, it was gradually transformed to crystalline phase. However, the orthorhombic peaks of mullite appeared at 1185°C to 1200°C.

Suzuki et al. [40] reported the formation of Al, Si-spinel at 900°C and subsequently to the spinel-to-mullite only above 1200°C. The specific surface area of their mullite powder was in the range of 147-466 m^2/g when calcinated at 800 -1100°C for 12 hours. Other workers following a similar processing method reported 980°C [41, 43], and 900°C [42] as the mullitization temperatures. Somiya et al. [44] prepared mullite by hydrothermal treatment through alkoxide route. They reported mullite particles of needle like to accicular in shape of 0.1 to 0.5 μm in size.

Consecutive Precipitation Method:

This preparation [4,6] consisted of hydrolization of tetraethyl silicate in the presence of $Al(OH)_3$. The $Al(OH)_3$ was prepared from $AlCl_3$ in presence of NH_4OH according to the reactions:

$$AlCl_3 + 3NH_4OH \longrightarrow Al(OH)_3 + 3NH_4Cl$$
$$Si(OC_2H_5)_4 + 4H_2O \longrightarrow Si(OH)_4 + 4C_2H_5OH$$
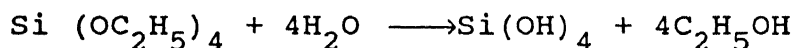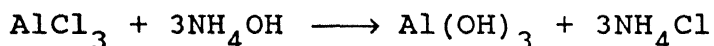
The precipitate was filtered and dried and mullite was obtained after calcining.

Since the hydrolysis of tetraethyl silicate was a slow process the authors [4,6] reported a very intimate mixing of hydrated SiO_2 and Al_2O_3. The X-ray crystallography showed that after calcination at 1000°C or 1100°C there was virtually no crystalline pattern visible, but at 1200°C the pattern was that of crystalline mullite with no evidence of the intermediate formation of crystalline Al_2O_3 or SiO_2.

Wet Chemical Methods:

Various wet chemical methods [7-10] are reported in the literature. The precursor materials were also varied in wide extent. Reynen and Faizullah [7] used three types of SiO_2 precursors namely finely milled quartz, silicic acid obtained by leaching of silicates and silicic acid obtained by hydrolysis of ethyl silicate. The Al_2O_3 - precursors were gibbsite [$Al(OH)_3$], $Al_2(SO_4)_3$ and $AlCl_3$. The authors [7] reported results carried out by small scale laboratory method or large scale spray drying/spray roasting methods. In laboratory method the salt solutions or suspensions were dispersed in kerosine with a high boiling point emulsifying agent. It was then flash dried and subsequently the

powder was dried in sand bath followed by calcination at 1300°C.

In spray-drying, mixtures of aluminium sulphate and stabilized suspensions of silicic acid in the ratio corresponding to 3:2 mullite were mixed and subsequently thermally decomposed at 1000°C. The spray drying and thermal decomposition were simultaneously carried out during spray roasting. But in this case $AlCl_3$ was used instead of $Al_2(SO_4)_3$ as Al_2O_3 precursor. The aforesaid wet chemical methods gave mullite with a surface area ranging from 2.23 to 22.95 m^2/g depending upon the precursor materials used. The powders also had a wide range of impurities like Fe_2O_3, TiO_2, MgO, Na_2O, K_2O, Cr_2O_3 and SO_3.

Sacks and Pask [8] prepared mullite from α-Al_2O_3 and silica flour (α-quartz) which had purities of ≈99.8% and ≃ 99.6% respectively. They studied compositions ranging from 60 - 90 wt% Al_2O_3, which were mixed and deagglomerated by wet milling. The mixtures were stir dried and calcined at 1700°C to get mullite. The surface area obtained after such a method was 1.9 to 1.7 m^2/g for 60 to 75% Al_2O_3 content. The phases obtained after calcining were mullite, aluminium silicate glass and alumina, depending upon the compositions studied.

Moya et al. [9] and Rincon and Thomas [10] prepared mullite from halloysite rock from Chihuahua (Mexico). The starting material was crushed and ground to a particle size of <60 μm and thermally treated at temperatures between 900 - 1000°C followed by treatment with aqueous dilute NaOH solution. Later on it was washed with water and calcined at 1000 - 1570°C. The sample prepared by this route gave exothermic peak at ~ 980°C which was attributed to the formation of premullite with the same chemical

composition of 3:2 mullite but a different tetrahedral / octahedral aluminium ratio and low crystallinity. The result also gave an exothermic peak at ~ 1250°C due to the abrupt ordering of premullite structure. This ordering was also reported at a temperature just slightly above 980°C exotherm but after a very long soaking period.

Mullites were also prepared by wet chemical methods from different raw materials like bauxite and fine SiO_2 [45], aqueous aluminium sulphate and fumed silica [46], and aqueous alumino silicate solutions [47, 48].

Sol-Gel Method:

Sacks and Pask [11] and Ismail et al. [5,12,13] prepared mullite by sol-gel method from the starting material of γ-Al_2O_3 and colloidal SiO_2 which had surface areas of 68 m^2/g and 130 m^2/g respectively. The γ-Al_2O_3 was hydrolized at a temperature greater than 90°C and was peptized with HNO_3. The colloidal SiO_2 was also dispersed in water and mixed with peptized γ-Al_2O_3 to form mullite sol, which was followed by gellation by the evaporation of excess water at a controlled pH. The as prepared mullite gel had a BET surface area of 277 m^2/g with an average particle size of 7 nm. On calcination at 1400°C the surface area of mullite was reduced to 1.7 m^2/g. The DTA heating curve showed endotherms at 96°C and 420°C representing the loss of moisture from gel and dehydration of bohemite to form the spinel phase (γ-Al_2O_3) respectively. The exotherm at 1296°C was attributed to the complete crystallization of mullite.

Sol-gel mullite were prepared by different investigators [49-56] from different Al_2O_3 and SiO_2 precursors as described

earlier. One interesting Sol-gel processing as described by Komarneni et al. [49] was preparation of mullite from diphasic gel which was nothing but a seeded gel.

Reaction Sintering/Reaction Bonding Method

Boch and Chartier [57] prepared mullite through the reaction sintering of Al_2O_3 and SiO_2 according to the following reaction :

$$3Al_2O_3 + 2SiO_2 \longrightarrow (3Al_2O_3 \cdot 2SiO_2)$$
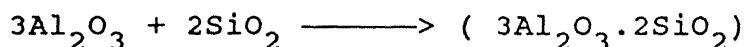
Reaction bonding technique was adopted to prepare mullite from Al, SiC and Al_2O_3 by Wu and Claussen [58]. In this method green compacts consisting of mechanically alloyed Al, SiC and Al_2O_3 were heat treated in two steps. During the first hold at 1200°C, Al and SiC were oxidized to form Al_2O_3 and SiO_2. On further heating, mullite was formed which then got sintered during the second hold at 1550°C.

I.2.2   Sintering

Depending upon the process parameters and powder characteristics, different types of sintering kinetics and different final densities are reported in the literature. Mazdiyasni el al.[1,14] got 99.995% theoretical density (3.18 to 3.19 gm/cc) from the alkoxy derived powder. The powder was calcined at 600°C for 1 hr and ground to effect comminution of the large agglomerates followed by vacuum uniaxially hot pressing at 5 kpsi at 1400 to 1600°C for 15 to 30 minutes. The specimen they got was transluscent.

Suzuki et al. [40] reported low density (94% Th.) product from the powder calcined below crystallization temperature. Calcination above the crystallization temperature resulted high density product. But full density was achieved only after hot

pressing above 1600°C. The sintered product was translucent. Mitachi et al. [43] reported higher density (> 99% Th.) for higher SiO_2 composition (69% Al_2O_3) than lower SiO_2 composition (79% Al_2O_3) where sintered density was 98% Th. after sintering at 1650°C for 4 hours. Somiya et al. [44] reported 98% Th. density after hot pressing at 1600°C under 40 MPa pressure for 30 min.

Mullite prepared by wet chemical method [7] gave a wide range of final density (2.18-2.99 gm/cc sintered at 1700°C). Classical mixing of raw materials such as [quartz + $Al(OH)_3$], exhibited a poor mullitization and low densification (2.30 gm/cc at 1700°c). The water soluble alumina precursors gave excellent results as compared to insoluble $Al(OH)_3$. The insoluble $Al(OH)_3$ caused demixing resulting into secondary phase formation. H_2SO_4 leached silicic acid from vermicullite contains upto 3.8 wt% unwashed SO_3. This is found to decrease densities from 2.99 to 2.18 gm/cm^3 due to swelling effect of its gasification when heated beyond 1500°C to 1700°C. Iron oxide and alkali impurities had several detrimental effects on the final products. These also showed a tendency to "demullitization" at higher temperatures.

Pask et al. [8] studied densification mechanism over a range of chemical compositions. A high densification rate was observed in compositions containing large amount of liquid phase possibly due to extensive particle rearrangement during sintering. The same effect was absent in the high alumina composition ranges. They observed, however, persistent glassy phase upto 74 wt% Al_2O_3 presumably because of metastable behaviour caused by the lowering of mullite-mullite interfacial energies. A sharp decrease in densification rate was observed on transition from the mullite

solid solution range to the mullite and alumina phase region which was associated with elimination of the residual glassy phase. The time dependence of densification for mullite compositions in the range of 73 to 75 wt% Al_2O_3 followed a semi-logarithmic relation between percent theoretical density and time. From this relation it was predicted that the apparent primary densification mechanism was grain boundary transport or diffusion, whose rate was significantly dependent on the presence or absence of the glassy film. The maximum density achieved in this process was 93-95% of the theoretical at $1730^{\circ}C$.

Mullite, prepared by Rincon and Thomas [10] from halloysite rocks, was deagglomerated by attrition milling in isopropyl alcohol media and subsequently iso-pressed at 200 MPa. After sintering at $1570^{\circ}C$ for 2.5 hrs, the mullite attained 98% of the theoretical density.

Nan and Xitang [45] reported enhanced densification for the mullite prepared from refined bauxite and SiO_2. The densification was greater than that for mullite prepared from $Al(OH)_3$ and SiO_2. They reported a sintered density of 2.96 gm/cm^3 after $1650^{\circ}C$ sintering for 3 hrs. Mizuno [46] reported 99.7% sintered density after hot pressing at $\geq 1575^{\circ}C$.

Ismail et al. [5] reported that mullite prepared by sol-gel method sintered quickly to the theoretical density for compositions which contained higher SiO_2. The authors' [5] observation was same as reported by Reynen and Faizullah [7]. Isostatically pressed (200 MPa) green compacts of mullite containing 68% Al_2O_3 reached full density after sintering at $1600^{\circ}C$. On the other hand, the compacts containing 72% Al_2O_3were

sintered to > 99% theoretical density at 1650°C for 1.5 hrs. The authors [5] also observed that sintered density increased with increasing temperature upto 1650°C and decreased slightly at 1700°C due to the formation of pores with exaggerated grain growth. Sacks and Pask [11] got 97.5% theoretical density at 1700°C for the stoichiometric mullite gel. They reported three stages of sintering based on geometrical changes during sintering.

Komarneni and Roy [49] reported that the densification of mullite prepared from diaphasic gels had greater densification than the mullite prepared from ordinary gel. They got 95.9-96.8%. theoretical density after sintering at 1400°C for 3 hrs. This enhanced densification was due to the heat of reaction during sintering of diaphasic gel which was compositionally heterogeneous on a nanometer scale. Ismail and Nakai [51] reported 99.1% theoretical density after sintering at 1640°C for 1.5 hours for the mullite containing 70 % Al_2O_3. The higher Al_2O_3 content had a reverse effect on densification.

Boch et al. [57] reported that the densification kinetics of reaction sintered mullite were sensitive to Al_2O_3:SiO_2 ratio. Below about 1350°C, the shrinkage rate was higher for the silica-rich mixtures, which could be due to the densification of the silica zones (viscous flow). Above 1350°C, the shrinkage rate was maximum for the 3/2 stoichiometric mullite and minimum for the 75% Al_2O_3 composition. The final density was also sensitive to the Al_2O_3 : SiO_2 ratio. The highest density, observed in 3/2 mullite, was 97% of the theoretical after 1600°C, 10 hours sintering. Wu and Claussen [58] reported 91 to 98% of the theoretical density in mullite sintered at 1550°C for 6 hours

prepared through reaction bonding route. They also reported a zero dimensional change during sintering.

I.2.3   Microstructure and Properties

Electron microprobe analysis of the vacuum hot pressed alkoxy derived mullite prepared by Mazdiyasni and Brown [1] indicated a homogeneous dispersion of SiO_2 in the Al_2O_3 matrix. The unique microstructural features of a typical thermally etched body prepared by this technique had interlocking needlelike, accicular, and polygonal grains arranged in an overall 'jigsaw' mosaic-type fine grained microstructure. This microstructure was reported to be contrary to the observations of other workers [4,5] who observed such type of structure only in the presence of liquid phase. The alkoxy derived mullite materials appeared to be a composite of a crystalline phase in a matrix of a different, perhaps, glassy phase. Thorough examination of the sample by X-ray diffraction and electron microprobe indicated only mullite present in the structure.

The alkoxy derived mullite [1] had an average thermal expansion of 5.6 x 10^{-6} in/in °C from 25°C to 1500°C. The exact cause of observed nonlinearity in thermal expansion around 1200°C is not known. However small hysteresis observed during cooling indicates only small structural change. The vacuum hot pressed sample also showed a very good thermal shock resistance during repeated quenching in cold water from heating at 1200°C for 15 minutes. This excellent thermal shock resistance of the sample was attributed to needlelike interlocking 'jigsaw' grain structure. The experimental Young's modulus of the above, measured by spherical resonance technique, was 32.0x10^6 psi (221

GPa) for the sample of 3.15 - 3.16 gm/cc bulk density. The room temperature flexural strength determined in 4 point bending was 39×10^3 (269 MPa)psi with compression strength exceeding 35×10^4 psi (2415 MPa). These results were in excellent agreement with those of other workers [15].

Creep resistance of the alkoxy derived mullite in compression at 1400°C as reported by Lessing et al. [16] was said to be good. It had a stress exponent of $\simeq 1$ which gave a strong indication of a creep process controlled by diffusion either through grain boundary diffusion or through bulk diffusion. Pask et al. [17] also suggested that such a creep was controlled by diffusion associated with grain boundary sliding. The creep studies by Lessing et al. gave an activation energy of $\simeq 164 \pm 9$ kcal/mol, which is very close to the value of 170 kcal/mol reported by Pask et al. [17]. These values also agreed well with the lattice diffusion of mullite ($\simeq 168$ kcal/mol). The strain rate, measured from 1350°C to 1450°C, decreased slightly when a specimen was tested at 1450°C and then returned to 1400°C. This discrepancy was reported due to small change in grain size during the test. Initial and final grain size of 4.5 and 5.7 μm respectively were measured by linear intercept technique. The creep rate was compared with that of pure Al_2O_3 at an equivalent grain size. The creep rate at 1450°C of such dense mullite was ≈ 1 order of magnitude less than that of pure (99.995%) Al_2O_3. However at higher temperatures, this difference decreased as a result of decrease of difference in creep activation energies (E_A 130 kcal/mol for Al_2O_3 and E_A 164 kcal/mol for mullite) for these two materials. The forgoing data indicated that alkoxy derived

mullite was significantly more creep resistant than Al_2O_3 from 1350°C to near the melting point of mullite. Also the compressive fracture stress at 1400°C appeared to exceed all reported values for polycrystalline oxide bodies.

Mah and Mazdiyasni [14] investigated the mechanical properties of alkoxy derived mullite. Using 4-point loading they found the room temperature flexural strength of 128 MPa, which increased with increasing temperature i.e. to 140 MPa at 1400°C and 145 MPa at 1500°C. Through the optical micrographic observations they found that crack initiated beneath the surface near the small grained porosity nests and showed a substantial slow crack growth (intergranular) before the specimen failed catastrophically (transgranular fracture). It was reported that below the slow crack growth temperature regime the material failed elastically in a transgranular brittle fashion and both the fracture stress and fracture toughness were temperature independent. Above the temperature regime of slow crack growth, the authors [14] observed two opposing phenomena: (i) plastic deformation by grain boundary sliding and microcracking due to the presence of a viscous grain boundary glassy phase and (ii) reduction of crack-tip stress intensity in the plastic zone by energy dissipation through plastic relaxation occuring in the viscous grain boundary glassy phase. Both these phenomena were strongly dependent on the viscosity of the grain boundary glassy phase at the testing temperatures. From the TEM analysis the presence of small amount of glassy phase was clearly observed at the multiple grain junctions or at the grain boundaries.

The fracture toughness, K_{IC}, of mullite was calculated by Mah

and Mazdiyasni [14] using fracture initiating flaws measured through SEM fractography. The equation used for the calculation was

$$\sigma_f \approx (1.68/Y)(K_{IC}/A^{1/4})$$

where the flaw area, A, was measured from the SEM fractographs; σ_f was the fracture strength, $Y \simeq 2$ for the surface flaw; $Y \simeq 1.8$ for subsurface flaws. K_{IC} measured in this fashion agreed with the values obtained by indentation surface-flaw technique. The reported values were 1.8 to 3.3 MPa.m$^{1/2}$ in the temperature regime of 25-1500°C. The increase in indentation fracture stress and K_{IC} with increasing temperature above the slow crack growth regime was also explained in the same way as before.

Suzuki et al. [40] reported that pressureless sintering of alkoxy derived mullite showed pore agglomeration but hot pressing gave fully dense transluscent body leading to higher flexural strength (σ_f). 1700°C sintered sample showed $\sigma_f \simeq 140$ MPa after pressureless sintering, whereas after hot pressing it was 210 MPa. Granulation followed by pressureless sintering showed higher σ_f (180 MPa) values than the samples without granulation. Mazdiyasni [59] reported interlocking needlelike, accicular and polygonal grain depending on both the composition of the powder and firing schedule of mullite derived through alkoxide route. There was no intergranular porosity in the TEM microstructure of average grain size of 1 μm.

Perry [4] reported that the microstructure of mullite, prepared by consecutive precipitation method, was of fine needlelike and interlocking in nature. But, with the decrease of SiO$_2$ content the structure transformed to uniaxial. He observed

~5μm uniaxial grains for 23.3% SiO_2 and ~ 10μm/3μm small needles for 27% SiO_2. In between the structure was mixed in nature. The observation was almost same as observed by Metcalfe and Sant [6]. But they observed ~ 10μm equiaxed grains for lowest SiO_2 content mullite.

The dielectric premittivity of commercial mullite (95% TD) as reported by Perry [4] was found to be 6.7, at 9.4 GHz, with a loss tangent of ~0.002 and temperature coefficient of permittivity (μ_T) of ~+125x10^{-6}K^{-1}. from room temperature to 400°C. For synthetic mullite, however, permittivity was 6.5 with improved loss tangent and μ_T= ~70x10^{-6}K^{-1}. The author [4] also observed a linear relationship between density and dielectric permittivity (ε). From the plot of density vs ε, he found ε = 7.0 for 100% dense mullite. Metcalfe and sant [6] reported the dielectric permittivity of 6.6 with an average μ_T= +50 x 10^{-6}K^{-1} at the same conditions. Mullite prepared by this route [6] showed the values of Young's modulus, E = 160-220 GPa for 12 to 0.3% porosity and flexural strength, σ_f = 117 MPa for 95% TD and σ_f= 152 MPa for 98% TD in 3 - point loading.

Mullite prepared by wet chemical methods [7] had interlocked prismatic and tabular crystals. But if the raw materials were mixed by classical mixing methods, they gave agglomerates of mullite crystals embedded in a glassy matrix. It was reported that mullite prepared by any wet chemical method [8-10] showed a small amount of liquid phase at the triple point. Ultimate engineering stress of the mullite prepared from α-Al_2O_3 (71.8-75% wt%) and SiO_2 flour was 620-815 MPa at 1200°C. For mullite containing 71.8 and 74% Al_2O_3 respectively these values were 250 and 610 MPa at

1400°C. However, mullite prepared from halloysite rock [9,10] had flexural stress of 250 MPa with fracture toughness of 2.1 MPa.m$^{1/2}$ for 98% TD.

Mizuno [46] reported σ_f of 345 - 364 MPa for the hot pressed mullite prepared from aqueous aluminium sulphate and fumed silica. The strength was also high (283-332 MPa) at 1350°C. But above 1350°C σ_f decreased due to the presence of glassy phase.

Microstructure of mullite prepared by sol-gel method [5,11-13] showed a typical microstructure with elongated grains at higher silica content. But it gradually transformed towards equiaxed with the increase in Al_2O_3 content. This observation was same as that of mullite prepared by consecutive precipitation method [6]. The average grain size for equiaxed, stoichiometric mullite was 2 μm. However for higher Al_2O_3 content (76 wt%) it was 10 μm. At the triple point a very small amount of glassy phase of mullite composition was observed. Ismail et al [5] reported that equiaxed grain had no secondary phase at the triple point. Mullite having $\geq$ 72% Al_2O_3 had no glassy phase at the triple point. These workers [13], however, found a small amount of glassy phase at the triple point of stoichiometric mullite.

The room temperature flexural strength of stoichiometric sol-gel mullite [5,12,13] was 405±18 MPa, which decreased to 350±27 MPa at 1300°C due to exaggerated grain growth. However in the case of high silica (32% SiO_2) composition, the room temperature flexural strength (350 MPa) increased to 380 MPa at 1200°C. This increase in strength was attributed to the formation of viscous glassy phase along the grain boundary leading to reduction in the creep propagation rate. The low silica (24%

SiO$_2$) content mullite showed the same trend as that of stoichiometric mullite. It's room temperature value (380 MPa) decreased to ~280 MPa at 1200°C due to the same reason. Other mechanical properties of stoichiometric mullite were reported as follows:

Fracture toughness, K$_{IC}$ = 2.73 MPa.m$^{1/2}$

Vickers hardness, Hv = 11.96 GPa

Young's Modulus, E = 246 MPa

The dielectric constant of sol-gel mullite [5] showed a direct effect on composition. The presence of glassy phase and pores lowered the dielectric constant. The reported values were 7.38, 7.63 and 7.68 for 68%, 72% and 76% Al$_2$O$_3$ content respectively.

Huling and Messing [50] reported that there was no grain boundary phase formation in homogeneous gel-derived mullite. However, amorphous grain boundary phase formation was present in heterogeneous gel-derived mullite. Ismail et al. [51] reported that stoichiometric mullite (72% Al$_2$O$_3$) had highest flexural strength of 400 MPa at room temperature. With the increase in Al$_2$O$_3$ content high temperature flexural strength decreased. The dielectric constant (7.63) was nearly constant within the solid solution limit. Hynes et al. [54] observed that mullite derived through sol-gel route had a stress exponent of 1.2 to 1.6 (68-73 wt% Al$_2$O$_3$) with the activation energies ranging from 742 to 819 kJ/mol tested under 100 MPa at 1724K. They observed that creep of high SiO$_2$ mullite (68% Al$_2$O$_3$) was consistent with rate control by the viscous flow of the glass. The creep behaviour of completely crystalline aluminosilicate was consistent with rate control by

diffusion creep.

Mullite prepared from refined bauxite and SiO_2 [57] through reaction sintering route showed equiaxed mullite grains for 3/2 mullite. For 75% Al_2O_3, it consists of a mixture of small equiaxed grains (5 μm) with large elongated grains (7 by 30 μm). The Al_2O_3:SiO_2 ratio also affected the mechanical properties. The SiO_2 rich material (68% Al_2O_3) exhibited the best mechanical properties. Its flexural strength (σ_f) at room temperature was 210 MPa which continuously increase to greater than 450 MPa at 1200°C. However, for higher Al_2O_3 content ($\geq$ 71.8%) mullite showed decreasing trend of σ_f after 600°C. Reaction-bonded mullite [58] exhibited high fracture toughness of 290 MPa at a density of 97% of the theoretical.

I.3. MULLITE-ZrO_2 COMPOSITES

I.3.1 Preparation

As already described earlier Mullite has relatively low fracture toughness. Further improvements in mechanical behaviour of mullite has been achieved by developing mullite-ZrO_2 composites. The preparation processes are Reaction Sintering, Sintering of Mullite/Premullite with ZrO_2, Hot Pressing of glass powder and Sol-gel method.

In reaction sintering process, [18-23] mixtures of zircon and alumina were attrition-milled followed by drying at 110°C or spray drying at selected temperatures. The resulting powders were isostatically pressed and sintered in air at greater than 1500°C or hot pressed to get the mullite-zirconia composite according to the following reaction:

$$2ZrSiO_4 + 3Al_2O_3 \longrightarrow 3Al_2O_3.2SiO_2 + 2ZrO_2$$
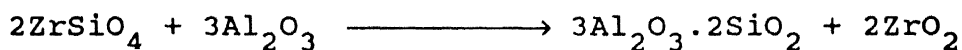
Moya and Osendi [24] prepared mullite-ZrO_2 composites from the active premullite powder, obtained by Moya et al. [9], and ZrO_2. The mixtures were attrition milled in isopropyl alcohol media followed by isostatic pressing at 200 MPa and subsequently sintering at 1570°C.

Yuan et al [25] prepared mullite-zirconia composite from high purity mullite and zirconia powder. The powders were ball milled and subsequently sedimented under various pH conditions to get submicron powder. The mixed powders were biaxially pressed at 250 MPa and sintered at 1610°C.

Boch et al. [60] prepared mullite-ZrO_2 composites from Al_2O_3 and zircon at 1600°C according to the reaction described earlier. Boch and Chartier [61] also prepared mullite-ZrO_2 composites by reaction sintering route from the tape cast mixtures of Al_2O_3, quartz and ZrO_2 powders.

Shyu and Chen [78] prepared mullite-ZrO_2 composites from alumina/zirconia particles coated with an amorphous silica layer. They reported that this type of composites could be sintered in the temperature range of 1100-1310°C.

McPherson [26] prepared mullite/5 wt% ZrO_2 composite from the glass obtained by rapid solidification of the melt of mixed hallides. The rapid solidification of hallides was carried out either in the tail flame of high frequency oxygen plasma or by in-flight melting and solidification of mullite and ZrO_2 powders in direct current plasma torch or in oxyacetelene flame. The composite was prepared by the hot pressing of the powder at 1040°C. Yoshimura et al. [62] prepared mullite-ZrO_2 composite from the glass powder of mullite-20 wt% ZrO_2 by hot pressing in a

temperature range of 1050-1600°C for 30 min. under 25 MPa pressure.

Ismail et al. [27] prepared mullite-zirconia composite by sol-gel method. Mullite sol was prepared by the method reported by the author [12] and was mixed with zirconia sol, which was prepared by using zirconyl chloride. The mixed sol was gelled at pH 2. The dried gel was ball milled and calcined at 800 to 1400°C followed by cold isopressing at 2 tons/cm^2 and sintering at 1600°C.

I.3.2   Sintering

In reaction sintering process, both the reaction and densification processes were reported to be important to get high density materials. Emiliano and Segadaes [22] studied sintering mechanism at temperatures ranging from 1350 to 1650°C. They observed relative density values above 100%, based on the theoretical density for complete reaction, which was reached at 1400-1450°C in the early stages of heat treatments. From this observation they reported that the sintering process of the reactants started before the reaction took place. Above 1400°C-1450°C, de-densification occured and minimum density was reached at 1500°C - 1550°C. The decline in densification rate was reported to coincide with the starting of zircon decomposition and the onset of the reaction to form mullite. This also agreed with Boch and Giry's results [21]. When the decomposition of zircon and the formation of mullite was approached towards completion, the relative densities of the two mixtures started rising again. The authors [22] also reported a certain time delay between the start of zircon decomposition and the beginning of mullite formation which was in agreement with the results of Di Rupo and

Anseau [28].

Boch and Giry [19,21] reported sensitivity of the reaction sintering process to powder characteristics. The authors [21] showed that the use of very fine particles (~0.5 μm) favoured densification rather than mullitization. They also reported the enhancement of densification of samples containing free ZrO_2. Holmstrom et al. [23] reported that zirconia accelerated both the densification and mullitization kinetics. Zircon appeared as a transitory phase and its ZrO_2 inclusions was reported to act as grain growth inhibitors. They also reported that even a low ZrO_2 content (1 vol%) was useful for improving reaction sintering. The product density was in the range of 95-99% of theoretical density at 1600°C, depending upon the powder characteristics.

Boch et al. [60] reported greater than 97% relative sintered density at 1600°C and preferred reassociated zircon to dissociated one for better sintering. In tape casting method greater than 98% relative sintered density was achieved at rather low sintering temperature, ie.1560°C for 2 hours.

Moya and Osendi [24] prepared mullite -ZrO_2 composites from premullite and ZrO_2 powders. They reported that the densification rate enhanced in the presence of ZrO_2. At 1570°C the density of mullite/ZrO_2 composite was 93.7% of TD, while the corresponding value for mullite was only 87.3% of TD.

Mullite prepared by Yuan et al. [25] from fused mullite and ZrO_2 powders gave density of 92.1 to 96.1% of theoretical density at 1610°C.

Shyu and Chen [78] reported that mullite-ZrO_2 composites prepared from Al_2O_3/ZrO_2 powders coated with an amorphous silica

layer could be densified through the viscous flow of the amorphous silica layer. For the ZrO_2 - free mullite ceramics the viscous densification kinetics was inhibited by increasing the content of the Al_2O_3 inclusion particles and by crystallization of the amorphous silica layer. However, for the zirconia-mullite ceramics, the addition of ZrO_2 inclusion particles accelerated the viscous densification kinetics. Mullitization kinetics was also enhanced by the addition of zirconia.

McPherson [26] reported 31% mean porosity of the mullite-ZrO_2 composites prepared from glass powder by hot pressing at 1040°C. However, the porosity at the outer 1mm thick rim was ≈10%. They suggested that extensive densification occurred in the outer region of the compact prior to crystallization, because of the temperature gradient through it, before any significant densification occurred in the interior.

Mullite-ZrO_2 composites prepared from glass powder [62] rapidly densified fully at about 950°C, around the glass transition and crystallization temperatures of the amorphous materials, probably due to the viscous flow mechanism.

Ismail et al. [27] prepared mullite-ZrO_2 composite by sol-gel method. They got densities of > 98% of TD irrespective of the composition studied.

I.3.3   Microstructure and Properties

The microstructure of reaction sintered mullite-ZrO_2 composites [18] exhibited the presence of ZrO_2 particles (0.5 to 1.0 μm) located primarily within the mullite grains (≈4 μm). The ZrO_2 particle size did not change even after long annealing. However, the fraction of tetragonal ZrO_2 particles decreased from

0.3 to <0.1 with the increase in annealing time from 1 to 16 hours at 1600°C.

Holmstrom et al. [23] observed the presence of equiaxed mullite grains in mullite-ZrO_2 composite sintered below 1620°C. The samples sintered at 1620°C, however, exhibited an elongated grains of 1-3 μm. The ZrO_2 grains were located in both intra- and intergranular positions. The former grains were very small with a size of about 0.1 μm, whereas latter were larger with a size varying from 0.5 to 1 μm. A coarsening of intergranular ZrO_2 grain was also observed for longer sintering time. The authors [23] also reported that a higher content of ZrO_2 produced larger ZrO_2 grains which were more amenable to transformation to the monoclinic phase.

Clausen and Jahn [18] measured the fracture toughness and bend strength of the mullite – ZrO_2 composite in 4- point loading. The samples sintered at 1600°C had fracture toughness of 4.5±0.3 $MPa.m^{1/2}$ and bend strength of 400±35 MPa. They also observed that the composites sintered at 1570°C retained their bend strength of 330±25 MPa upto at least 1280°C, indicating the retention of very little glassy phase in the grain or phase boundaries. Boch and Giry [19,21] measured bend strength of 320 MPa at room temperature for the composites sintered at 1600°C. They reported that coarse microstructure at higher temperature lowered the bend strength of the materials. Room temperature Young's modulus and shear modulus had values of 220 GPa and 155 GPa, which was slightly higher than pure mullite materials. Fracture toughness of the composite was 3.3 $MPa.m^{1/2}$ in comparison to 2 $MPa.m^{1/2}$ for pure mullite. Dilatometric measurement gave a mean thermal expansion coefficient

of $6x10^{-6}K^{-1}$ in the range of 20 to 1000°C. Observed hysteresis in the curve was attributed to phase transformation of monoclinic-ZrO_2 into tetragonal-ZrO_2 on heating and vice versa.

Reaction sintered mullite - ZrO_2 composites prepared by Boch et al. [60] showed a mixture of accicular and equiaxed mullite grains in the 68% Al_2O_3 material. However, >68% Al_2O_3 containing materials showed only equiaxed mullite grains. Excessive grain growth was reported in the 75% Al_2O_3 mullite. High silica (68% Al_2O_3) mullite exhibited very good flexural strength (≈195MPa) upto 1200°C, whereas its ZrO_2 containing counterpart did not show similar trend. Tape cast followed by reaction sintered mullite-ZrO_2 composites [61] showed flexural strength of 265 to 328 MPa for 5 to 15 vol% ZrO_2 addition. The K_{IC} for the same condition was in the range of 2.8 to 3.5 MPa.m$^{1/2}$.

Moya and Osendi [24] observed increase in fracture toughness value of mullite-ZrO_2 composite from 2 to 3.2 MPa.m$^{1/2}$ with increase in ZrO_2 addition from 0 to 20 vol%.˙ Relative content of t-ZrO_2 did not affect these values. However flexural strength increased with the increase in t-ZrO_2. The reported values of flexural strength was in the range of 213±23 to 288±20 MPa for 0 to 20 vol% total ZrO_2 content. Strengthening of composite was attributed to microcracking due to the martensitic transformation of t-ZrO_2 to m-ZrO_2 (on cooling) added in addition to solid solution strengthening. This view has also been supported by Osendi et al. [29].

Yuan et al. [25] reported the increase in flexural strength and fracture toughness of Mullite from 15 to 30% by the addition of 5 to 25 vol% fine (1 μm) ZrO_2 in the as fired (1610°C)

condition. The values for pure mullite were 100 MPa and 2.01 MPa.m$^{1/2}$ respectively. The flexural strength of the mullite composites (15 to 25 vol% of fine or medium ZrO_2) after three thermal shock cycles (from 1200°C to room temperature) was nearly tripled compared to that of pure mullite. An increase of 20 to 30% in K_{IC} both before and after one thermal shock was also obtained by introducing 20 vol% fine ZrO_2. Young's moduli of the quenched composite samples did not decrease, as it was expected, but slightly increased for some strengthened specimens.

Mullite - ZrO_2 composites prepared from amorphous silica coated Al_2O_3/ZrO_2 powders [78] and sintered in the range of 1100-1310°C, exhibited a duplex, porous, microstructure specially at the higher sintering temperature. With the increase in sintering temperature and ZrO_2 content, a coarsening of ZrO_2 grains was observed, resulting in a decreased tetragonal to monoclinic ratio. K_{IC} increased with the increase in ZrO_2 content. Mullite- 20 vol% ZrO_2 composite sintered at 1600°C had a K_{IC} of 3.8 MPa.m$^{1/2}$.

The microstructure of mullite/ 5 wt% ZrO_2 composites prepared from glass powder [26] and sintered at 1300°C showed $\simeq$ 0.02 μm crystals of t-ZrO_2 dispersed in a polycrystalline mullite matrix with grain size of $\approx$0.1μm. Heating at higher temperatures resulted in increase in size of grains of both zirconia and mullite. Heating at 1600°C gave a microstructure of $\simeq$ 0.2 μm spherical t-ZrO_2 particles dispersed within the mullite grains of $\approx$2 μm size.

The microstructure of hot pressed mullite-ZrO_2 composites from glass powder [62] showed large amount of glassy phase at

1050°C. This glassy phase decreased with the increase in hot pressing temperature. The samples hot pressed at 1600°C exhibited a fracture toughness of 2.2 MPa.m$^{1/2}$.

Mullite-ZrO_2 composites prepared by sol-gel method [27] gave microstructure of homogeneously dispersed ZrO_2 in the mullite matrix. The ZrO_2 particles were mainly intergranular. The average grain sizes of mullite and ZrO_2 in the specimen (15 vol% ZrO_2 composite) sintered at 1600°C for 2.5 and 3.0 hours were 0.8, 0.40 μm and 0.8, 0.45 μm for the respective periods.

Authors [27] reported increase in fracture toughness of the mullite-ZrO_2 composites (prepared by sol-gel method) with increase in total ZrO_2 content as a result of microcrack toughening due to spontaneous transformation (tetragonal to monoclinic) of ZrO_2. The fracture toughness value of the 15 vol% ZrO_2 specimen was 4.9 MPa.m$^{1/2}$. Whereas, the flexural strength was 520 MPa. Beyond 15 vol% ZrO_2 it decreased due to both microcrack formed by the t-m transformation on cooling and the release of strain caused by thermal expansion mismatch between the mullite and ZrO_2, which resulted in extensive microcracking in the sintered body. The flexural strength increased with the increase in transformable t-ZrO_2 upto 45 vol% for the specimen of 15 vol% total ZrO_2 content. After 45 vol% it again decreased due to the same reason. The flexural strength decreased to 300 MPa with increase in temperature upto 1300°C due to the coarsening of ZrO_2 particles as a result of thermal expansion mismatch within the mullite matrix. The Young's modulus of the 15 vol% ZrO_2-mullite composite had a value of 219 GPa, which decreased to 213 GPa due to the microcracking.

1.4 MULLITE-BN COMPOSITES:

This particular composite was prepared by Lewis et al. [30] from submicron size α-Al_2O_3, colloidal silica and fine BN powders. The powders were mixed by wet milling and then hot pressed (at 1700-1750°C and 35 MPa) to almost theoretical density.

The microstructure of the composite was anisotropic and laminar in character. The BN crystallites were generally oriented with the thickness direction (c-axis) parallel to the HPA. The BN crystallites were 0.1 - 0.2 μm in thickness and $\simeq$ 5μm in lateral dimension. The mullite grains were $\simeq$ 5μm in size. The composite had a very good thermal shock resistance, as measured by room temperature water quench technique. It also showed an exponential dependence of Young's modulus on composite density. The properties of mullite - 30 vol% BN composites were as follows:

Density (gm/cc)   =   2.75-2.81

Young's modulus (GPa)   =   66-90 ($\parallel$ HPA), 100-130 ($\perp$ HPA)

(HPA: Hot pressing axis)

Flexural strength (MPa)   =   200-350

Dielectric constant   =   5

Thermal shock resistance ΔT_c(°C)=   400-450

I.5 COMPLEX MULLITE BASED COMPOSITES:

I.5.1   Mullite-ZrO_2-MgO/CaO/Y_2O_3 Composites

Orange et al. [31] prepared mullite-ZrO_2-MgO composites from zircon/dissociated zircon, alumina and magnesia by reaction sintering method, as per the following reaction:

$$2ZrSiO_4 + 3Al_2O_3 \xrightarrow{\text{1.8 wt\% MgO}} 2ZrO_2 + 3Al_2O_3.2SiO_2$$
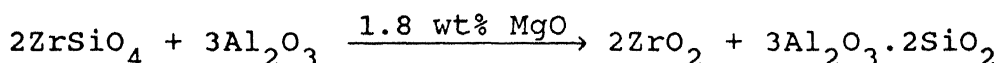
The stoichiometry of the above equation was also modified slightly to get multiphase ceramic composites of the

zirconia/alumina/mullite/magnesia, according to the following reaction:

$$2ZrSiO_4 + (3+x)Al_2O_3 \xrightarrow{1.8\ wt\%\ Mgo} 2ZrO_2 + 3Al_2O_3 \cdot 2SiO_2 + xAl_2O_3$$
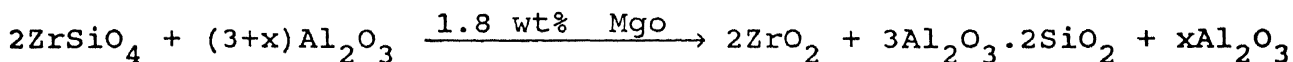
The individual powders were mixed using mechanical procedure with an organic binder, uniaxially pressed at 50 MPa and finally sintered at 1450-1650°C. In all the cases ZrO_2 content was 20 vol%. Yuan et al. [32] prepared mullite-ZrO_2-Y_2O_3 composites from sol-gel mullite and submicron fine (<0.2 μm) ZrO_2 powders. The powders were mixed by ball milling in Al_2O_3 grinding media and subsequently pressed into discs and sintered at 1600°C. Pena et al. [33] prepared mullite-ZrO_2-CaO composites from zircon, alumina and $CaCO_3$/$CaSiO_3$ by the reaction sintering process. The raw materials were milled, homogenized and iso-pressed at 200 MPa and then sintered at 1425°C and 1450°C.

Mullite-ZrO_2/MgO/Y_2O_3/TiO_2 composites were also prepared by different workers through reaction sintering [63-67] or through sol-gel [63, 68] processing technique. Leriche [63] prepared mullite - ZrO_2 composites with MgO/TiO_2 addition through different routes. Moya and Miranzo [64] prepared mullite-ZrO_2-MgO composites by reaction sintering of $ZrSiO_4$, Al_2O_3 and MgO. They used both direct reaction sintering method as well as pressureless sintering of isopressed reaction-sintered composite powder. Das et al. [66, 67] prepared mullite-ZrO_2/MgO/Y_2O_3 composites by the reaction sintering of zircon, Al_2O_3 and MgO/Y_2O_3 powder mixtures. Shiga et al. [68] prepared MgO doped mullite-ZrO_2 composites by the sol-gel method.

In the reaction sintering process [31] MgO was used to decrease the dissociation of zircon and produce a small amount of

transient liquid phase contributing to simultaneous densification with the reaction. Yuan et al. [32] reported that addition of Y_2O_3 enhanced the retention of t-ZrO_2 and also lowered the sintering temperature. They synthesized composites of 97.5 to 99% of the theoretical density at 1600°C. Pena et al. [33] observed that $CaCO_3$ and $CaSiO_3$ addition enhanced the sintering rate and also decreased the final sintering temperature of reaction-sintered composites. They found that CaO addition as $CaSiO_3$ resulted into lower sintering rate than that of $CaCO_3$ addition. This difference was higher in case of compositions containing free Al_2O_3. They also observed that presence or absence of free Al_2O_3 in the mullite-ZrO_2 composites did not modify the sintering behaviour.

Orange et al. [31] reported that the microstructure of reaction sintered mullite-ZrO_2-MgO composites consisted of needlelike mullite grains with two types of ZrO_2 particles: rounded intragranular grains of 2.5 μm and well-faceted intergranular grains of 1.0 μm in size. Glassy phase was observed in the tridimensional skeleton of mullite. Yuan et al. [32] reported that Y_2O_3 addition in mullite ZrO_2 composite aided the retention of t-ZrO_2 in the composite structure. This t-ZrO_2 did not undergo stress-induced transformation during grinding.

Orange et al. [31] reported room temperature flexural strength and fracture toughness value of 270-330 MPa and 4.6 - 5.25 MPa.m$^{1/2}$ respectively for the reaction sintered mullite-ZrO_2-MgO composites. They observed that flexural strength and fracture toughness slightly decreased with the increase in temperature upto 600°C. But both these properties increased from 600°C to 800°C due to the presence of highly viscous glassy phase

along the grain boundaries. Beyond 800°C the properties again decreased due to the fluidization of grain boundary glassy phase. Mullite-ZrO_2-Y_2O_3 composites prepared by Yuan et al. [32] (through sol-gel route) gave Young's modulus and fracture toughness values of 160-185 GPa and 2.3-2.5 MPa.m$^{1/2}$ respectively.

Leriche [63] reported 98 to 99% relative sintered density of mullite-ZrO_2 composites prepared through different routes at a temperature ranging from 1570 to 1650°C. Reaction sintered material in the presence of MgO and TiO_2 presented similar mechanical properties, although very different microstructures. The MgO composites were characterized by a crosslinked mullite grain arrangement with the presence of an intergranular glassy phase, whereas the microstructures of the titania composites and the sol-gel materials were constituted of equiaxed grains without an intergranular glassy phase. The sol-gel composites showed the highest flexural strengths and the most homogeneous microstructures. However, the toughness value was lower than that of the MgO doped composites because of lower tetragonal ZrO_2 content and the absence of a crosslinked mullite grain arrangement. Das et al. [66, 67] reported 97.5 to 99.59% relative sintered density for the isopressed reaction sintered mullite-ZrO_2- MgO/Y_2O_3 composites, sintered at 1550 to 1600°C for 2 hours. They observed a homogeneous distribution of ZrO_2 in the mullite matrix, and reported flexural strength of 116 to 243 MPa depending upon the nature of dopant. The fracture toughness was in the range of 2.40 to 5.15 MPa.m$^{1/2}$. However, uniaxial pressing of the green compacts showed poor sintered properties. In this case flexural strength was in the range of 110 to 165 MPa for the

samples sintered at 1600°C for 2 hours. Shiga et al. [68] reported 99% relative density for the sol-gel processed mullite-ZrO_2-MgO composites, sintered at 1450°C with 1.5 wt% MgO. They also reported the formation of $ZrSiO_4$ with greater than 0.3 wt% MgO due to the liberation of SiO_2 from mullite grains. The flexural strength of 560 MPa and fracture toughness of 5.8 MPa.m$^{1/2}$ for the 1.5 wt% MgO doped composites fired at 1475°C was reported.

I.5.2   Mullite - ZrO_2 - TiO_2 Composites

This group of composite was prepared by the reaction sintering process [34-38] from the raw materials of zircon, alumina and titania, according to the following reactions:

$$2ZrSiO_4 + (3+x)Al_2O_3 + xTiO_2 \longrightarrow 2ZrO_2(ss) + Al_4Si_2O_{13}(ss)$$
$$\text{with } x = 0.25$$

$$2ZrSiO_4 + (3+x)Al_2O_3 + xTiO_2 \longrightarrow 2ZrO_2(ss) + Al_4Si_2O_{13}(ss) + Al_2TiO_5$$
$$\text{with } x = 1.0$$
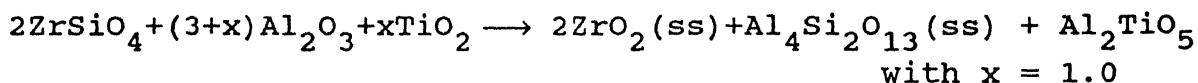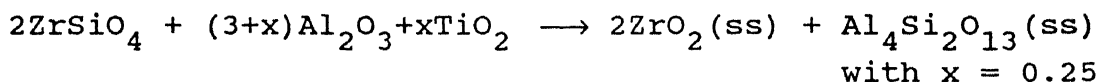
The powders were homogenized by attrition milling in isopropyl alcohol. After drying and sieving, the raw compositions were isostatically pressed at 200 MPa followed by sintering at 1500-1550°C.

Leriche et al. [35] reported that the addition of TiO_2 in Mullite-ZrO_2 composite enhanced the densification and zirconia dissociation reaction. Several workers [34,37, 38] observed that the composition containing 1 mol TiO_2 was situated beyond the solid solubility limit of TiO_2 and ZrO_2 in the quaternary system Al_2O_3-ZrO_2-TiO_2-SiO_2. The formation of transitory $ZrTiO_4$ therefore occurred at temperatures around 1300°C. This phase formed a transitory liquid phase at 1400°C, accelerating the densification. However, Melo and Moya [34] reported this phase as

Al_2TiO_5. The composite formulated with 1 mol TiO_2 reacted and densified at a lower temperature of 1500°C incomparison to usual sintering temperature 1550°C for composite with 0.25 mol TiO_2. Since the latter composition was located inside the solid solubility limit sintering process took place in the absence of any liquid phase. The density obtained in this process was 98-99% of the theoretical.

The microstructure of such reaction sintered composite [36] was characterized by fine equiaxed mullite grains, intergranular ZrO_2 and a very small amount of glassy phase, when sintered at 1500°C- 1550°C. It was reported that ZrO_2 was the only TiO_2 incorporating phase. As a result, addition of TiO_2 increased the ZrO_2 grain size causing decrease in unit cell parameters of ZrO_2 with increasing TiO_2 additions due to smaller ionic radius of Ti^{4+} compared to Zr^{4+} in quasi-octahedral coordination.

Melo and Moya [34] did not observe any noticeable variation in the final density of mullite-ZrO_2-TiO_2 composite with the increase in ageing temperature or time. Only pore size changed. Bending strength of composite was 250±20 MPa at room temperature. The strength degradation, observed at ≥1450°C and ≥1400°C for 0.25 and 1.0 mol TiO_2 respectively, was due to the pore coalescence and ZrO_2 particle coarsening. On the other hand, fracture toughness values increased from 4 to 4.8 MPa.m$^{1/2}$ with the increase in temperature from 20°C to 1500°C. Such a behaviour was attributed to the existence of a significant plasticity zone infront of crack tip as well as microcrack-toughening as a consequence of higher average grain size of zirconia particles.

I.5.3   Mullite - ZrO_2 - SiC Composites

This group of composite was prepared by Hoffmann et al. [39] from mullite and ZrO_2 powders and purified SiC whiskers. A slurry of the mixtures of mullite, ZrO_2 and SiC was prepared by tumble mixing and then dried in a rotation evaporator. Densification was achieved after uniaxial hot pressing at temperatures between 1500 - 1650°C.

The grain size of the mullite-20 vol% SiC composite after hot pressing at 1600°C was ≤2 μm. Incorporation of 10 vol% ZrO_2 reduced the densification temperature by 50°C.

The microstructure of 10 vol% ZrO_2 content sample showed a homogeneous distribution of the ZrO_2 particles in the mullite matrix. The whisker containing composites exhibited an anisotropic microstructure with alignment of the SiC-whiskers parallel and a random uniform distribution within the planes perpendicular to the hot pressing direction.

Addition of 20 vol% whiskers increased the bending strength of mullite from 300 to 473 MPa and the fracture toughness from 3.0 to 5.0 MPa m$^{1/2}$. Impurities in the unsedimented whiskers reduced bending strength from 470 to 330 MPa. Fractographic analysis revealed the initiation of fracture from the metallic impurities and hard whisker agglomerates. It was observed that fracture toughness remained nearly constant with the increase in hot pressing temperatues from 1500 to 1650°C. However, bending strength increased from 390 to 470 MPa due to the reduction of critical flaw size. A further improvement of the mechanical properties was observed due to ZrO_2-toughening and whisker reinforcement. The maximum bending strength of 580 MPa was

observed for the samples containing 10 vol% ZrO_2 and 20 vol% SiC. The maximum fracture toughness of 6.9 MPa.m$^{1/2}$ was observed for the samples containing 10 vol% ZrO_2 and 30 vol% SiC. Bending strength of the latter sample was lower than the former due to insufficient deagglomeration of the whiskers. Fracture surfaces of the whisker reinforced composites were noticeably rougher than that of mullite matrix and roughness increased with increase in whisker content. From these observations authors [39] explained strengthening behaviour due to crack deflection by the whiskers.

Oxidation resistance of the SiC whisker reinforced composite was good at temperatures ≤1000°C. In this temperature region a thin oxide film formed on the surface which prevented further degradation of bulk material. However at higher temperature (≥1200°C) SiC-whiskers severely oxidized resulting in the degradation of high temperature mechanical properties.

Mullite-ZrO_2/SiC composites were also prepared by other workers [69-75] through different routes namely reaction sintering, sol-gel processing followed by sintering, colloidal processing followed by sintering and transient viscous sintering. Moya [69] prepared the composites from $ZrSiO_4$, Al_2O_3 and SiC by the process of reaction sintering at 1450°C for 1.5 hours. CaO, MgO and TiO_2 were also used as additives in order to develop a transient liquid phase. Rahaman and Jeng [70] prepared the composite from the sol-gel processing of mullite and 15 vol% SiC whisker after sintering at 1550°C for 1 hr to 85% relative density. Tiegs et al. [71] prepared mullite-20 vol% SiC composite from the mullite and SiC whisker by either hot pressing or pressureless sintering at a temperatures of 1500-1675°C to >97%

sintered density. Takada et al. [73] prepared the composite from mullite and SiC powder by pressureless reaction sintering at 1700°C. Nischick et al. [74] prepared SiC platelet reinforced mullite-ZrO_2 composites by both conventional powder processing and a pressure filtration route with constant filtration rate. The samples were sintered at 1690°C for 30 to 120 min. Sacks et al. [75] prepared this composite by transient viscous sintering of composite powders. In this process α-Al_2O_3 powders were coated with amorphous SiO_2 and then mixed with SiC followed by compaction and sintering at ~1300°C. Finally they were converted to dense fine grained mullite at higher temperature ($\geq$1500°C) by reaction between Al_2O_3 and SiO_2. In this process an enhanced densification was observed compare to other recent studies of sintering of mullite based composites.

Microstructure of SiC reinforced mullite ZrO_2 composites prepared through sol-gel processing route exhibited better uniformity than other processing routes. The fracture surfaces were irregular in nature. Moya [69] reported moderately high toughness (4.5-5.5 $MPa.m^{1/2}$), hardness (10-14 GPa) and bending strength (250-400 MPa) for the composites of mullite-20 vol% SiC whisker. Tiegs et al. [71] showed that the addition of 20 vol% SiC whisker to mullite increased the flexural strength from 200 to 425 MPa and fracture toughness from 2.2 to 4.7 $MPa.m^{1/2}$.

I.6 SCOPE OF THE PRESENT INVESTIGATION

As described in the introduction section, mullite ceramic has extensive uses in different structural and electrical applications because of its high melting point, low thermal expansion, high creep resistance, chemical inertness, enhanced flexural strength

at high temperature and good dielectric constant. However, the relatively low fracture toughness of mullite is the main barrier to be overcome for efficient structural applications. Development of mullite based composites is therefore one of the solutions.

As highlighted earlier mullite can be processed by various methods, the most prominent being fusion and sol-gel routes. The former grade ceramic is naturally much cheaper than the latter. The present investigations aims to investigate the comparative properties of mullites obtained from processing of powders of these two grades under similar conditions. In the case of mullite based particulate composites, the most prominent addition is the pure ZrO_2 in its straight or modified forms. Processing of these composites were proposed to be carried out through different routes such as prealloyed fusion route, reaction sintering of zircon and Al_2O_3 and milling/sintering route of ceramic premixes. Very little attention has been directed towards study of mechanically milled mullite composite. While there is some effort [25] in this direction on fused mullite - ZrO_2 composite, there seems no work on sol-gel based milled mullite composites. Ismail et al. [27] investigated mullite based composites by sol-gel route in which all the constituents were chemically mixed in the form of sol followed by gellation at a particular pH. Keeping in view the capital cost involvement of hot presses or Hips, the present selected processing route viz milling/pressureless sintering is naturally more attractive economically, at least for the production of technical grade mullite and its based refractory products.

The earlier workers [31,32, 63, 64, 66-68] have mostly used

either straight ZrO_2 additive or singly modified ZrO_2 (eg. ZrO_2-MgO, ZrO_2-Y_2O_3, etc.) However in the present investigation an effort has been done to investigate the effects of doubly modified ZrO_2 additives such as ZrO_2-MgO-Y_2O_3. In addition special care during present investigation has been taken to keep the powder characteristics (eg. average grain size, packing density, etc.) of both ZrO_2-MgO and ZrO_2-MgO-Y_2O_3 identical, so that the role of Y_2O_3 or MgO could be focussed better.

The stoichiometry of Al_2O_3/SiO_2 in mullite is 1.5. However there may be some departure from stoichiometry during preparation. Keeping this in view the mullites having two different stoichiometries ie. 1.5 and 1.51 have been used in the present investigation.

either straight ZrO_2 additive or singly modified ZrO_2 (eg. ZrO_2-MgO, ZrO_2-Y_2O_3, etc.) However in the present investigation an effort has been done to investigate the effects of doubly modified ZrO_2 additives such as ZrO_2-MgO-Y_2O_3. In addition special care during present investigation has been taken to keep the powder characteristics (eg. average grain size, packing density, etc.) of both ZrO_2-MgO and ZrO_2-MgO-Y_2O_3 identical, so that the role of Y_2O_3 or MgO could be focussed better.

The stoichiometry of Al_2O_3/SiO_2 in mullite is 1.5. However there may be some departure from stoichiometry during preparation. Keeping this in view the mullites having two different stoichiometries ie. 1.5 and 1.51 have been used in the present investigation.

CHAPTER II
EXPERIMENTAL PROCEDURE

Mullite and its composites were prepared through three different routes namely (i) premix milling, compaction and sintering, (ii) reaction sintering and (iii) prealloyed powder compaction and sintering. In premix milling, compaction and sintering route mullites, ZrO_2, ZrO_2-MgO and ZrO_2-MgO-Y_2O_3 powders were used. Reaction sintered mullite-ZrO_2 composites were prepared from zircon and Al_2O_3 powders. Prealloyed powder was directly used to prepare the composite. The important aspects of preparation and characterization consisting of the details of (i) raw materials, (ii) preparation of composites and (iii) their characterization are presented in the following section.

II.1 RAW MATERIALS

The chemical compositions of various raw materials were provided by the suppliers. As these raw materials had to be milled further, the average particle size of each powder (raw materials) was estimated by Coulter counter analysis. The equipment (Model Z_B and B) developed by [Coulter Electronics Ltd., U.K.) was used. After milling the average particle size fell below coulter counter limit and so it was measured on JEOL 840A scanning electron microscope. For each set a large number of electron micrographs from different regions were used for averaging the particle size estimation.

The chemical and physical characteristics of raw materials used in the present investigation are as follow:

II.1.1   Mullite Powders

Three different types of mullite powders were used in the present investigation.   One of them (MC) was prepared by electrofusion of calcined Al_2O_3 and high grade silica sand.   Other two types, MP-20 and MP-40 were prepared by sol-gel process with $Al_2O_3:SiO_2$ ratio of 1.5 and 1.51 respectively.   Powder characteristics of these mullites and their sources are given below.

(a) **MC Mullite**

Supplier : Carborundum Universal Ltd., Madras, India

Average particle size (as received)   : 7.83 μm

Apparent Density   : 0.99 g/cm^3

Al_2O_3 : SiO_2 Ratio   : 1.70

Chemical Composition (mass %) : Al_2O_3 75.50, SiO_2 22.50, Fe_2O_3 0.05, alkalies 1.94, TiO_2 0.01

(b) **MP-20 Powder**

Supplier : Chichibu Cement Co. Ltd, Japan

Average particle Size (as received) :   1.30 μm

Apparent Density   :   0.59 g/cm^3

Al_2O_3 : SiO_2 Ratio   :   1.50

Chemical Composition (mass %) : Al_2O_3 71.80, SiO_2 28.19, Na_2O 0.01

(c) **MP-40 Mullite**

Supplier : Chichibu Cement Co. Ltd, Japan

Average particle size (as received) : 1.36 μm

Apparent Density   : 0.58 g/cm^3

Al_2O_3 : SiO_2 Ratio   : 1.51

Chemical composition (mass %) : Al_2O_3 71.80, SiO_2 28.05, TiO_2 0.10, Na_2O 0.01

II.1.2 ZrO_2 powder

Supplier : Magnesium Elektron Ltd, U.K

Average particle size (as received) : 0.90 μm

Apparent Density   : 1.06 g/cm^3

Chemical composition (mass %) : ZrO_2 99.63, SiO_2 0.15, TiO_2 0.20, Fe_2O_3 0.02

II.1.3 ZrO_2-MgO Powder

Supplier : Dynamit Nobel, Germany

Average particle size (as received) : 50% < 0.6 μm

Apparent Density   : 0.45 g/cm^3

Chemical composition (mass %) : ZrO_2 94.70, SiO_2 0.06, TiO_2 < 0.05, Fe_2O_3 0.04, CaO 0.04, MgO 3.41, Al_2O_3 0.05, HfO_2 1.69, Na_2O 0.01, K_2O < 0.01

II.1.4 ZrO_2-MgO-Y_2O_3 Powder

Supplier : Dynamit Nobel, Germany

Average particle Size (as received) : 50% < 0.60 μm

Apparent Density   : 0.38 g/cm^3

Chemical composition (mass %) : ZrO_2 92.00, SiO_2 0.05, TiO_2 <0.05, Fe_2O_3 0.04, CaO 0.04, MgO 2.50, Al_2O_3 0.06, HfO_2 1.60, Na_2O 0.01, K_2O < 0.01, Y_2O_3 3.7

II.1.5   Zircon Flour

Supplier : Indian Rare Earths Ltd., Bombay, India

Average Particle Size (as received) : 20.00 μm

Chemical Composition (mass%):

ZrO_2 59.72, SiO_2 31.94, Al_2O_3 6.76, Fe_2O_3 0.17, TiO_2 trace, CaO 1.03, MgO trace, K_2O trace

II.1.6 Al_2O_3 Powder

Supplier : Indian Aluminium Co., Belgaum, India

Average Particle Size : 2 μm

Chemical Composition (mass %) : Al_2O_3 99.50, Alkalies 0.50

II.1.7 Mullite - ZrO_2 Prealloyed Powder (MZ)

This powder was prepared by electric arc fusion of zircon sand and calcined alumina to form large ingot followed by crushing. The chemical and physical properties of the powder and its supplier are given below.

Supplier : Universal Abrasives Ltd., U.K.

Average Particle Size : 7.24 μm

Al_2O_3 : SiO_2 ratio   : 1.67

Chemical Composition (mass%) :

Al_2O_3 46.30, SiO_2 16.30, TiO_2 0.08, Fe_2O_3 0.04, CaO 0.05, MgO <0.05, Na_2O/K_2O 0.15, ZrO_2 + HfO_2 36.00

II.2 PREPARATION OF COMPOSITES

Mullite and its composites were prepared by conventional powder metallurgy route involving following steps: powder milling, green compaction and sintering.

II.2.1 Powder Milling

The mullite powder with 0 to 25 vol% ZrO_2 and its modified versions were separately milled by the conventional ball milling technique. Wet milling of the powders was performed in isopropyl alcohol medium for a period of 3 hours. The ratio of powder to ball was kept at 1:3 (by mass). Zircon (57wt%) and Al_2O_3 (43 wt%) powders mixture was also similarly wet ball milled. This composition was selected so as to react all the SiO_2 in Zircon with Al_2O_3 to form stoichiometric mullite. The powder so obtained

were dried in an oven at 110°C. The zircon mullite prealloyed powder (ZM) was used in as received condition. The particle sizes of MC, MP-20, MP-40, ZrO_2, ZrO_2-MgO, ZrO_2-MgO-Y_2O_3 and zircon powders after milling the premixes were 3.72, 0.76, 0.85, 0.76, 0.49, 0.46 and 10.20 μm respectively.

II.2.2 Green Compaction

Rectangular pellets, of the ball milled powder, measuring 25 mm x 8 mm x 2.5 mm were compacted in a uniaxial hydraulic press (10 ton capacity) at a pressure ranging from 300-350 MPa, in order to impart sufficient green strength. Polyvinyl alcohol solution (0.5% mass in water) was used as a green binder. Steel die was lubricated with a thin layer of zinc stearate prior to each compaction. The pellets were dried in an over at 110°C and green densities were calculated from their physical dimensions and mass.

II.2.3 Sintering

The sintering of green compacts were carried out for 1 hour in super kanthal resistance heated muffle furnace with a hot zone of 10 cm at three different temperatures, namely 1600℃, 1650℃ and 1700℃ in ambient atmosphere. The 1600°C temperature was selected only for MP-20 based mullite with ZrO_2 additive in order to probe the adequacy of sintering condition. The other two temperatures were used invariably for all the composites. The rate of heating was 5°C/min. During heating the temperature was held at 450°C for 15 minutes for efficient binder removal.

II.3 MEASUREMENT OF SINTERED DENSITY AND POROSITY

The sintered densities were measured with the help of a Mercury Densometer (Fairey Tecramics Ltd., U.K. make) using the following relation:

$$\text{Sintered density (g/cm}^3) = \frac{W_1 \times d}{W_2}$$

where

W_1 = Weight of the sample in air (g)

W_2 = Weight of the sample in mercury (g)

d = Density of mercury (g/cm^3)

Sintered porosities were calculated from the measured and theoretical densities of the composites. The calculation of theoretical densities were done from the rule of mixtures, assuming that no interaction of individual mullite and ZrO$_2$ powders takes place. In case of reaction sintering route the theoretical density was calculated assuming complete mullitiztion.

II.4 MEASUREMENT OF MECHANICAL PROPERTIES

Mullite based composites developed in the present case were mainly studied for their transverse rupture strength (TRS) and fracture toughness (K_{IC}). Details of the measurement are given below:

II.4.1 Transverse Rupture Strength

The TRS of the as sintered samples were measured under three point bending load in an Instron machine with a cross head speed of 0.2 mm/min. TRS was calculated from load at the point of failure using following formula:

$$\text{TRS (MPa)} = \frac{1.5 \ PL}{WD^2} \times 9.806$$

where

P = Breaking load (kg)

L = Span length (mm)

W = Width (mm)

D = Thickness (mm)

The average value was obtained for each set of preparation using tests on six specimens.

II.4.2   Fracture Toughness

Three point bending fracture toughness (K_{IC}) was measured according to the single edge-notch bend (SENB) method described by Larson et al. [76]. In this method a 0.15 mm width notch was cut at the middle of the as sintered sample by means of a Buehler, Isomet (USA) low speed diamond cutter. The tests were performed in an Instron machine with a cross head speed of 0.05 mm/min. The formula [76] used for the calculation was:

$$K_{IC} = \frac{3PLC^{1/2}}{2WD^2}\left[A_o + A_1\left(\frac{C}{D}\right) + A_2\left(\frac{C}{D}\right)^2 + A_3\left(\frac{C}{D}\right)^3 + A_4\left(\frac{C}{D}\right)^4\right]$$
$$\times (1000)^{-1/2}, \text{ MPa.m}^{1/2}$$

where

P   =   Breaking load (N)

L   =   Span length (mm)

D   =   Thickness (mm)

W   =   Width (mm)

C   =   Notch length (mm), generally $C \simeq D/2$

A_o =   1.90 + 0.0075 (L/D)

A_1 =   -3.39 + 0.0800 (L/D)

A_2 =   15.40 - 0.2175 (L/D)

A_3 =   -26.24 + 0.2815 (L/D)

A_4 =   26.38 - 0.1450 (L/D)

Three test samples were broken for each set for the averaging purposes.

II.5 MICROSTRUCTURAL STUDIES

Microstructural studies were accomplished using JEOL 840A scanning electron microscope. The three main aspects namely (i) the microstructure, (ii) EDX dot mapping of Zirconium and (iii) fractography, as discussed below, were mainly covered.

II.5.1   Microstructure

For microstructural studies the sintered samples were polished with SiC powders of 200, 400, 800 mesh size respectively. Later on they were polished with 7 μm and 1 μm diamond pastes respectively followed by etching in 10% HF solution. The samples were vacuum coated with silver film to make the surface electron beam conductive. The secondary electron image at 15 kV operating voltage was used for studies. These microstructural studies were conducted for the samples sintered only at 1650°C.

II.5.2   EDX Dot Mappings of Zirconium

The EDX dot mappings of zirconium for MP-20 and MP-40 mullite based composites, sintered at 1650°C were carried out to see the distribution of ZrO_2 in the matrix. The samples were prepared in the same way as described in section II.5.1. Point analyses of different oxides present in the composites at selected points were also carried out at 15 kV beam voltage.

II.5.3   Fractography

The fractured samples from TRS studies were used for SEM fractography after vacuum coating the fractured surface with silver. The secondary electron image mode was used at 15 kV electron beam voltage.

II.6 X-RAY DIFFRACTION ANALYSIS

X-ray diffractometry was used for calculating the fractional tetragonal and monoclinic zirconia present in the as sintered samples. The intensity of ($11\bar{1}$) monoclinic ZrO_2 and (111) tetragonal ZrO_2 peaks were used for the calculation. Rich. Seifert and Co. (Germany), Model III diffractometer was used at a scanning rate of $1.2°/min$ (2θ) and time constant of 10 seconds with CuK_α radiation.

II.7 MEASUREMENT OF DIELECTRIC CONSTANT

Dielectric constant (k') values were measured in Hewlett Packard 4194A Impedance/Gain-Phase Analyser, using polished and silver coated rectangular specimens at 1 MHz frequency. The formula used for the calculation is given below.

$$k' = 1 + \frac{C_p - C_o}{\varepsilon_o A} \times t$$

where

C_p = Capacitance of specimen (F)

C_o = Capacitance of air (F)

t = Thickness (m)

A = Area (m^2)

ε_o = Permittivity of free space (8.85×10^{-12}, F/m)

II.8 MEASUREMENT OF THERMAL SHOCK RESISTANCE

Thermal shock resistance was measured according to the method described by Tomono et al. [77]. In this method rectangular polished specimens, measuring 10 mm x 7 mm x 2 mm (all sides polished) were heated in a vertical tubular furnace and quenched in water (Fig. 2.1). Later on they were observed in an optical microscope at 100 X to identify the crack, if any. The

temperature difference ($\Delta T = T_1 - T_2$) was reported as the thermal shock resistance of the composites, where

T_1 = Maximum temperature (K) at which there was no crack in the sample after quenching.

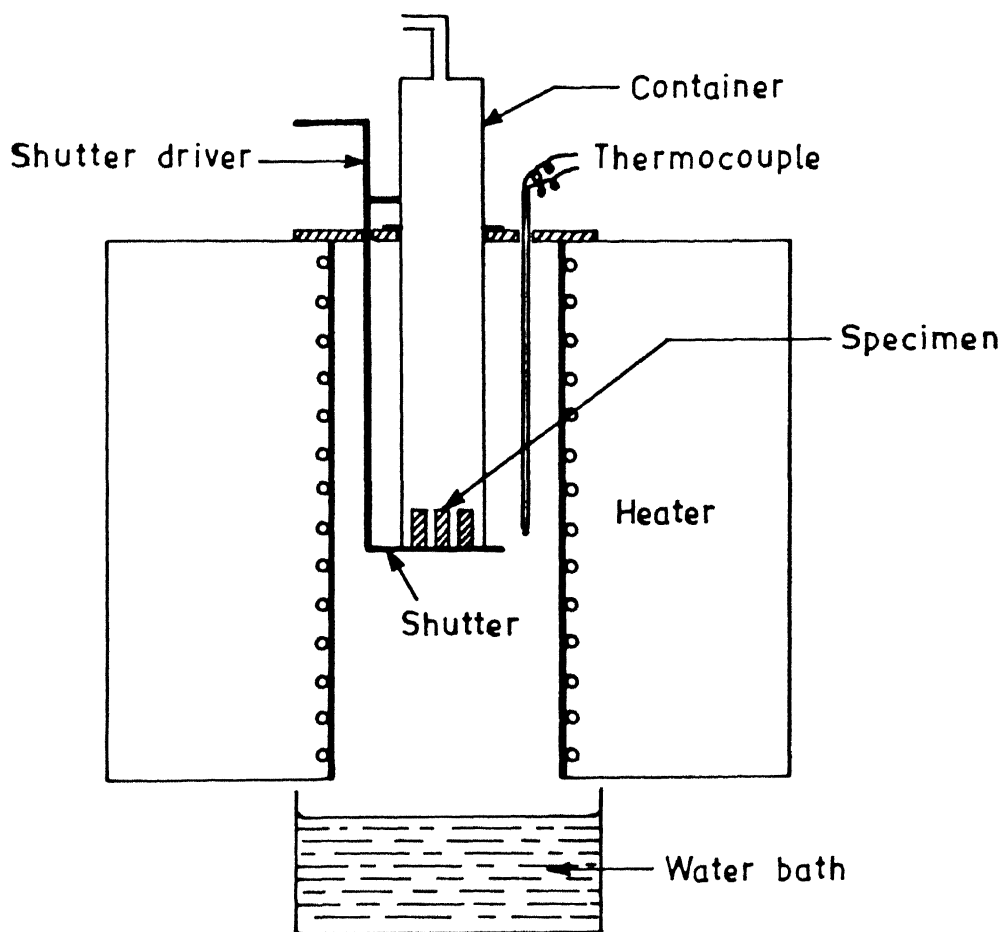T_2 = Quenching temperature (K) of water.

Fig.2.1 Set up for thermal shock resistance measurement.

CHAPTER III
RESULTS

III.1   SINTERED PROPERTIES OF MULLITES

The properties of different types of mullites are enumerated in Table   3.1.   From the table it is clear that sintered porosities of MC mullite remain same at either sintering temperature ie. 1650 or 1700°C. This value (26%) is highest among all the mullites. Sintered porosities of both MP-20 and MP-40 mullite decrease with increase in sintering temperature.   In absolute value lowest sintered porosity (5%) is observed for MP-40 based mullite sintered at 1700°C.

TRS values of all the mullites increase with increase in sintering temperature. The MP-20 mullite gives highest TRS values after sintering either at 1650°C or 1700°C. The lowest TRS value is observed for MP-40 mullite sintered at 1650°C.

Fracture toughness (K_{IC}) values of all the mullites increase with increase in the sintering temperature with the exception for MP-20   mullite   where K_{IC} remains   same   at   either   sintering temperature.   Like TRS values K_{IC} values are also highest for MP-20 mullite sintered, at 1650°C or 1700°C.   Lowest K_{IC} was observed for MP-40 based mullite sintered at 1650°C.

Microstructure of MC mullite shows elongated mullite grains with almost homogeneously distributed pores (Fig. 3.1). The grain size of this mullite is largest among all the types studied. Unlike MC mullite, MP-20 and MP-40 mullites show equiaxed mullite grains with homogeneously distributed pores.

Table 3.1 : Properties of Different Types of Mullites

Powder Type → Properties ↓	Electrofused Mullite (MC) Sintering Temp. ($^{\circ}$C)		Sol-gel Mullite (MP – 20) Sintering Temp. ($^{\circ}$C)			Sol-gel Mullite (MP – 40) Sintering Temp. ($^{\circ}$C)	
	1650	1700	1600	1650	1700	1650	1700
Sintered density (g/cm^3)	2.26	2.26	2.48	2.98	3.01	2.92	3.04
Sintered porosity (%)	26	26	22	7	6	8	5
TRS (MPa)	61±8	76±14	56±17	121±24	144±46	53±22	88±41
K_{IC} (MPa.m$^{1/2}$)	1.4±0	1.5±0.07	–	3	3±0.02	1.1±0.2	3.0±0.4
Grain size of mullite (μm)	4±2	6±2	1.1±.6	1.5±.8	1.5±.8	1.2±.5	1.9±.8
Dielectric constant	5.91	5.93	–	7.18	7.53	7.68	7.79
Thermal shock resistance, ΔT (K)	1050	1075	–	1000	1050	1025	1075

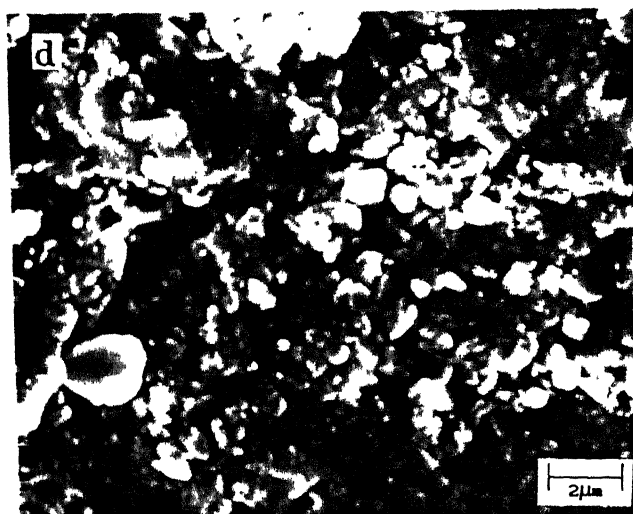Fig.3.1 Microstructures of Different Sintered Mullites

a.   MC (Sint. Temp. 1650°C)
b.   MP-20 (Sint. Temp. 1600°C)
c.   MP-20 (Sint. Temp. 1650°C)
d.   MP-40 (Sint. Temp. 1650°C)

Fractographic analyses of all the mullites show intergranular fracture (Fig. 3.2 and 3.3). Distribution of pores is also uniform for all the mullites. Grain size of all the mullites increases with increase in sintering temperature (Table 3.1) with the exception for MP-20 mullite where the grain size remains almost same after $1650^{\circ}C$ or $1700^{\circ}C$ sinterings. In absolute value the grain size is largest for MC mullite, which is elongated in nature, while smallest for MP-20 mullite, which is equiaxed in nature.

Dielectric constant (k') value increases with increase in sintering temperatures for all the mullites. However, k' values are almost same for MC mullite. Highest k' values are observed for MP-20 mullite and lowest for MC mullite.

Thermal shock resistance (ΔT) for all the mullites increases with increase in sintering temperature. Lowest value of ΔT is observed for MP-20 mullite sintered at $1650^{\circ}C$.

III.2 SINTERED PROPERTIES OF MULLITE - 25 VOL% ZrO_2 COMPOSITES PREPARED THROUGH DIFFERENT ROUTES

The properties of mullite - 25 vol% ZrO_2 composites prepared through different routes are given in Table 3.2. From the results it is clear that sintered porosities of MC based composites are highest among all the composites and it remains same at either sintering temperature. Sintered porosity of MP-20 based composites decreases from 8 to 7% with increase in sintering temperature from $1650^{\circ}C$ to $1700^{\circ}C$. RSMZ composites give 21% sintered porosity (at $1650^{\circ}C$) which decreases to 8% with increase in sintering temperature.
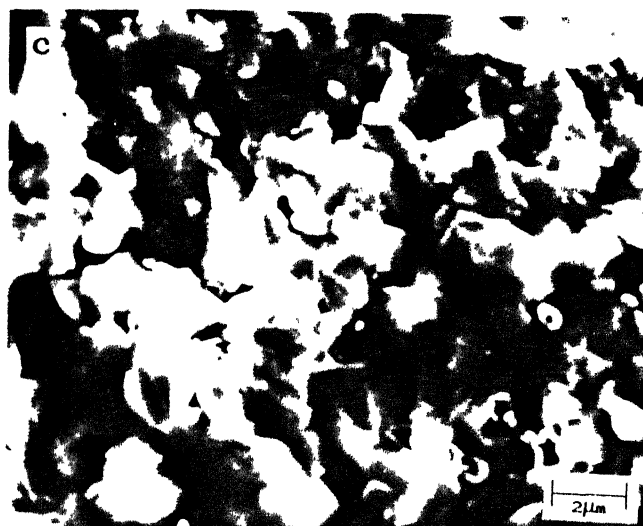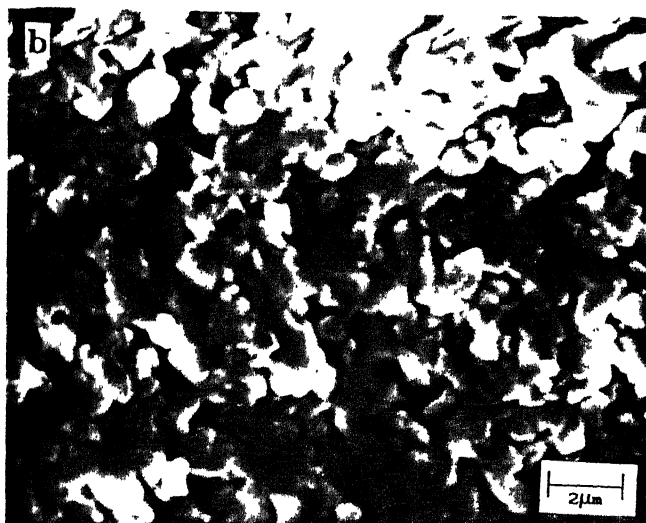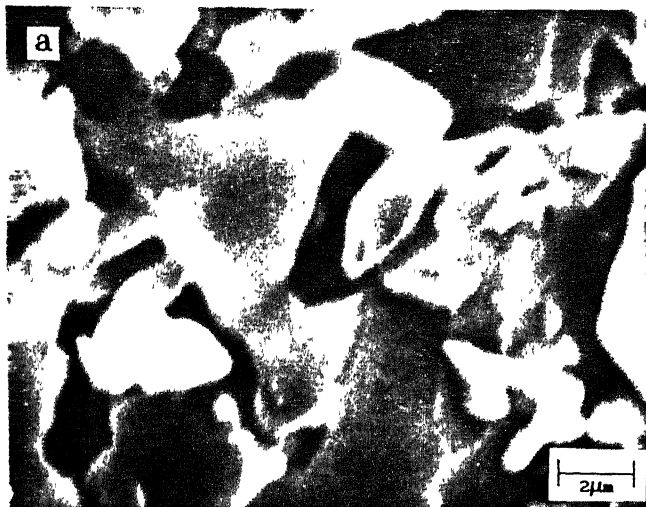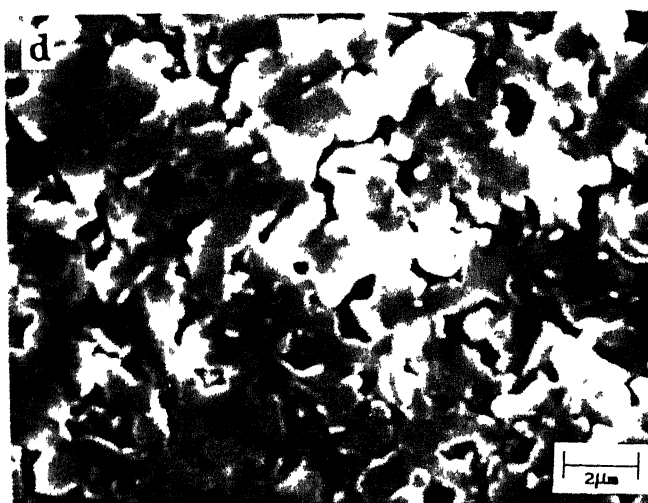
Fig.3.2 SEM Fractographs of Different Sintered Mullites

    a.   MC (Sint. Temp. 1650°C)
    b.   MP-20 (Sint. Temp. 1600°C)
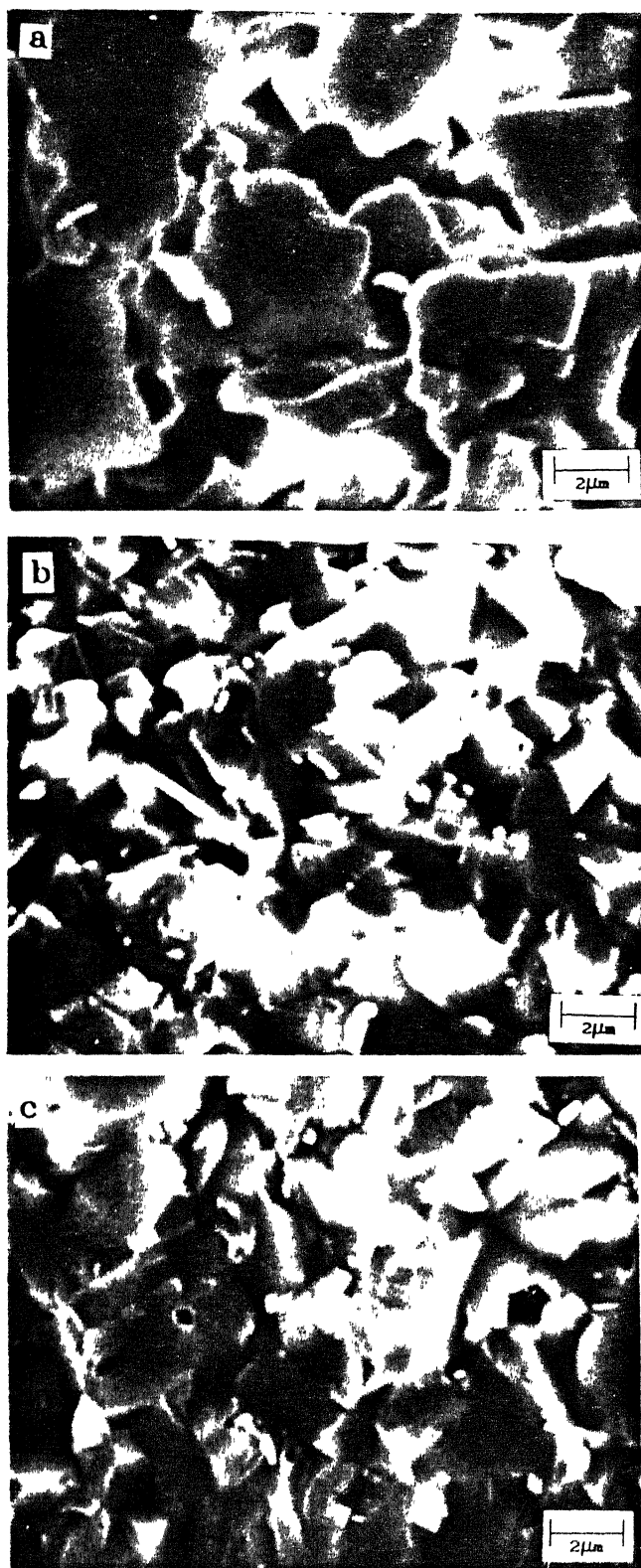   c.   MP-20 (Sint. Temp. 1650°C)
    d.   MP-40 (Sint. Temp. 1650°C)

Fig. 3.3 SEM Fractographs of Different Types of Mullite, Sintered at 1700°C

Table 3.2 : Properties of Mullite - 25 vol% ZrO_2 Composites

Powder Type → Properties ↓	Electrofused Mullite Powder (MC) Sintering Temp. (°C)		Sol-gel Mullite Powder (MP - 20) Sintering Temp. (°C)			Reaction Sintered Composites (RSMZ) Sintering Temp. (°C)	
	1650	1700	1600	1650	1700	1650	1700
Sintered density (g/cm^3)	2.75	2.75	2.98	3.53	3.55	2.95	3.45
Sintered porosity (%)	21	21	22	8	7	21	8
TRS (MPa)	93±15	105±6	94±28	118±44	79±17	81±13	86±8
K_{IC} (MPa m$^{1/2}$)	1.73±.02	2.73±0.11	–	2.37±.5	2.9±0.13	2.52±0.05	2.84±.17
Grain size of mullite (μm)	4±3	4±1	1.2±.4	1.8±.06	1.5±.5	3±1	3±2
Particle size of ZrO_2 (μm)	1.0±.4	1.6±.5	0.84±.3	1.6±0.4	–	1.5±.9	1.9±.8
Fractional tetragonal ZrO_2 (f_t)	0.11	0.09	–	0.11	0.03	0.10	0.04
Dielecctric constant	7.69	7.91	–	10.03	10.70	7.03	7.75
Thermal shock resistance, ΔT (K)	1050	1175	–	1025	1175	1075	1100

TRS values for MC based and RSMZ composites increase with increase in sintering temperature, whereas, it is reverse for MP-20 based composites. However, in absolute magnitude MP-20 based sintered composite gives highest TRS values after 1650°C sintering.

K_{IC} of all the composites increases with the increase in sintering temperature. Among all the grades investigated, K_{IC} is highest for MP-20 based sintered composites.

Microstructure of MC based composites, sintered at 1650°C reveals a homogeneous distribution of rounded ZrO_2 particles in the matrix of elongated shaped mullite (Fig. 3.4). Like MC based composites MP-20 based composites also show homogeneous distribution of ZrO_2 particles throughout the matrix. However, in this case the mullite grains are equiaxed in nature. The EDX dot mappings of zirconium (Fig. 3.5) for MP-20 based composites also confirm a homogeneous distribution of ZrO_2 throughout the mullite matrix.

From the fractographic analysis (Fig. 3.6 and 3.7) it is clear that MC based composites give rise to rather elongated mullite grains with intergranular fracture. The distribution of both ZrO_2 particles and pores are uniform throughout the matrix. After sintering at high temperature the microstructures become more homogeneous with the reduction of average mullite grain aspect ratio from 2.5 to 1.6. MP-20 based composites exhibit equiaxed mullite grains with homogeneously distributed ZrO_2 particles. The fracture mode is intergranular in nature. Grain size of mullite for MP-20 based composites decreases from 1.8 to
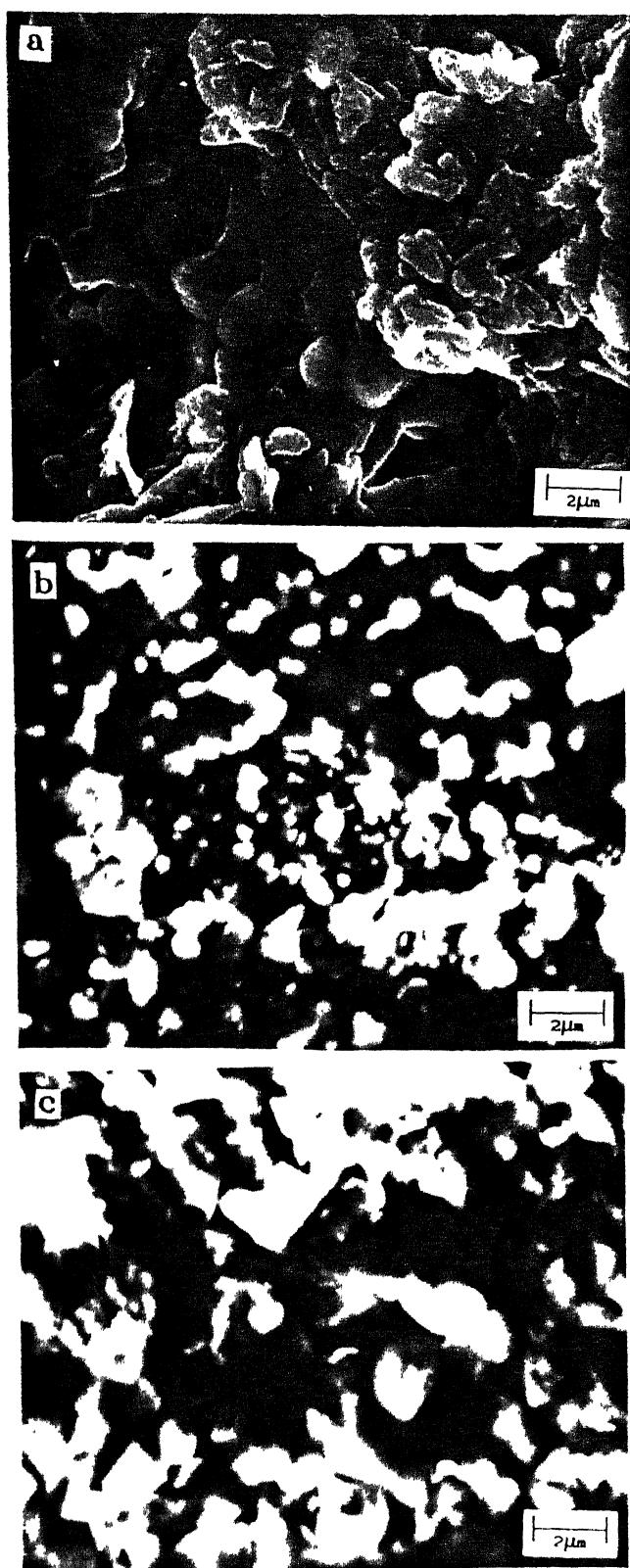
Fig.3.4 Microstructures of Sintered Mullite-25 vol% ZrO_2
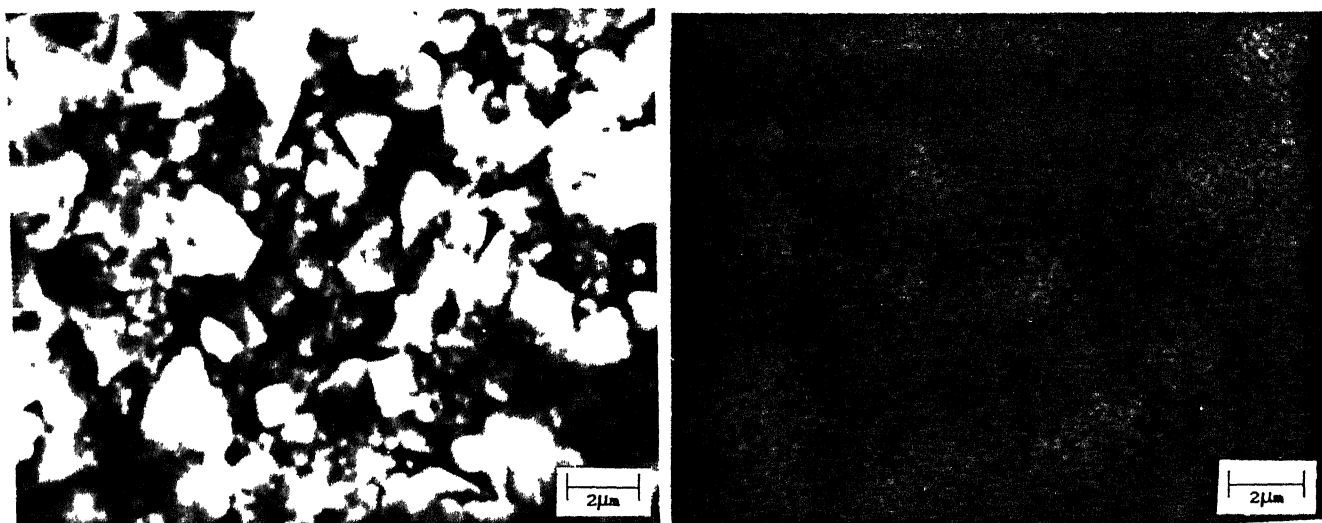Composites

a.   MC (Sint. Temp. 1650°C)
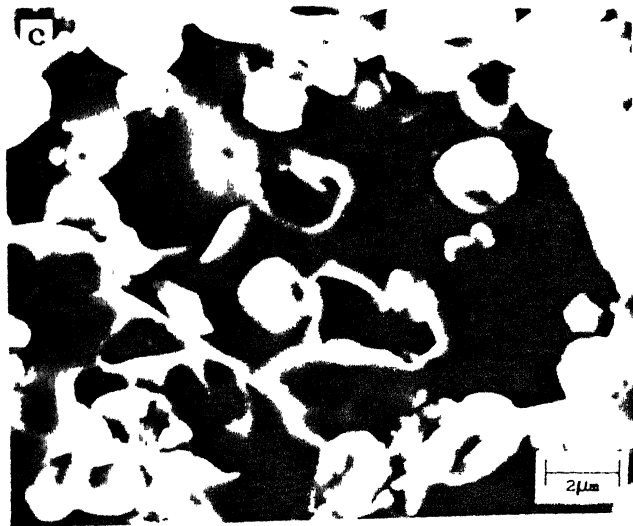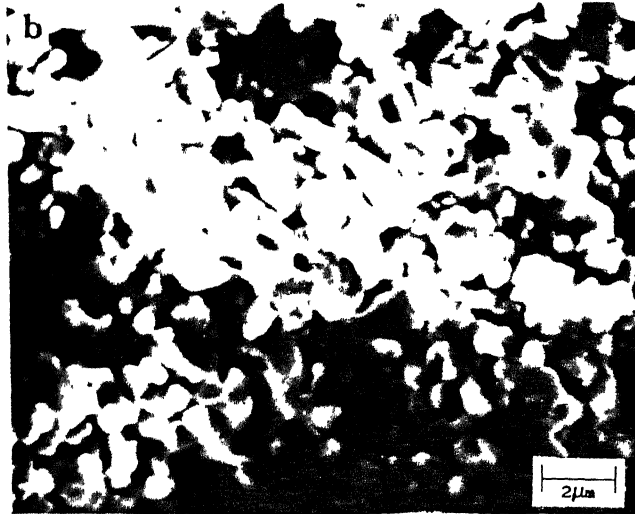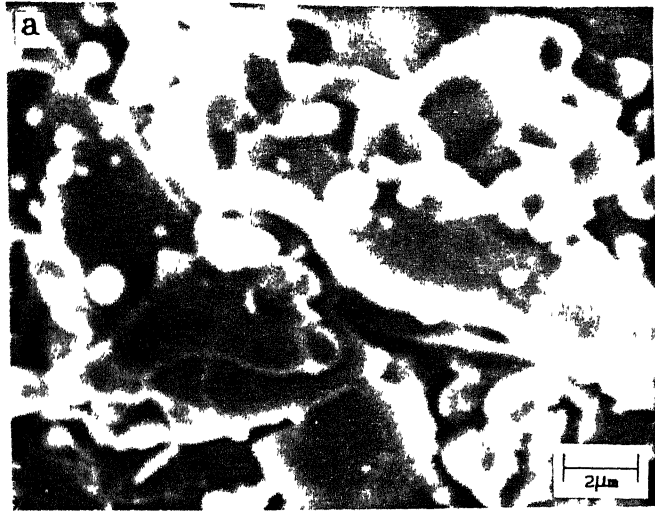
Fig.3.5 EDX Dot Mappings of Zirconium in MP-20 based
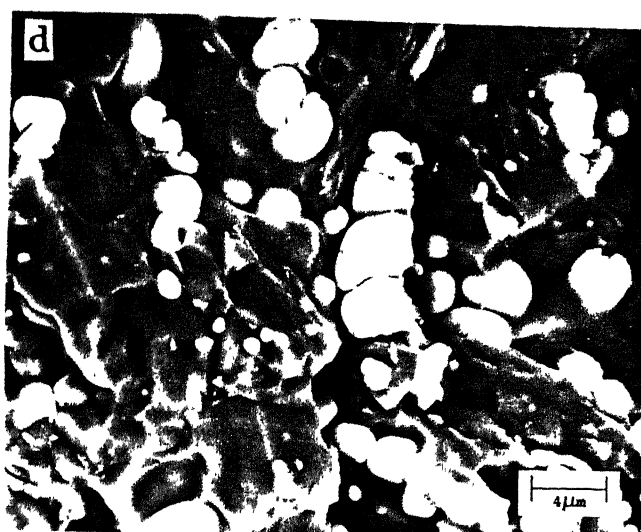   Mullite-25 vol% ZrO_2 Composites, Sintered at
        1650°C.

Fig.3.6 SEM Fractographs of Sintered Mullite-25vol% ZrO_2
Composites

    a.   MC (Sint. Temp. 1650°C)
    b.   MP-20 (Sint. Temp. 1600°C)
    c.   MP-20 (Sint. Temp. 1650°C)
    d.   RSMZ (Sint. Temp. 1650°C)

Fig.3.7 SEM Fractographs of Mullite-25 vol% ZrO_2 Composites, Sintered at 1700°C

(a) MC. (b) MP-20 (c) RSMZ

1.5 μm with increase in the sintering temperature from 1650°C to 1700°C. However, the grain shape remains equiaxed in nature. In RSMZ composites a wide distribution of ZrO_2 particles in equiaxed mullite grains (Fig. 3.6 and 3.7) is observed in case of 1650°C sintered samples. On the other hand in case of sintering at a still higher temperature viz. 1700°C the size of ZrO_2 particles increases from 1.5 to 1.9 μm. Average mullite grain size remains same at either sintering temperature. Fractographs (Fig. 3.6 and 3.7) reveal that reaction sintering gives rise to rather coarser ZrO_2 particles than other three types of preparation routes. In reaction sintered composites along with intergranular fracture mode, some of the ZrO_2 particles particularly bigger ones appear to be fractured ones.

X-ray diffraction analysis shows (Table 3.2) that fractional tetragonal ZrO_2 decreases with increase in the sintering temperature for all the composites prepared through different routes.

Dielectric constant values increase with the increase in the sintering temperature for any type of composite. However, MP-20 based composites show highest values among all types of composites.

Thermal shock resistance increases with the increase in sintering temperature for all the composites.

III.3 FUSED MULLITE-38 VOL% ZrO_2 PREALLOYED POWDER BASED COMPOSITES (MZ)

From the results (Table 3.3) it is clear that the sintered porosity of this type (MZ) of composites is maximum among all the

Table 3.3 : Properties of Fused Mullite - 38 vol% ZrO_2 Prealloyed Composites

Properties	Sintering Temp. ($^\circ$C)	
	1650	1700
Sintered density (g/cm^3)	2.74	2.82
Sintered porosity (%)	34	32
TRS (MPa)	39±2	42±2
K_{IC} (MPa.m$^{1/2}$)	1.45±0.08	1.76±0.17
Grain size of mullite (μm)	6±4	6±3
Particle size of ZrO_2 (μm)	1.6±0.7	3±1
Fractional tetragonal ZrO_2 (f_t)	0.05	0.08
Dielectric constant	6.81	7.03
Thermal shock resistance, ΔT (K)	1075	1100

composites studied in the present investigation. It is about 4 times higher than sol-gel mullite (MP-20) based composites. The sintered porosity of MZ composites decreases from 34% to 32% with the increase in sintering temperature from 1650°C to 1700°C.

TRS value is also lowest among all the composites. It is 39 MPa after 1650°C sintering and increases to 42 MPa after 1700°C sintering.

K_{IC} increases from 1.45 to 1.76 MPa.m$^{1/2}$ with the increase in sintering temperature from 1650 to 1700°C. These values are slightly lower than those for MC based composites sintered at 1650°C.

Fractographs of the sintered composites (Fig. 3.8) show intergranular fracture with rounded ZrO_2 particles distributed homogeneously throughout the large equiaxed mullite matrix. A wide distribution of ZrO_2 particles is observed for the composites sintered at 1650°C. However, after 1700°C sintering ZrO_2 particle distribution becomes more homogeneous. An increase in ZrO_2 particle is observed with increase in sintering temperature. Average mullite grains, however, remain same at either sintering temperature.

X-ray diffraction analysis shows that the fractional tetragonal ZrO_2 unlike other types of composites increases from 0.05 to 0.08 with the increase in sintering temperature.

Similar to other preparation routes, the dielectric constant of MZ composites increases with increase in sintering temperature.

Fig.3.8 SEM Fractographs of Mullite-38 vol% ZrO_2
Prealloyed Composites (MZ)

(a) Sint. Temp. $1650^{\circ}C$
(b) Sint. Temp. $1700^{\circ}C$

Fig.3.8 SEM Fractographs of Mullite-38 vol% ZrO_2 Prealloyed Composites (MZ)

(a) Sint. Temp. 1650°C
(b) Sint. Temp. 1700°C

Thermal shock resistance (ΔT) increases with increase in sintering temperature. In absolute value, ΔT is similar to the values for the composites processed through other routes.

III.4 SINTERED PROPERTIES OF MULLITE -ZrO$_2$ (0-25 VOL% PURE OR MODIFIED) COMPOSITES FROM FUSED OR SOL-GEL BASED POWDERS

In this section sintered properties of fused (MC) and sol-gel (MP-20 and MP-40) based composites are discussed.

III.4.1 Densification Behaviour

Sintered densities of all the composites increase with the increase in vol% additive as evidenced from Fig. 3.9-3.12. Sintered porosity of MC based composites decreases with the increase in vol% additives at either sintering temperature (Fig. 3.13). In absolute value the sintered porosity is lower for 1700°C sintered composites than 1650°C sintered ones. Sinterability increases in the order of ZrO$_2$ → ZrO$_2$-MgO → ZrO$_2$-MgO-Y$_2$O$_3$ addition at either sintering temperature. Unlike MC based composites, MP-20 based composites show an increasing trend of sintered porosity with the increase in vol% additive at either sintering temperature (Fig. 3.14). However, sintered porosity is slightly decreased up to 10 vol% additives at lower sintering temperature (1650°C). On an average the % total porosity is lower for 1700°C sintered composites than 1650°C sintered ones with some scattering in the results. Like MC based composites, sintered porosity for MP-40 based composites decreases with increase in vol% additives, sintered at 1650°C (Fig. 3.15). However, composites sintered at 1700°C shows reverse trend. The scattering
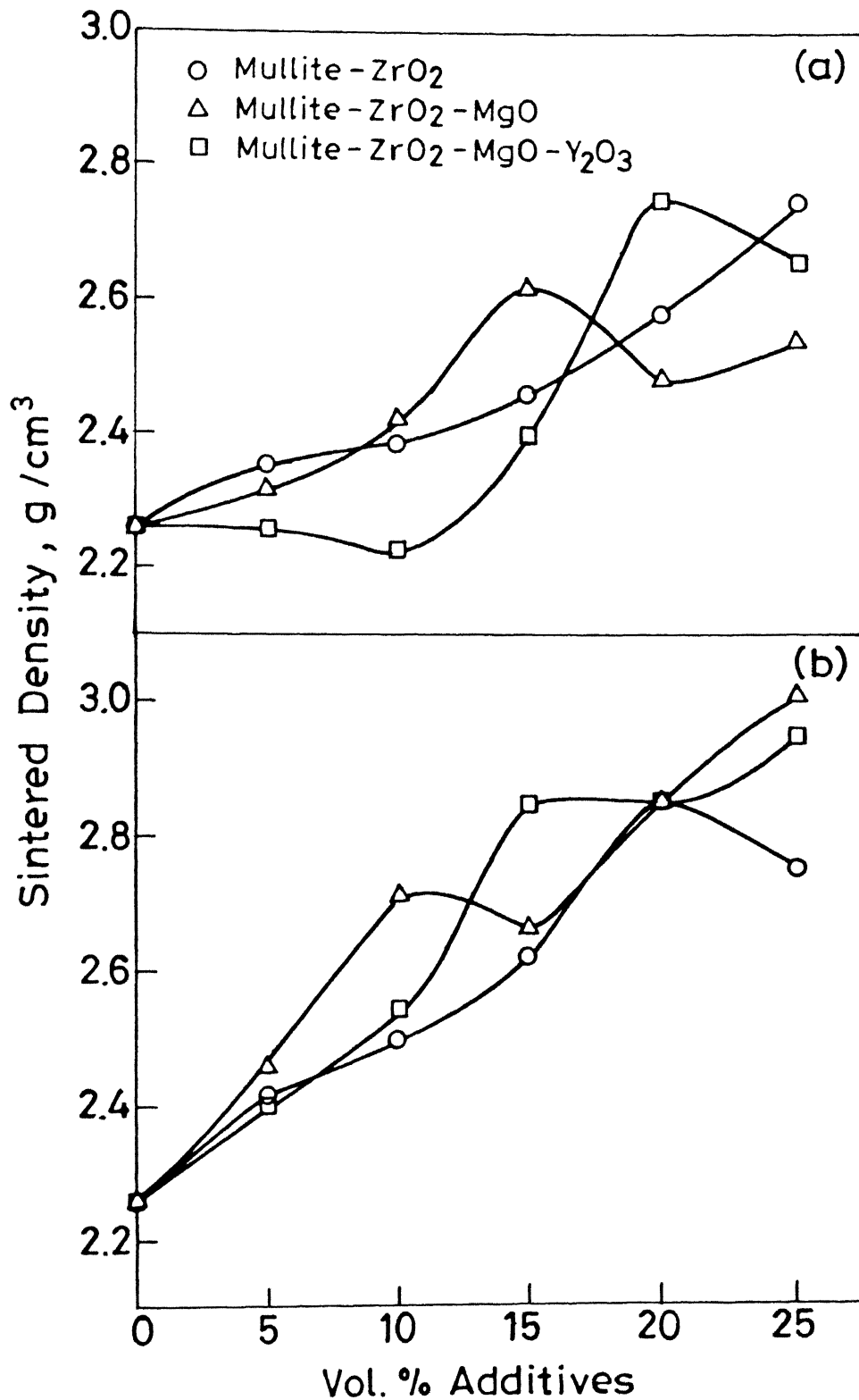
Fig. 3.9 Variation of sintered density of MC mullite based composites (a) sint. temp. 1650°C, (b) sint. temp. 1700°C.
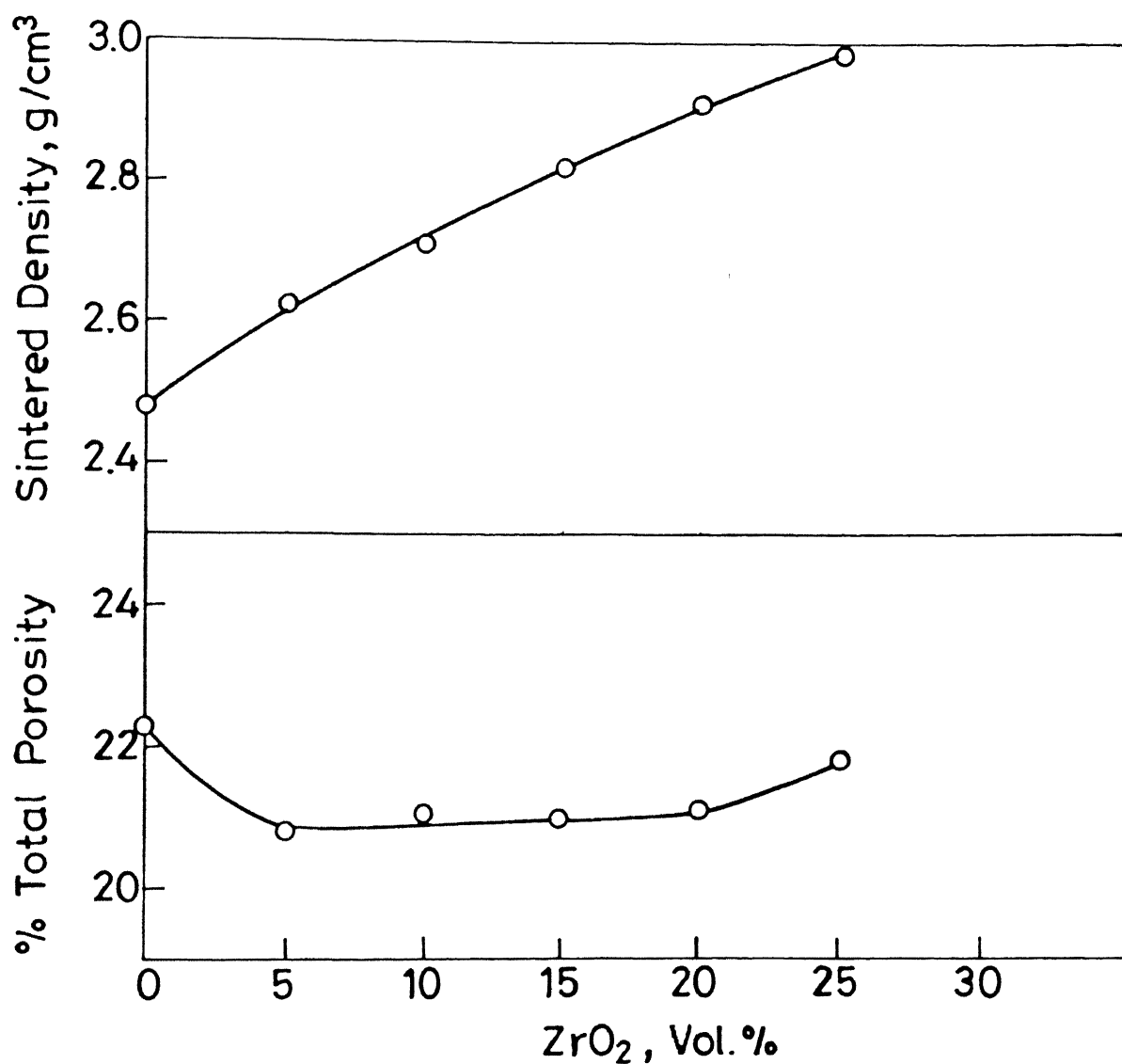
Fig. 3.10 Variation of sintered density and % total porosity of MP-20 based mullite-ZrO₂ composites, sintered at 1600°C.
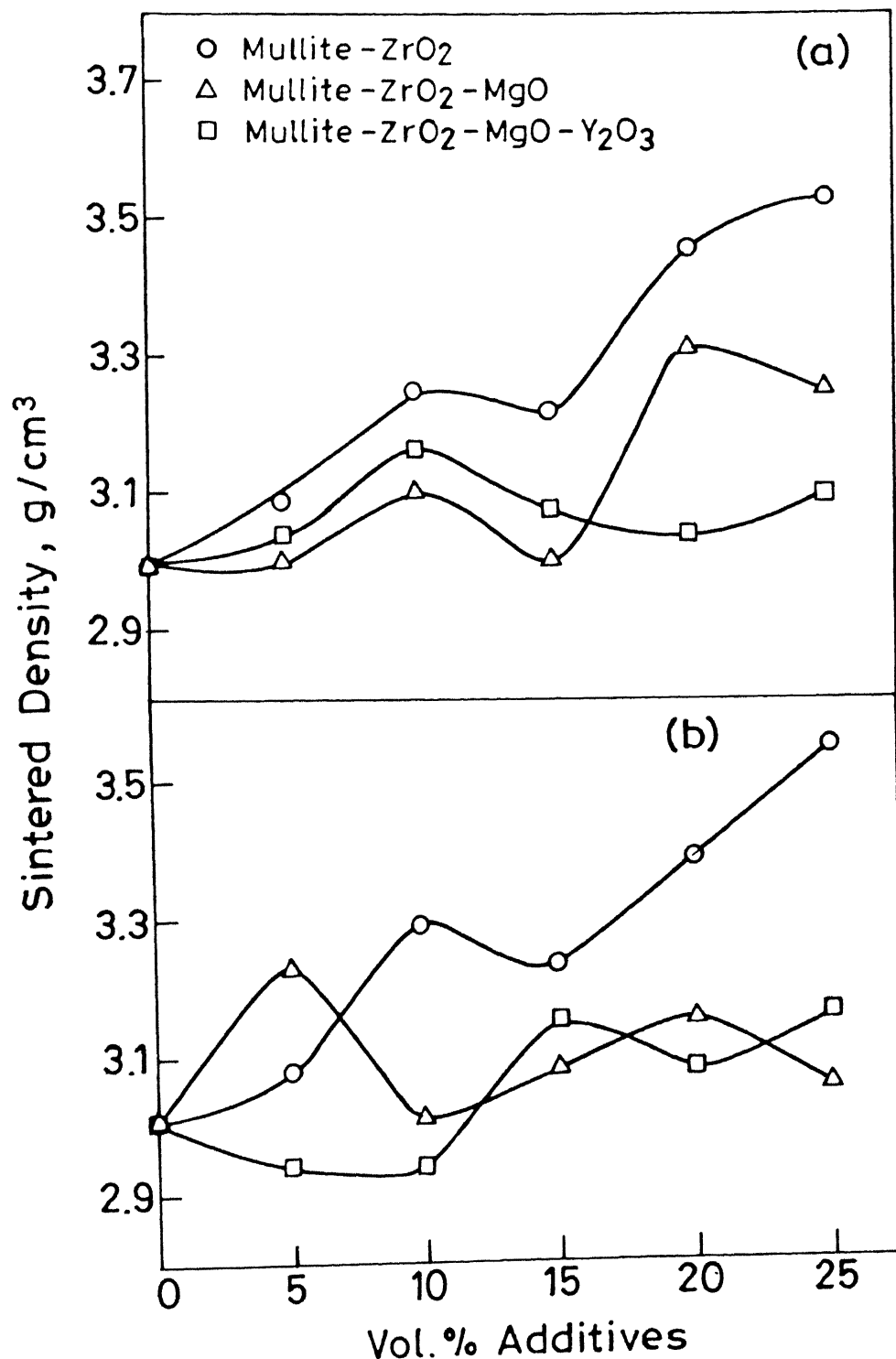
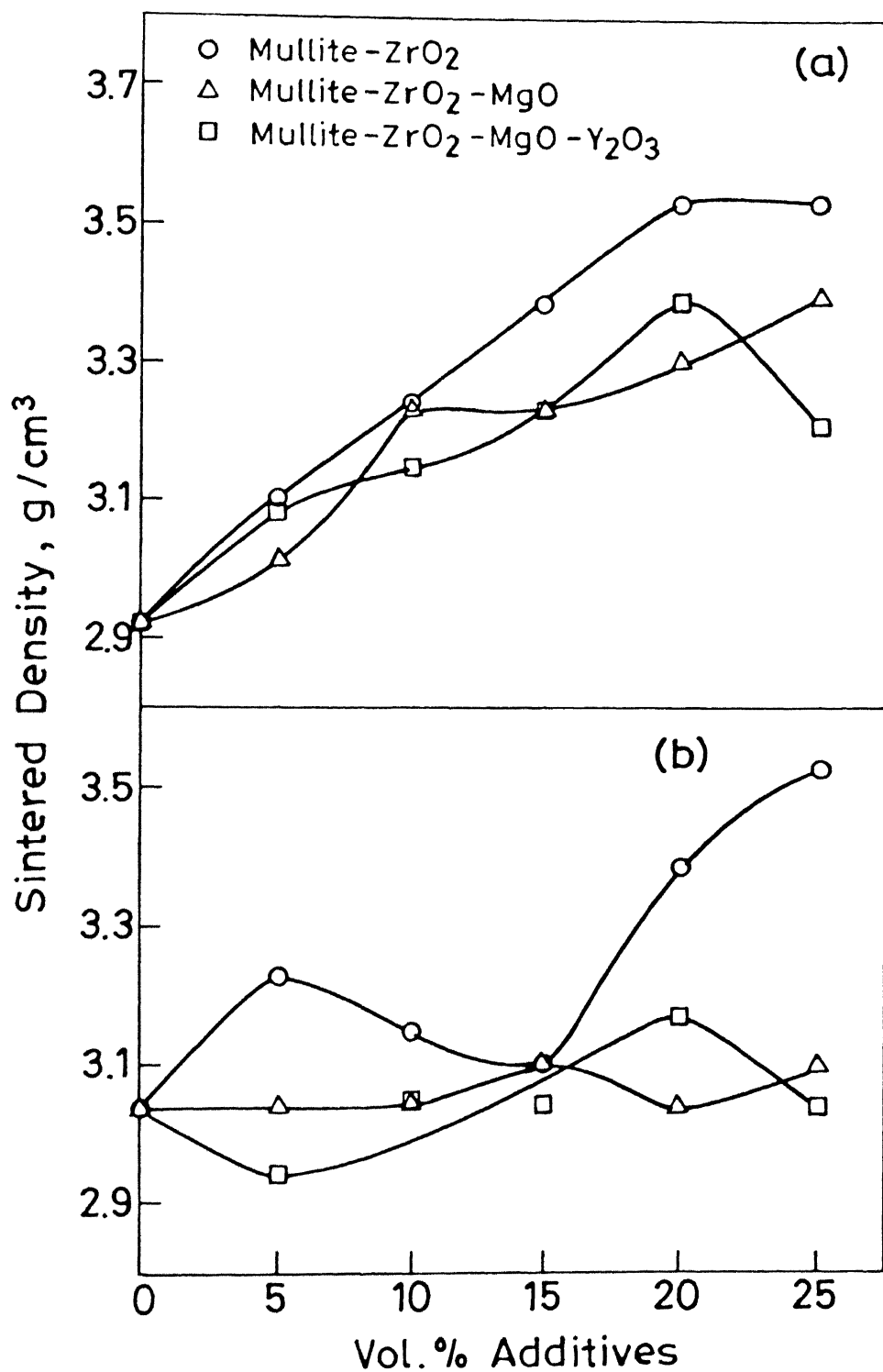Fig. 3.11 Variation of sintered density of MP-20 mullite based composites (a) sint. temp. 1650°C , (b) sint. temp. 1700°C.

Fig. 3.12 Variation of sintered density of MP-40
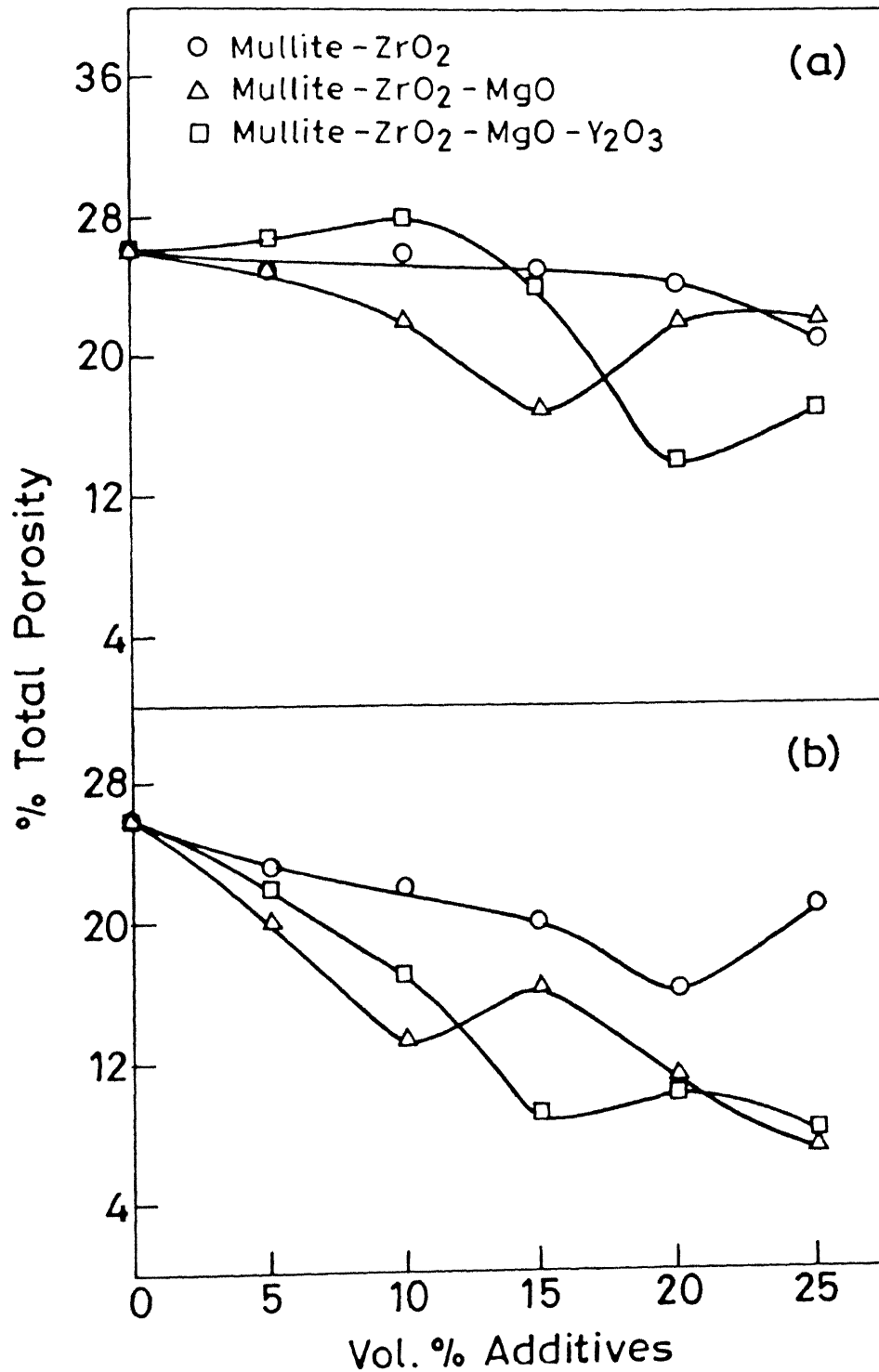mullite based composites (a) sint. temp.

Fig. 3.13 Variation of % total porosity of MC mullite
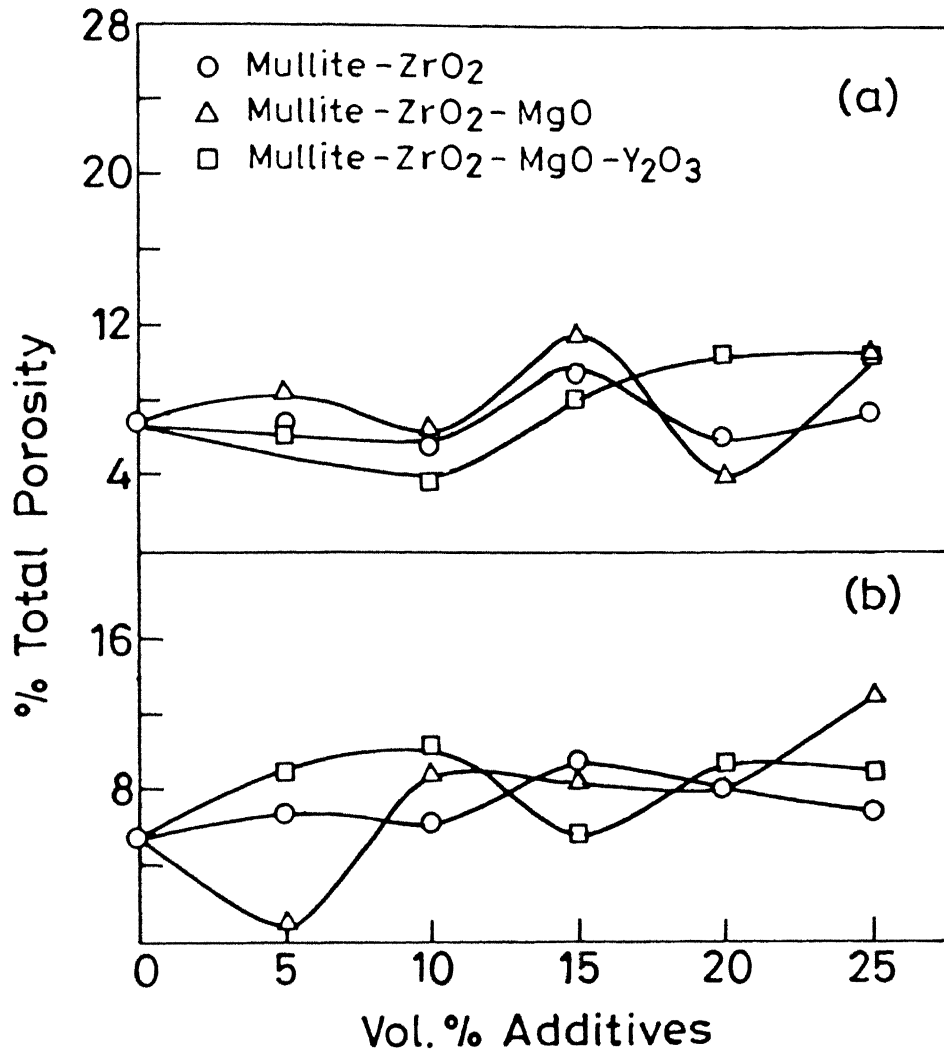based composites (a) sint. temp. 1650°C,

Fig. 3.14 Variation of % total porosity of MP-20 mullite based composites (a) sint. temp. 1650°C, (b) sint. temp. 1700°C.
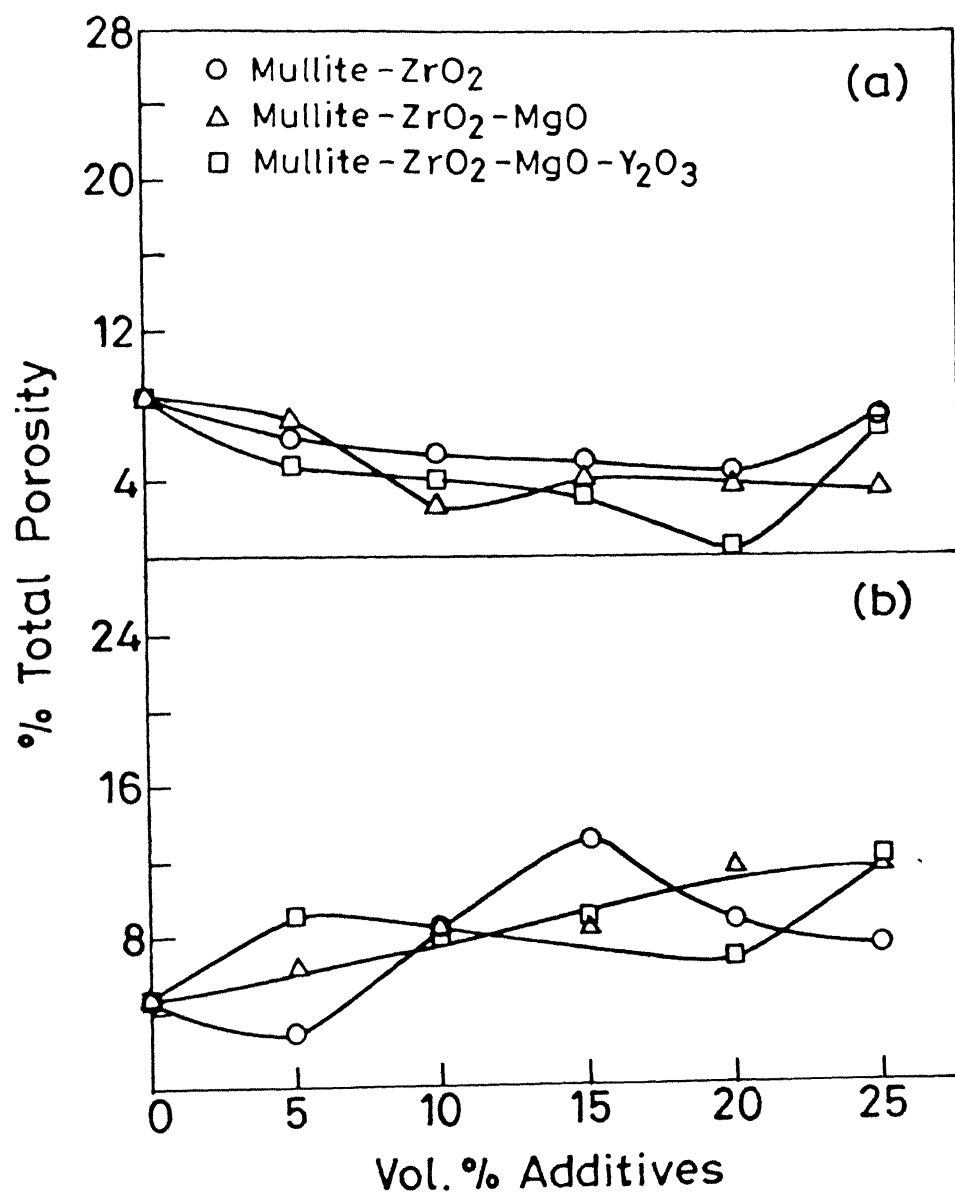
Fig. 3.15 Variation of % total porosity of MP-40 based composites (a) sint. temp. 1650°C, (b) sint. temp. 1700°C.

in the sintered density is ± 0.10 g/cm^3.

III.4.2   Transverse Rupture Strength

TRS values for MC based composites (0-25 vol% ZrO$_2$) marginally increases with the increase in vol% additives at either sintering temperature (Fig. 3.16). In absolute magnitude TRS values after 1700°C sintering is higher than 1650°C sintering ones. Unlike MC based composites, TRS values for MP-20 based composites show a maximum at a particular composition pertaining to individual ZrO$_2$ powders (Fig. 3.17 and 3.18). Decrease in TRS values at higher vol% additives than a critical for composites sintered at 1700°C is more prominent than those sintered at 1650°C. A similar feature as for MP-20 based composites is present for MP-40 based composites also sintered at 1700°C (Fig. 3.19). However, the TRS values for the composites sintered at 1650°C continuously increase with the increase in vol% additives. An additional characteristic feature is observed for MP-40 based composites, sintered at 1650°C, where MgO and MgO-Y$_2$O$_3$ additives are present in ZrO$_2$, show higher values of TRS than the straight ZrO$_2$ containing ones.

In terms of absolute values the MP-20 based sintered composites show highest TRS values, while the MC based ones show lowest values. One more characteristic feature of MP-20 and MP-40 based composites is that the absolute values of TRS are always lower after 1700°C sintering than after 1650°C one. Scattering in the result is $\pm$ 25 MPa.
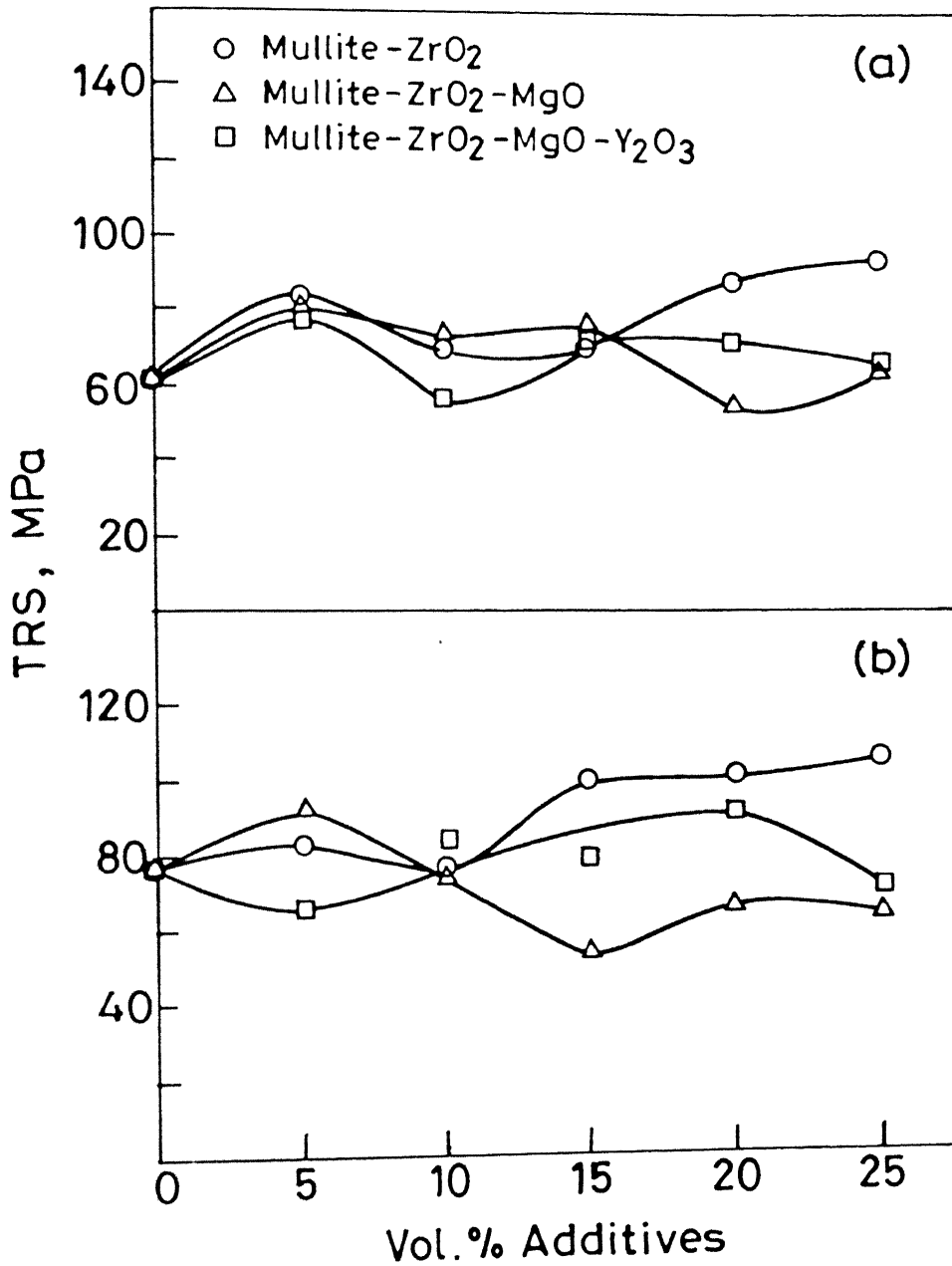
Fig. 3.16 Variation of transverse rupture strength
of MC mullite based composites (a) sint.
temp. 1650°C, (b) sint. temp. 1700°C.
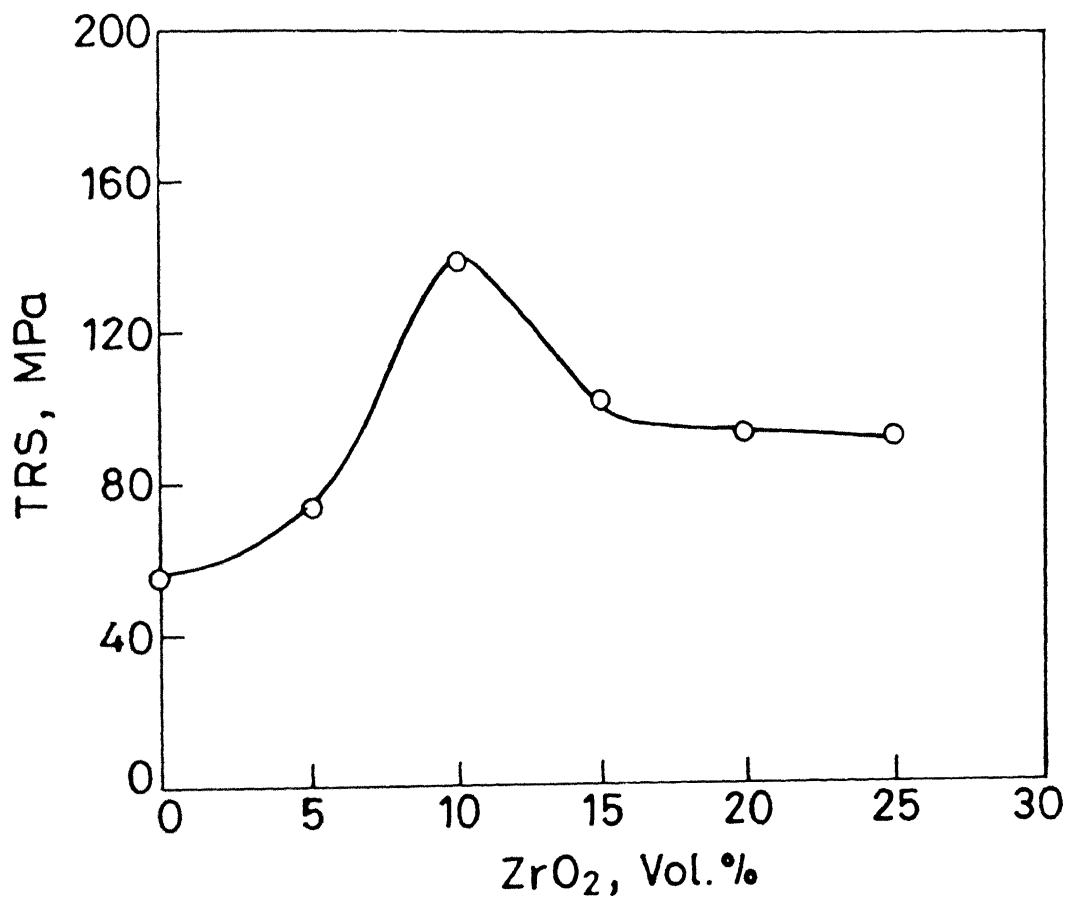
Fig. 3.17 Variation of transverse rupture strength of MP-20 based mullite-ZrO_2 composites sintered at 1600°C.
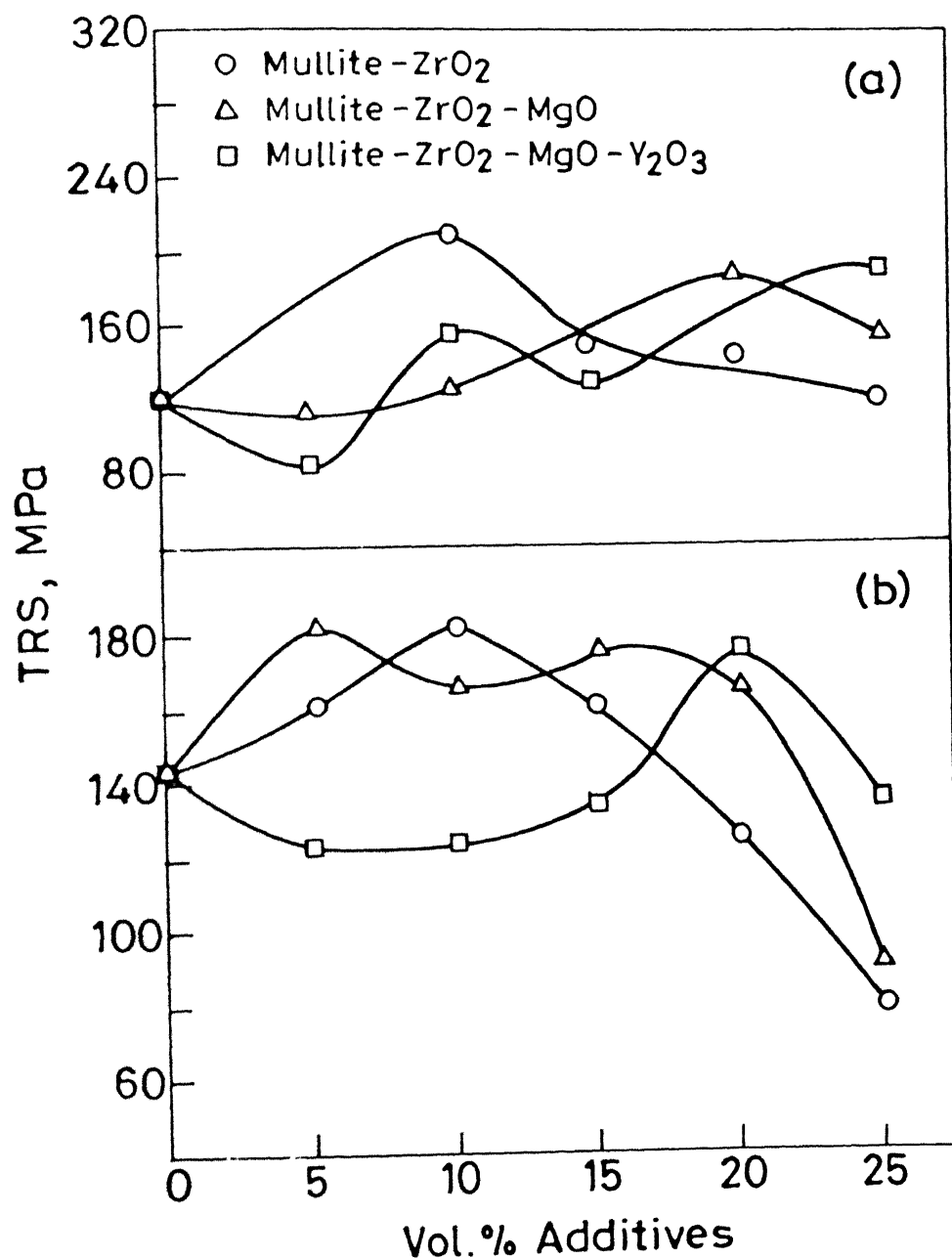
Fig. 3.18 Variation of transverse rupture strength
of MP-20 mullite based composites
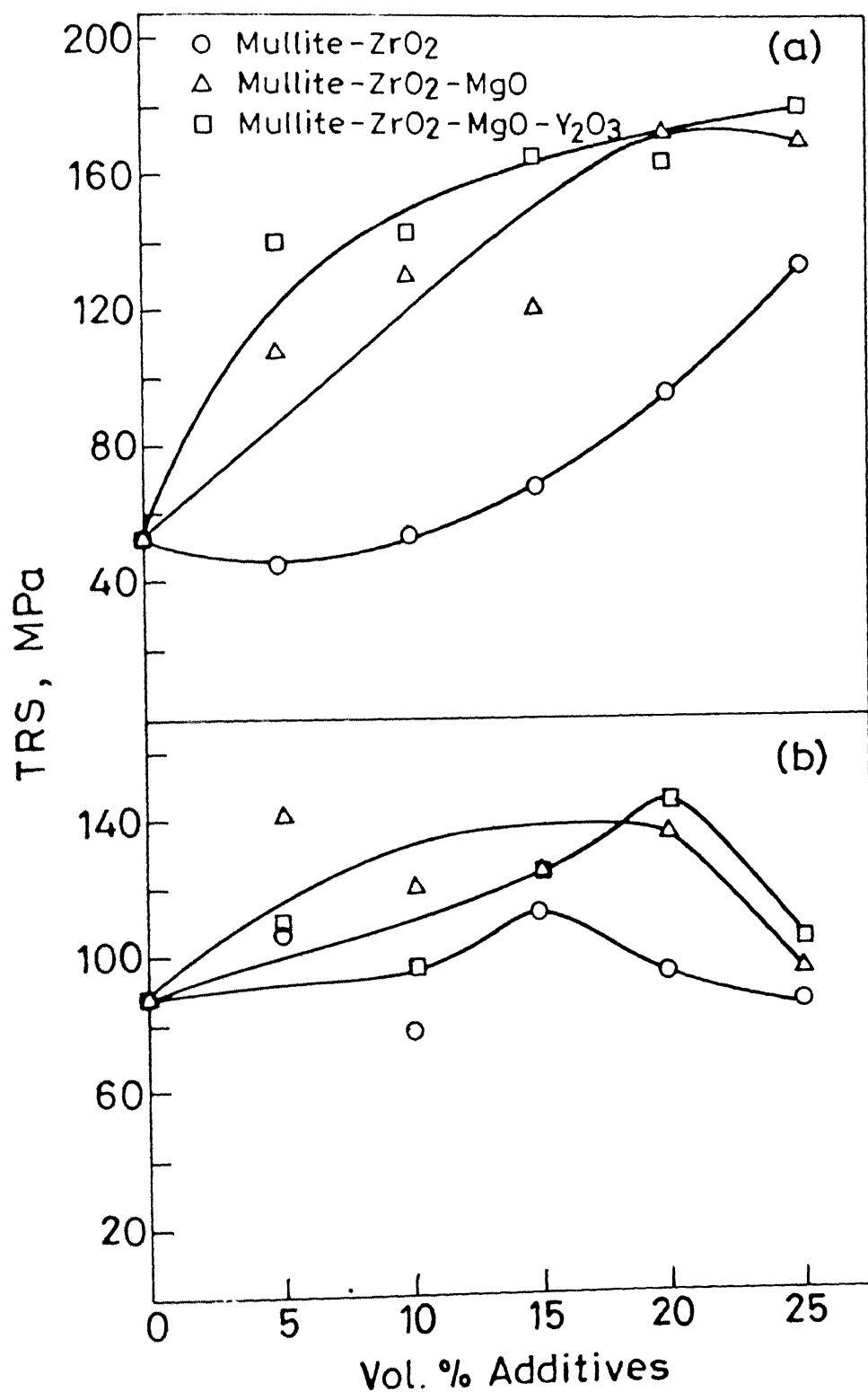(a) sint. temp. 1650°C, (b) sint. temp. 1700°C.

Fig. 3.19 Variation of transverse rupture strength
of MP-40 mullite based composites
(a) sint. temp. 1650°C. (b) sint. temp. 1700°C.

III.4.3   Fracture Toughness

K_{IC} values for all the composites irrespective of the type of mullite powders increase with increase in vol% additive with some variation, which is highest in MP-20 based composites sintered at 1650°C (Fig. 3.20, 3.21 and 3.22). In absolute magnitude all the composites after higher temperature (1700°C) sintering show higher K_{IC} values than 1650°C sintering with the exception for MP-20 based composites where the trend is reverse. The scattering in the K_{IC} values is ± 0.22 MPa.m$^{1/2}$.

III.4.4   Microstructural Studies

From the microstructure of MC based composites sintered at 1650°C it is clear that the rounded ZrO_2 particles are homogeneously distributed throughout the elongated mullite matrix (Fig. 3.23). The microstructure of MP-20 based composites sintered at 1600°C and 1650°C show a homogeneous distribution of ZrO_2 particles throughout the equiaxed mullite grains (Fig. 3.24). A large volume fraction of pores are visible in the microstructures, after 1600°C sintering. Like MP-20 based composites, microstructure of MP-40 based composites, sintered at 1650°C show a homogeneous distribution of ZrO_2 particles throughout the equiaxed mullite matrix (Fig. 3.25).

From the EDX dot mapping of zirconium for MP-20 and MP-40 based composites, sintered at 1650°C a homogeneous distribution of ZrO_2 particles throughout the mullite matrix is also observed (Fig. 3.24 and 3.25). In some of the MP-20 based composites (>10 vol% additives) ZrO_2 agglomerates are visible.

Fig. 3.20 Variation of fracture toughness of MC mullite based composites (a) sint. temp. 1650°C, (b) sint. temp. 1700°C.
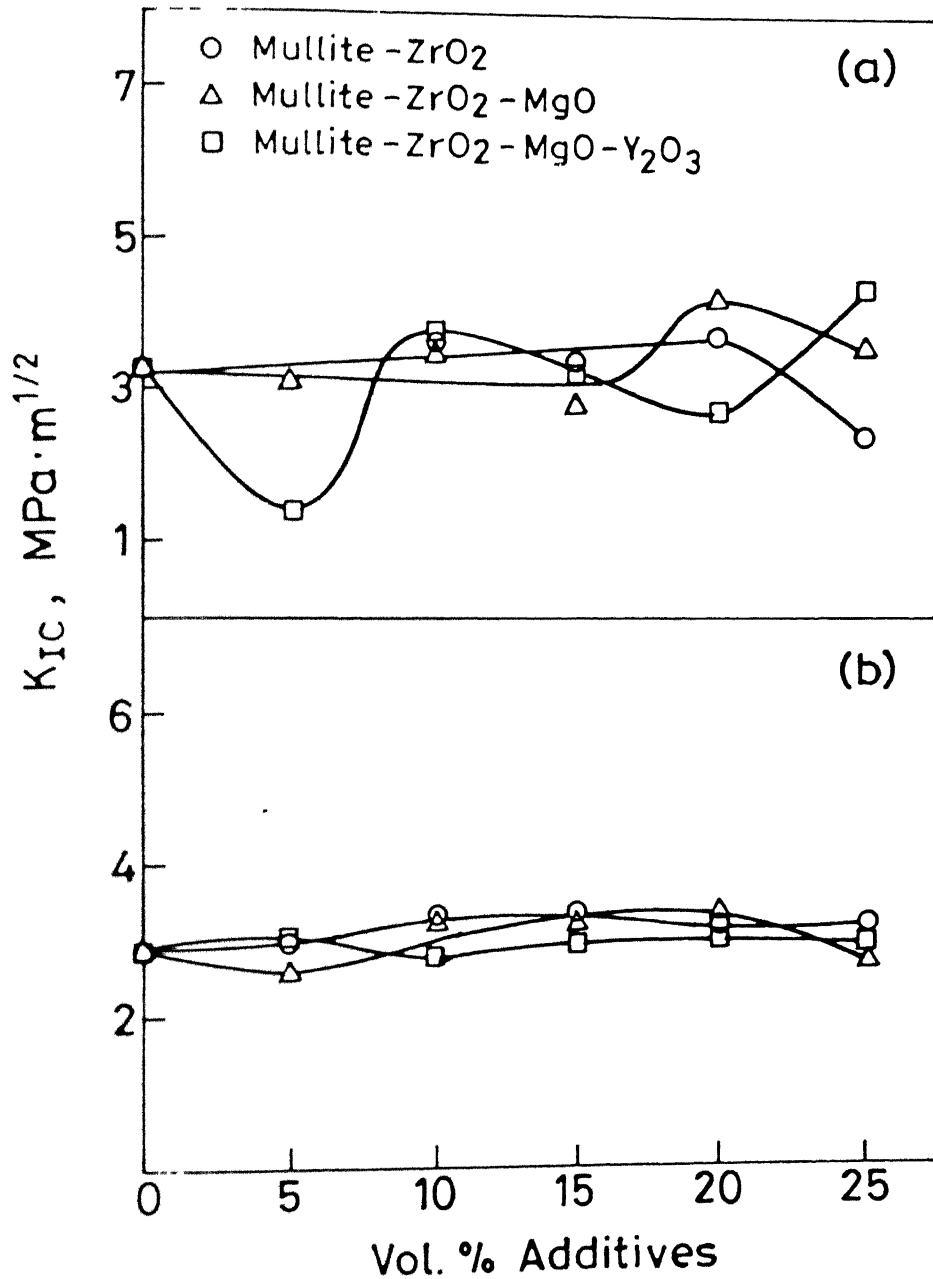
Fig. 3.21 Variation of fracture toughness of MP-20 mullite based composites (a) sint. temp. 1650°C, (b) sint. temp. 1700°C.
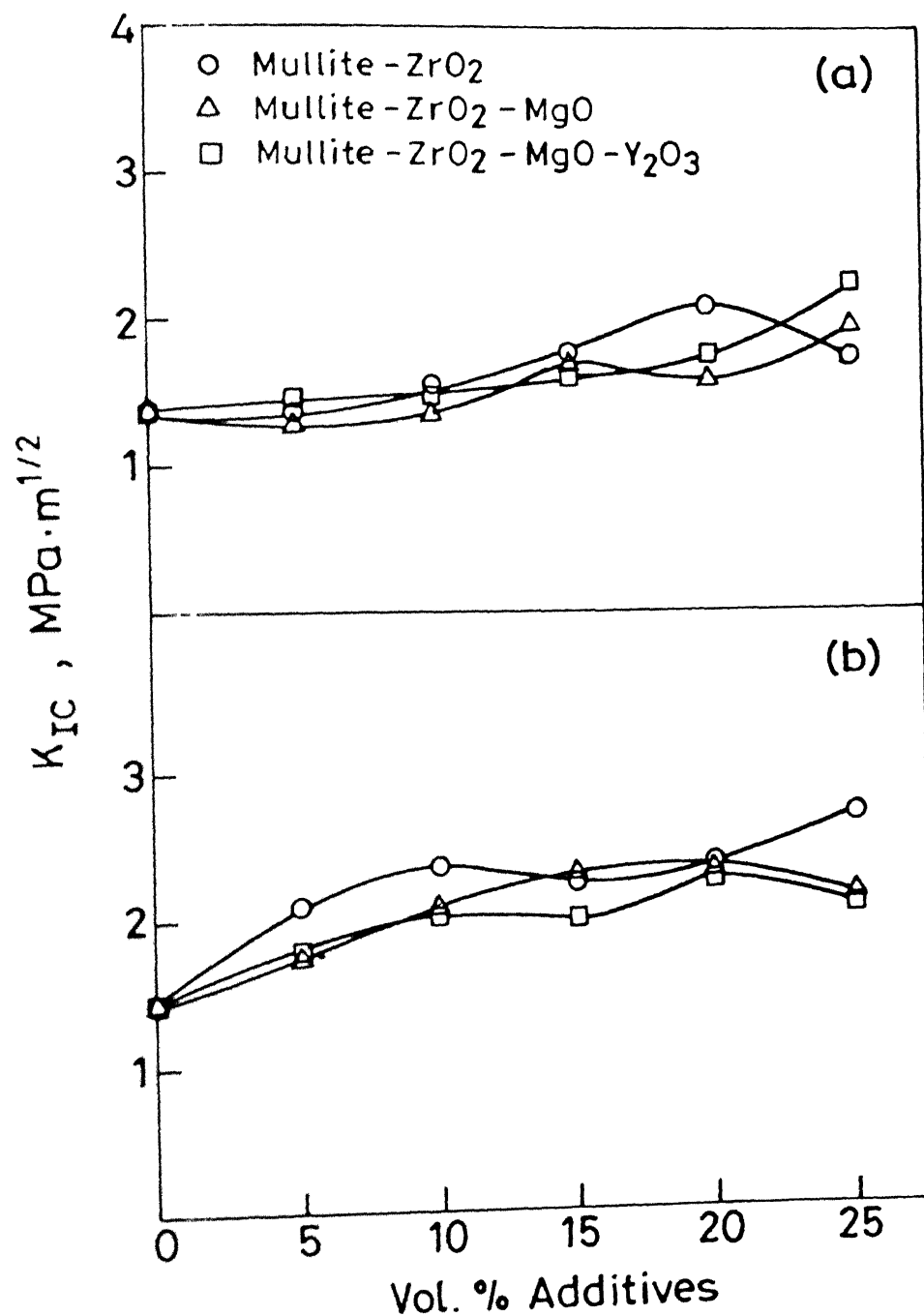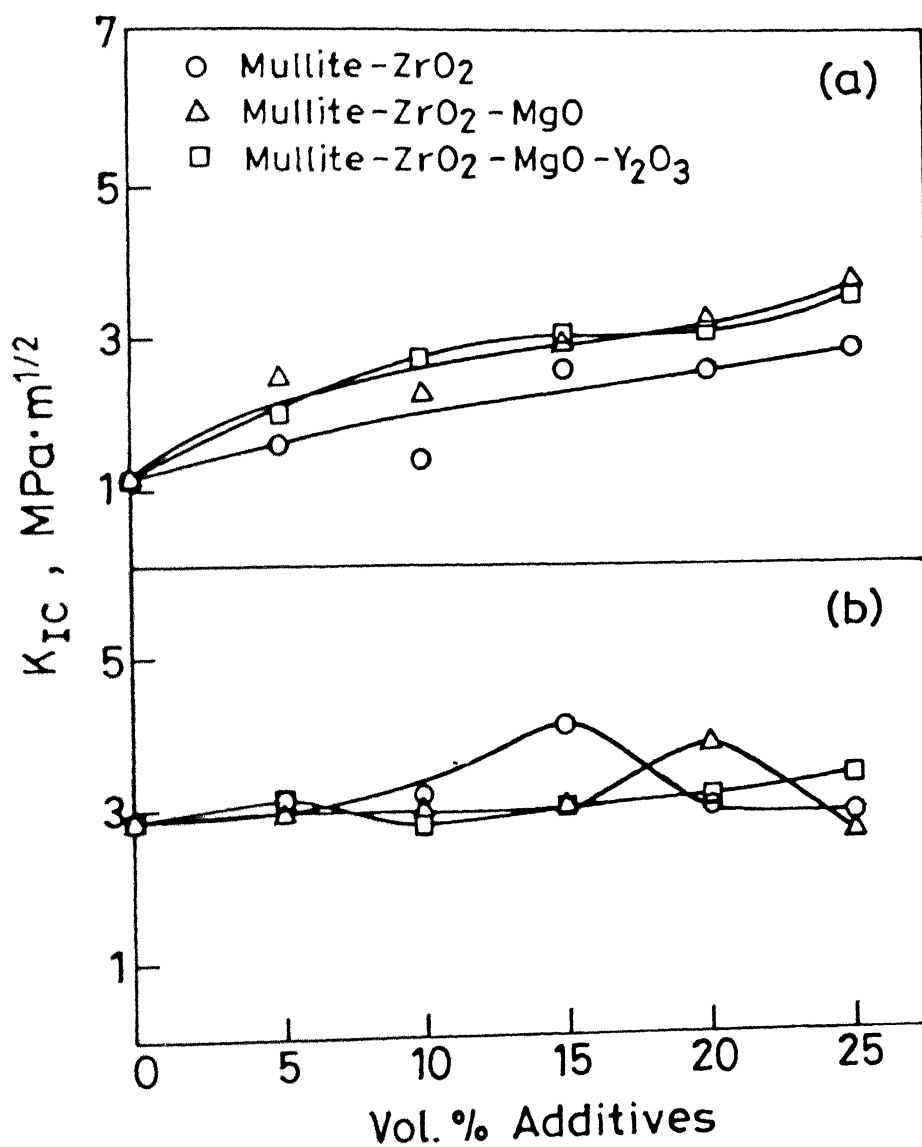
Fig. 3.22 Variation of fracture toughness of MP-40 mullite based composites (a) sint. temp. 1650°C, (b) sint. temp. 1700°C.

Fig.3.23 Microstructure of MC Mullite Based Composites
Containing 5 vol% Additive, Sintered at 1650°C
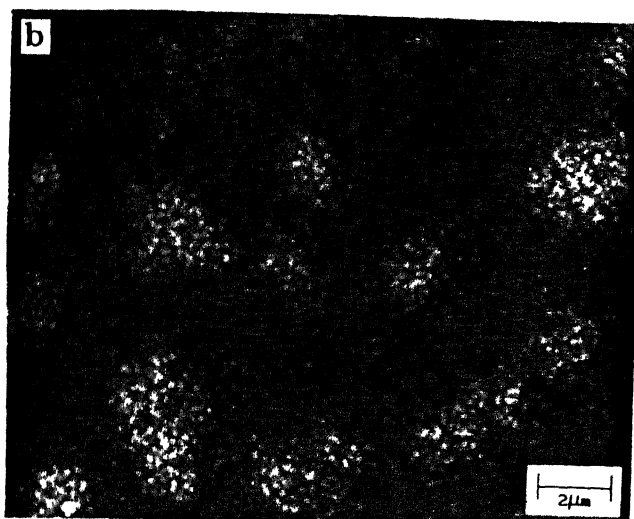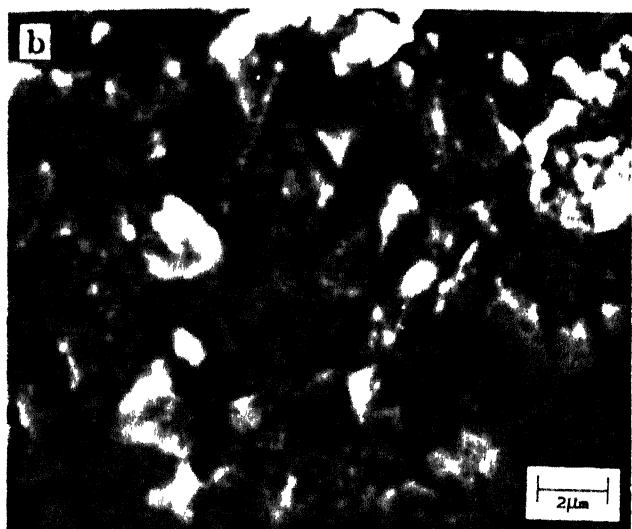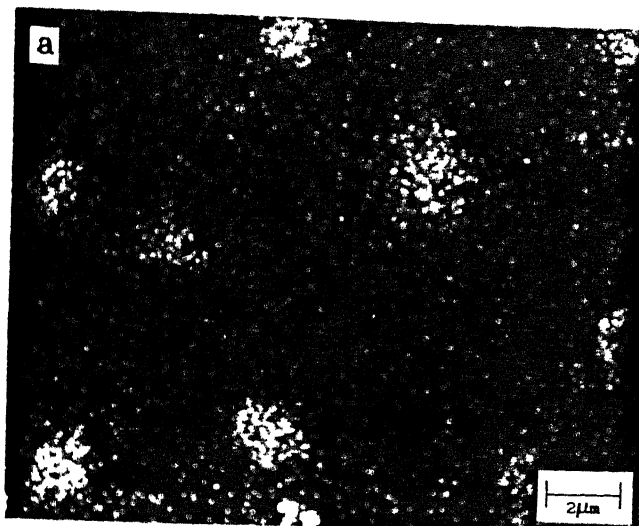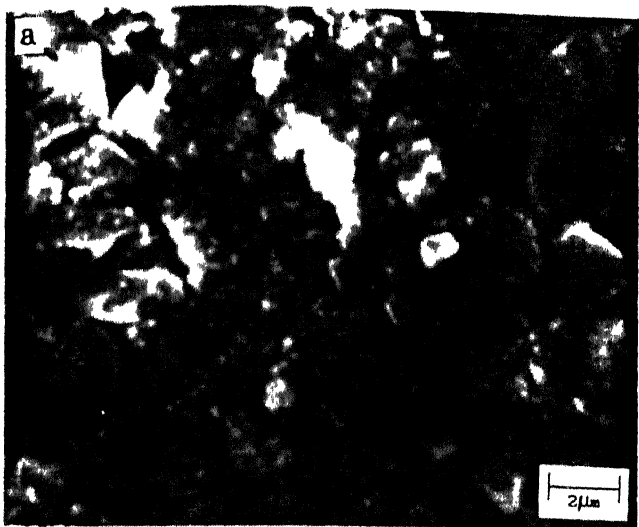
i) ZrO_2 additive
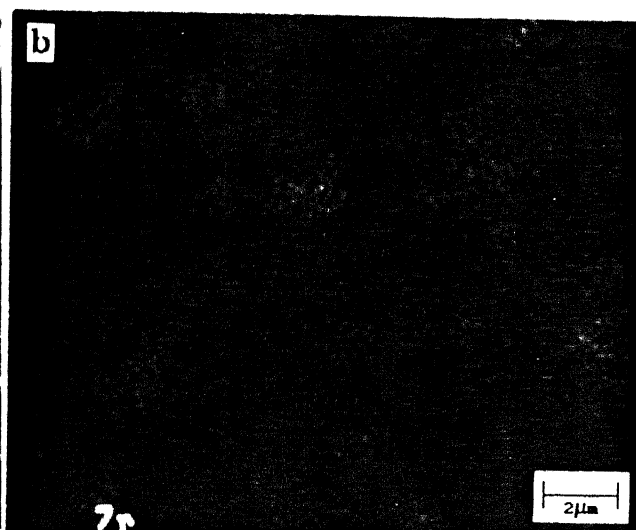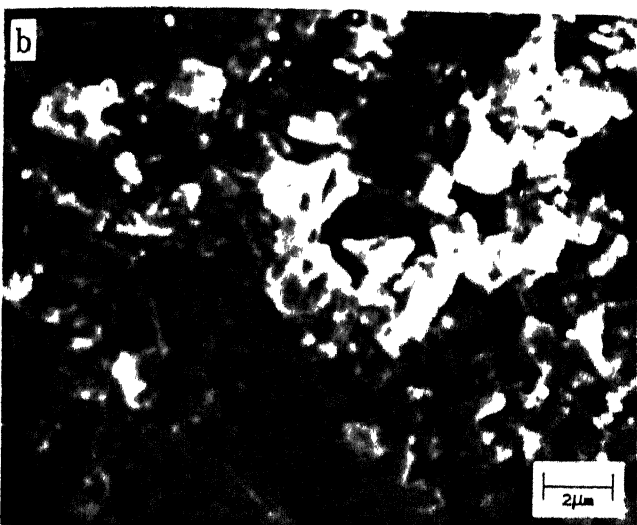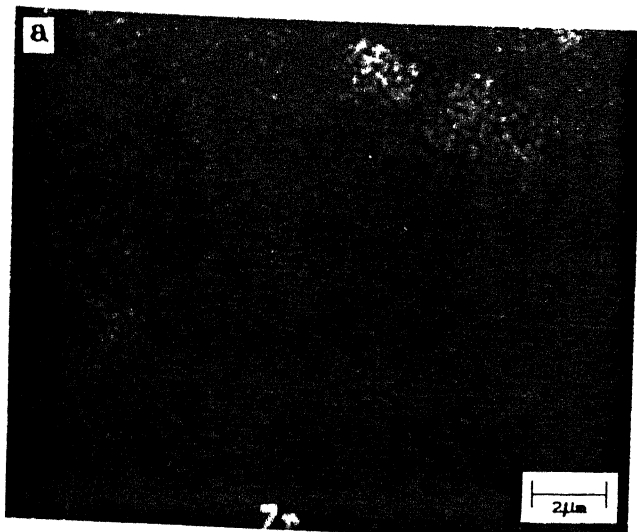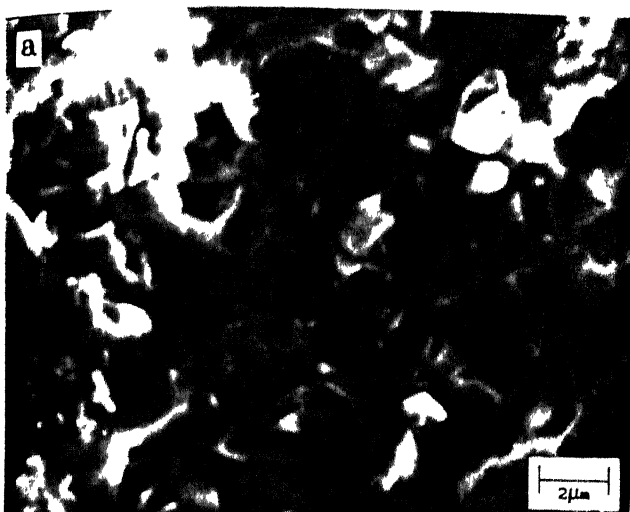
a)   5 vol%   b)   25 vol%

ii) ZrO_2-MgO additive
  a)   5 vol%   b)   25 vol%
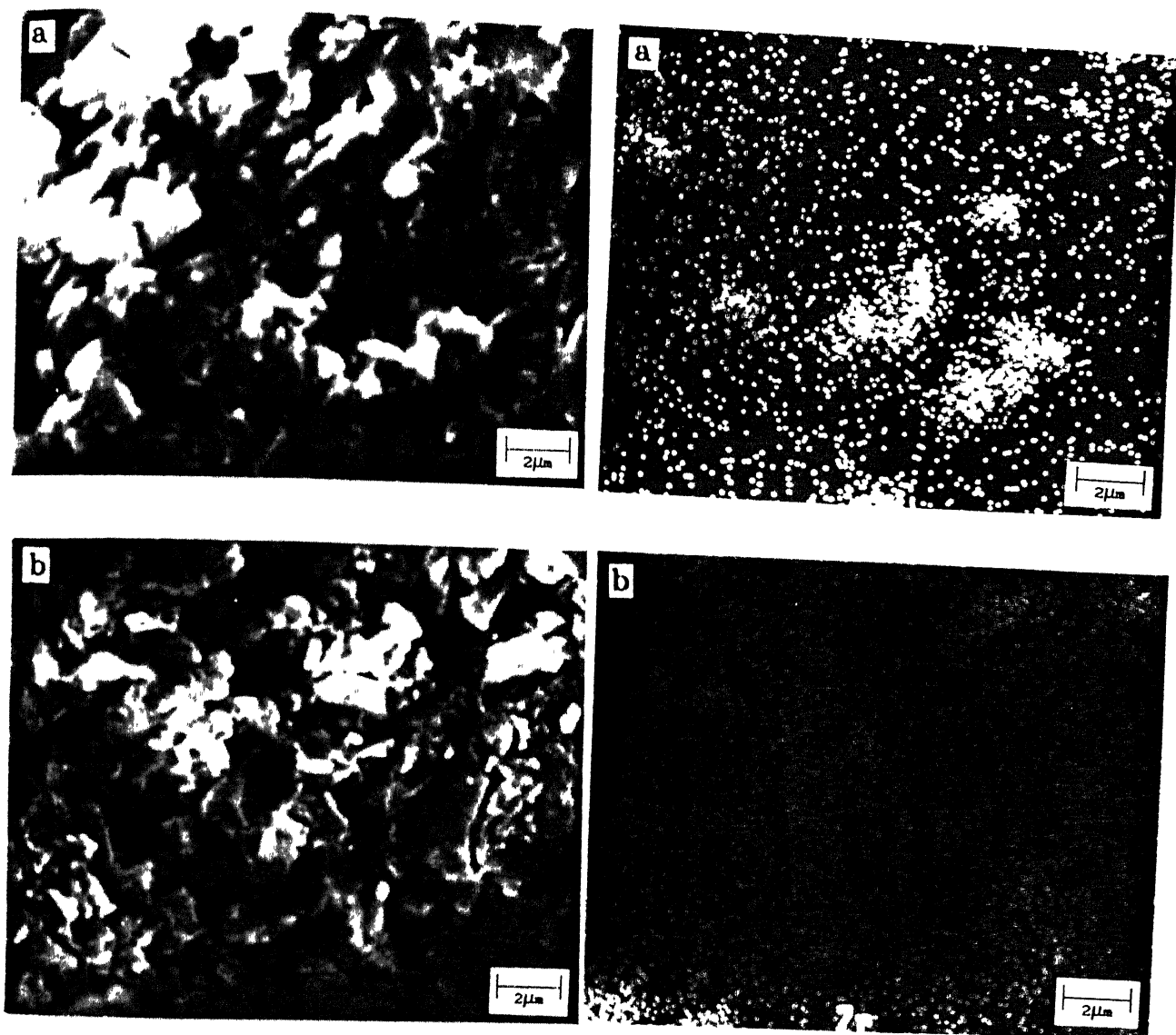
iii) ZrO_2-MgO-Y_2O_3 additive

a)   5 vol%   b)   25 vol%

Fig.3.24 Microstructures and EDX Dot Mappings of Zirconium
        for MP-20 Mullite Based Composites, Sintered at
        1650°C
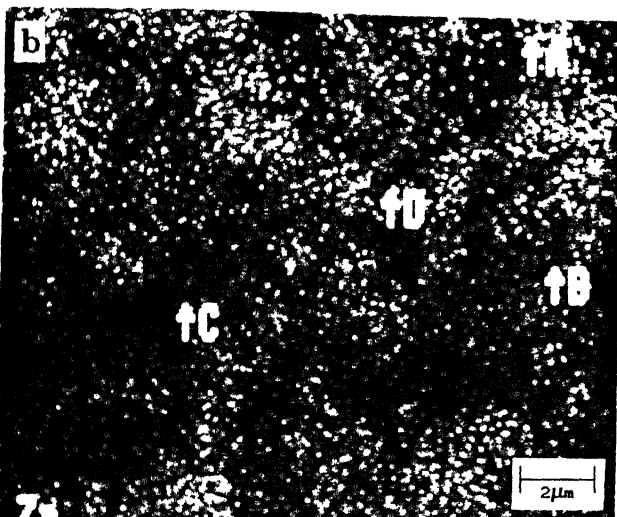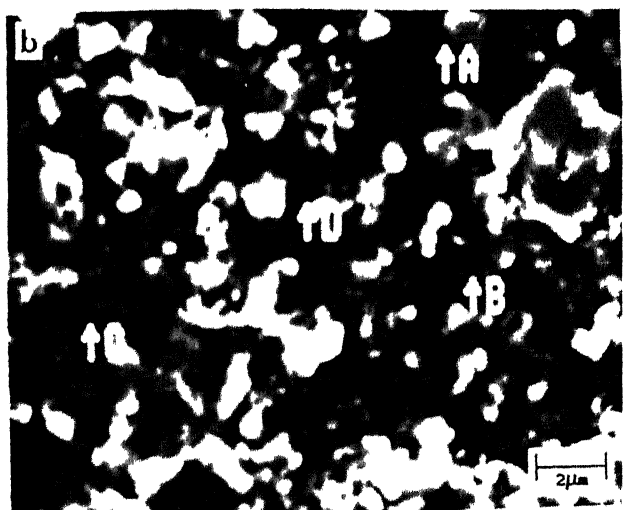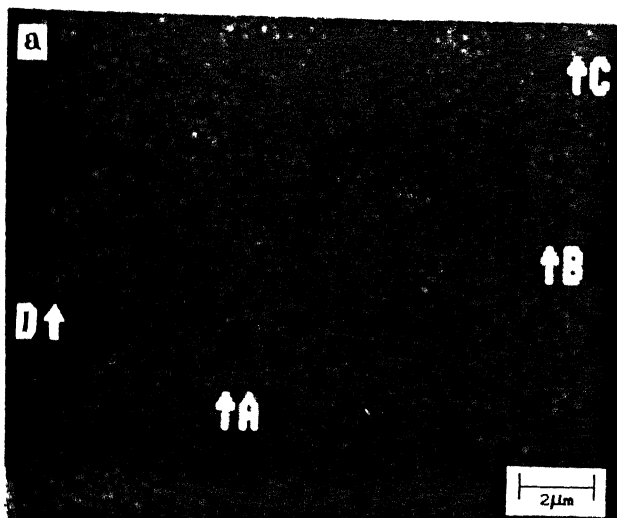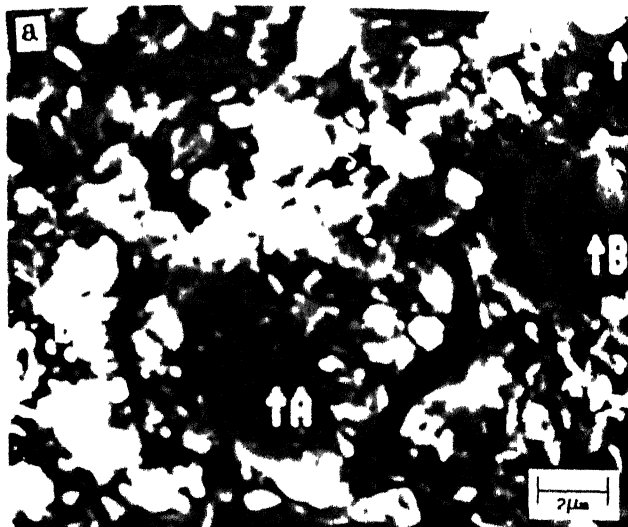
i) ZrO_2 additive
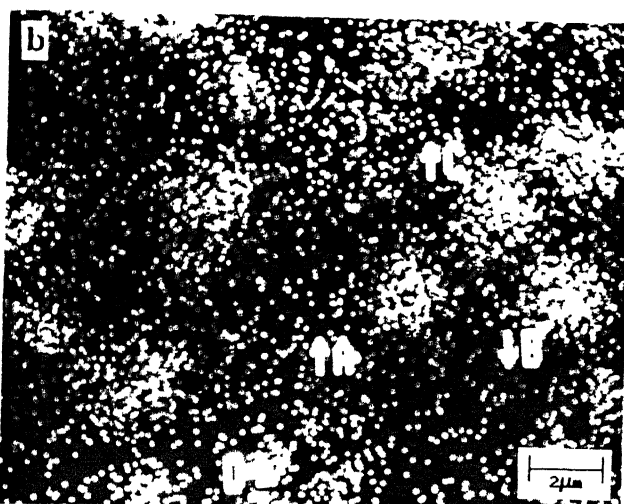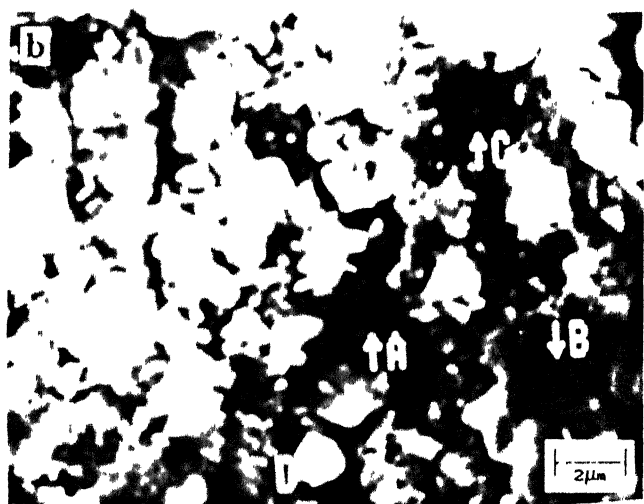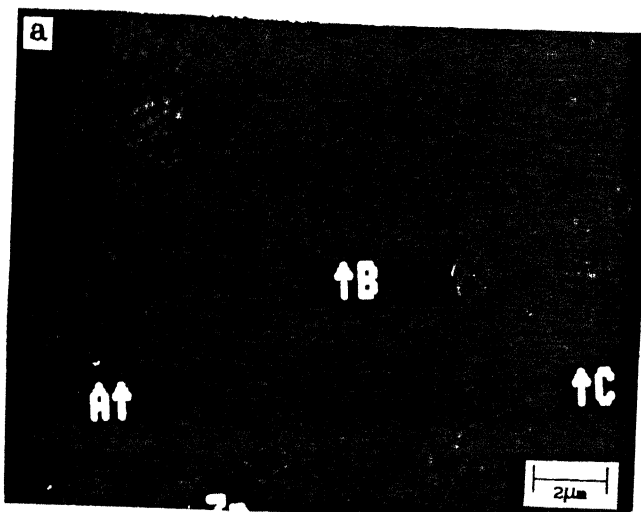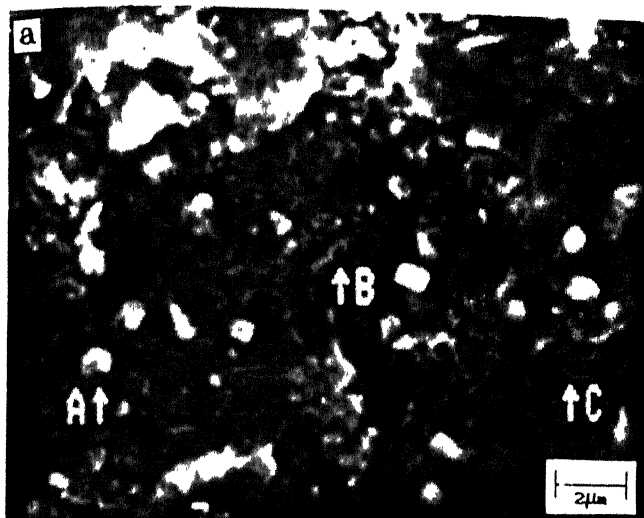
a)   5 vol%   b)   25 vol%

ii) ZrO$_2$-MgO additive
   a)   5 vol%   b)   25 vol%
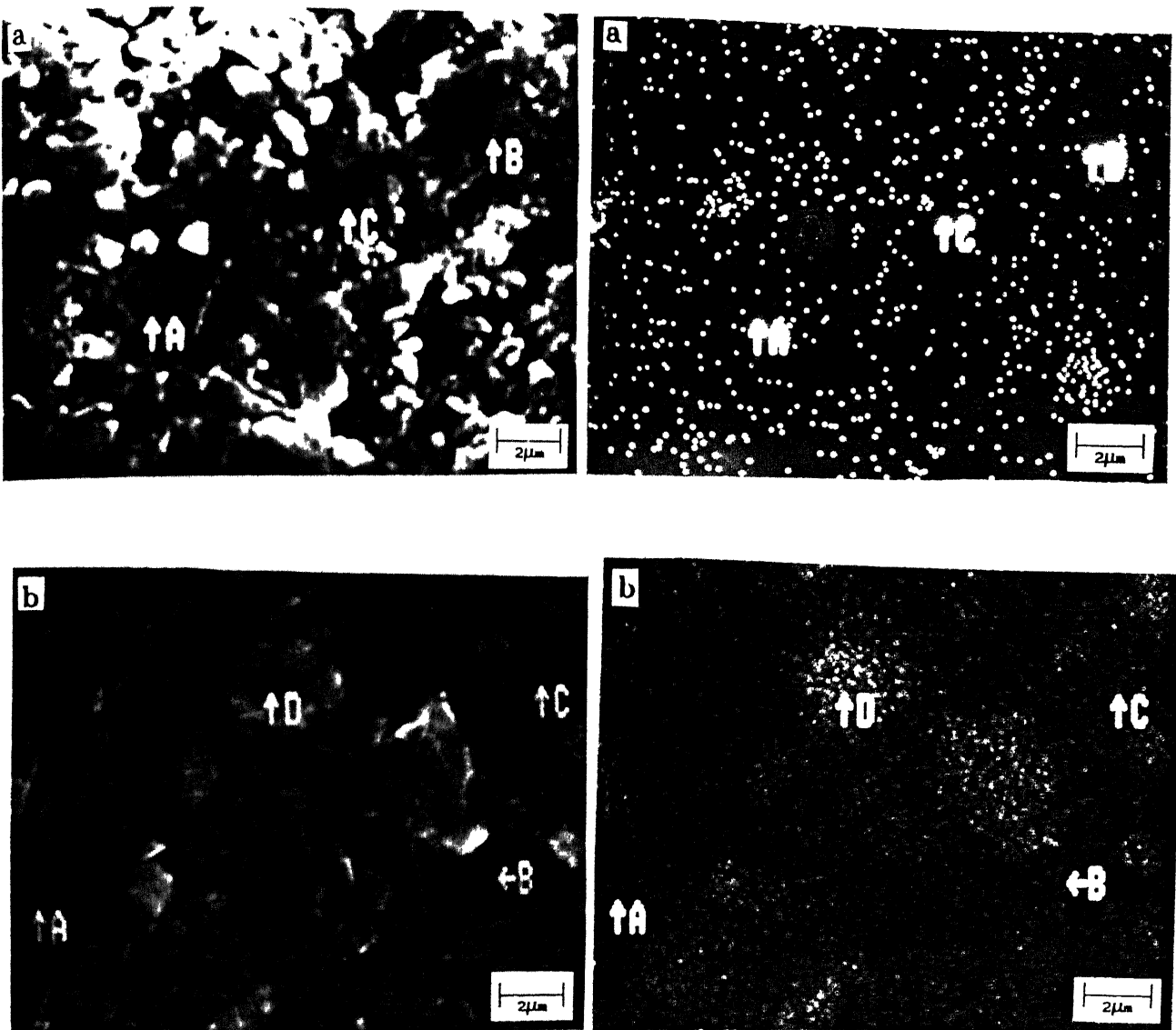
iii) ZrO_2-MgO-Y_2O_3 additive
a)   5 vol%   b)   25 vol%

Fig.3.25 Microstructures and EDX Dot Mappings of Zirconium
For MP-40 Mullite Based Composites, Sintered at
1650°C ('D' in micrographs designate ZrO_2 phase)

Table 3.4 shows the chemical composition of different oxides near the mullite grain boundary and at the ZrO_2 grains as designated in Fig. 3.25. The results do no doubt have appreciable error but they suffice to give a qualitative trend. With the increase in volume fraction of ZrO_2 in the composites, the estimated values of ZrO_2 after EDX analysis increases. So does the amount of other oxides viz. MgO and Y_2O_3. Since after communition the particle size of ZrO_2 additive decreases, during EDX analysis it naturally analyses the spot for Al_2O_3 and SiO_2 as well, giving a weighted value.

Fractographic analysis of MC based composites (Fig 3.26, 3.27) shows a homogeneous distribution of ZrO_2 particles throughout the elongated mullite matrix at either sintering temperature. However at higher sintering temperature (1700°C) microstructure becomes more homogeneous (Fig 3.27). From the quantitative microstructural analysis of fractographs (Fig 3.32, 3.33) it is clear that mullite grain size increases with the increase in vol% additives with some scattering except for straight ZrO_2 containing composites where the trend is reverse. Higher sintering temperature (1700°C) obviously increases the mullite grains size (Fig. 3.33). ZrO_2 particle size also increases with the increase in vol% additives (Fig. 3.34).

Fractographs of MP-20 (Fig 3.28, 3.29) and MP-40 (Fig 3.30, 3.31) based composites show a homogeneous distribution of ZrO_2 particles in the mullite matrix which is equiaxed in nature at either sintering temperature. At higher sintering temperature grain coarsening is also observed in some cases. Mullite grain

Table 3.4 : Chemical Composition of Oxides in ZrO_2 Dispersoids in Mass% in MP-40 Mullite Based Composites (Sintered at $1650^{\circ}C$).

Additive		At ZrO_2 Grain			At Mullite Grain		
Vol%	Mass%	ZrO_2	MgO	Y_2O_3	ZrO_2	MgO	Y_2O_3
5 ZrO_2	8.64	16.56	–	–	3.09	–	–
10 ZrO_2	16.65	87.65	–	–	2.52	–	–
15 ZrO_2	24.08	83.44	–	–	17.02	–	–
20 ZrO_2	31.00	85.17	–	–	18.03	–	–
25 ZrO_2	37.47	93.19	–	–	26.90	–	–
5 ZrO_2-MgO	3.89	–	–	–	8.79	0.20	–
15 ZrO_2-MgO	11.95	79.38	0.44	–	1.23	0.27	–
25 ZrO_2-MgO	20.41	68.60	0.13	–	4.92	0.56	–
5 ZrO_2-MgO -Y_2O_3	3.26	–	–	–	0.53	0.23	0.21
15 ZrO_2-MgO -Y_2O_3	10.15	70.55	0.20	6.81	3.46	0.42	0.96
25 ZrO_2-MgO -Y_2O_3	16.58	89.23	0.00	8.88	2.99	0.05	1.27

Fig.3.26 SEM Fractographs of MC Mullite Based Composites
Containing 15 vol% Additive, Sintered at 1650°C

a) ZrO_2 b) ZrO_2-MgO   c) ZrO_2-MgO-Y_2O_3
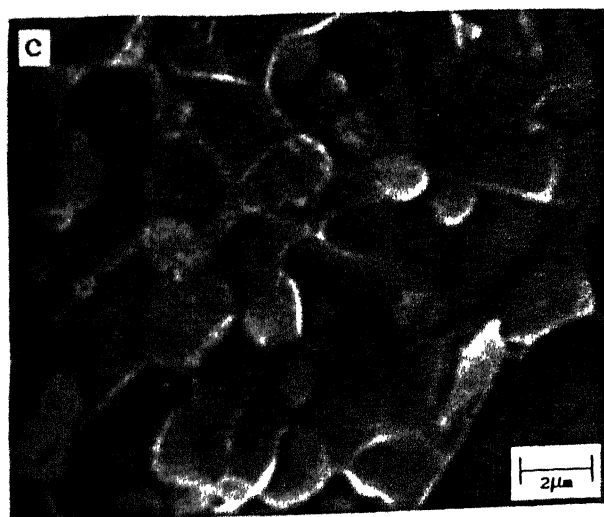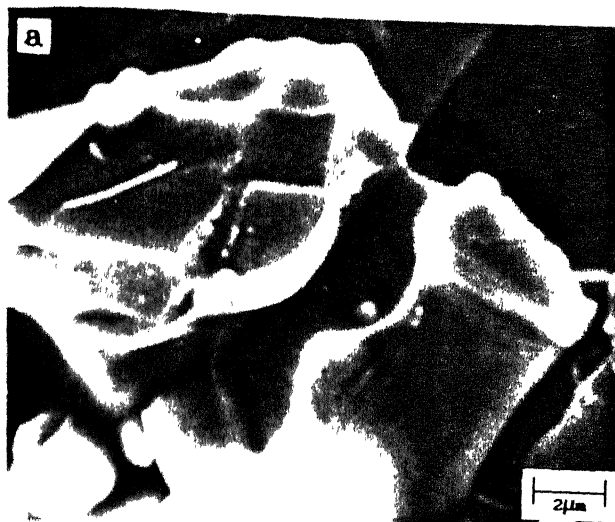
i) ZrO_2 additive

ii) ZrO_2-MgO additive
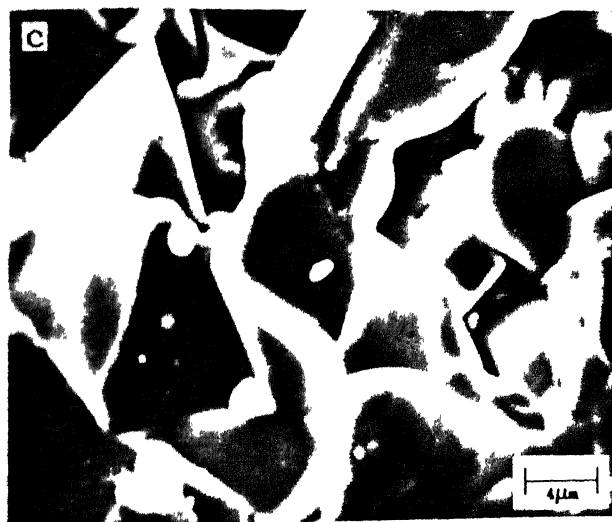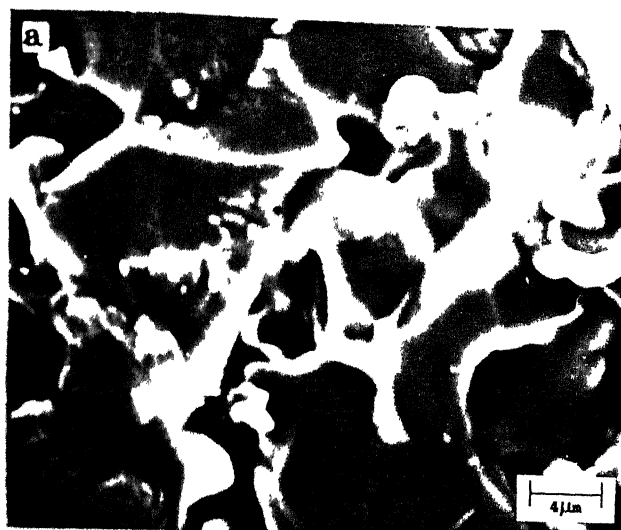
a) 5 vol%   b) 15 vol%   c) 25 vol%

iii) ZrO_2-MgO-Y_2O_3 additive
a)   5 vol%   b)   15 vol%   c)   25 vol%
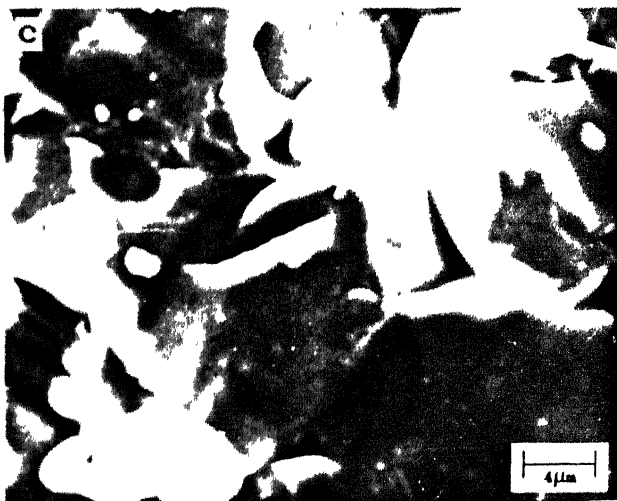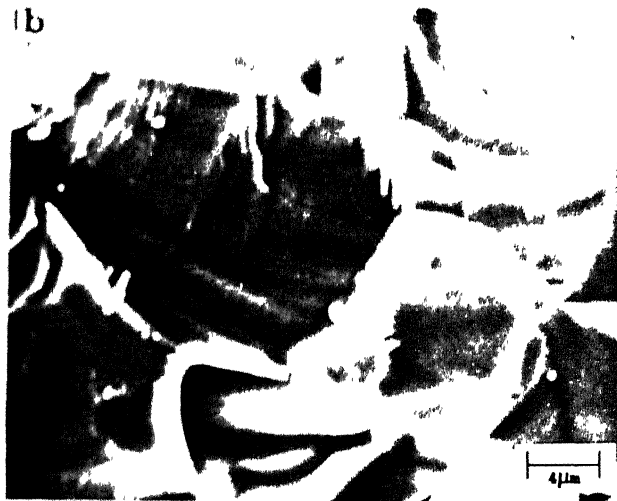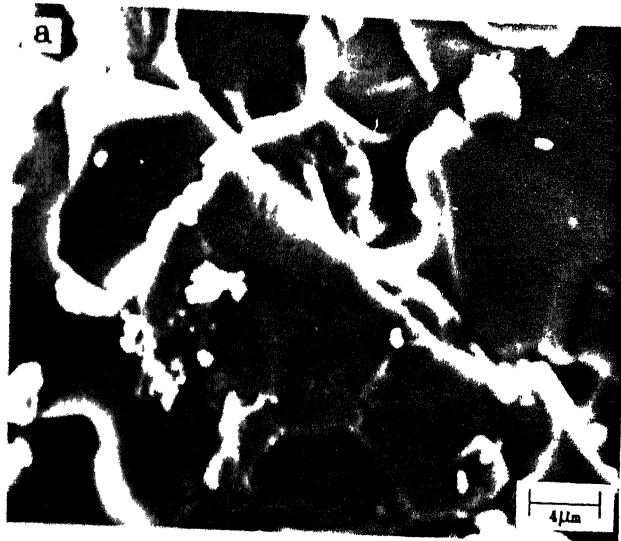
Figure   ...   of MC Mullite Based Composites,
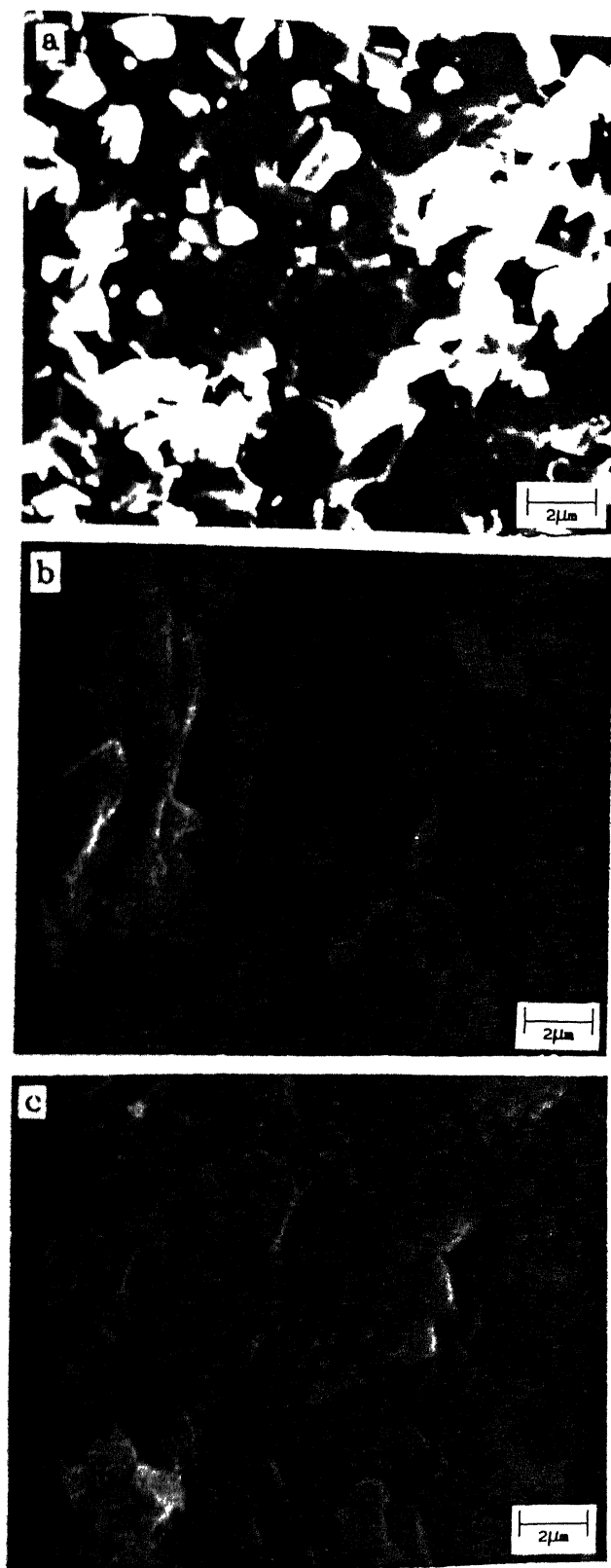
Fig.3.28 SEM Fractographs of MP-20 Mullite Based Composites Containing 15 vol% Additive, Sintered at 1650°C

a)   ZrO₂   b)   ZrO₂-MgO   c) ZrO₂-MgO-Y₂O₃

i) ZrO_2 additive
a)   5 vol%   b)   15 vol%   c)   25 vol%

ii) ZrO$_2$-MgO additive

  a)   5 vol%   b)   15 vol%   c)   25 vol%

iii) ZrO_2-MgO-Y_2O_3 additive

a)   5 vol%   b)   15 vol%   c)   25 vol%

Fig.3.29 SEM   Fractographs   of   MP-20   Mullite   Based
Composites, Sintered at 1700°C

Fig.3.30 SEM Fractographs of MP-40 Mullite Based Composites
Containing 15 vol% Additive, Sintered at 1650°C

a) ZrO_2 b) ZrO_2-MgO   c) ZrO_2-MgO-Y_2O_3
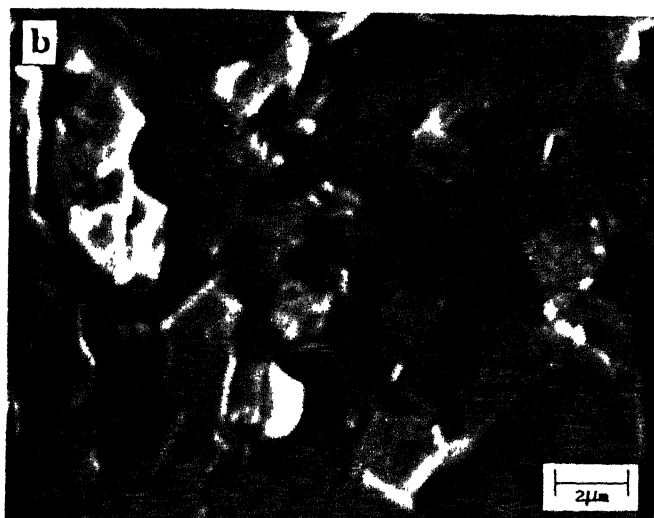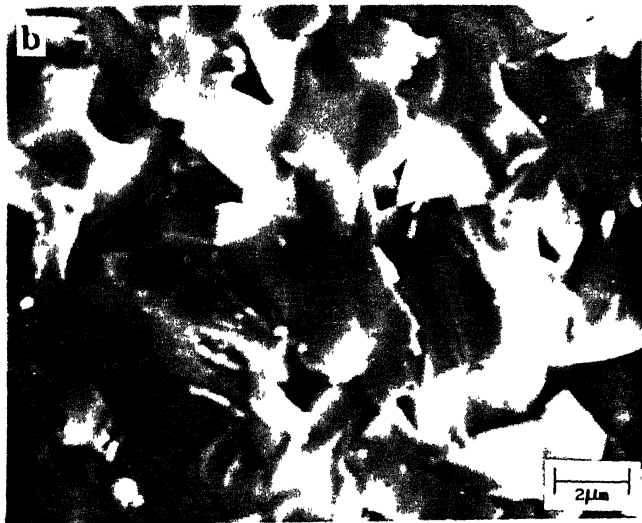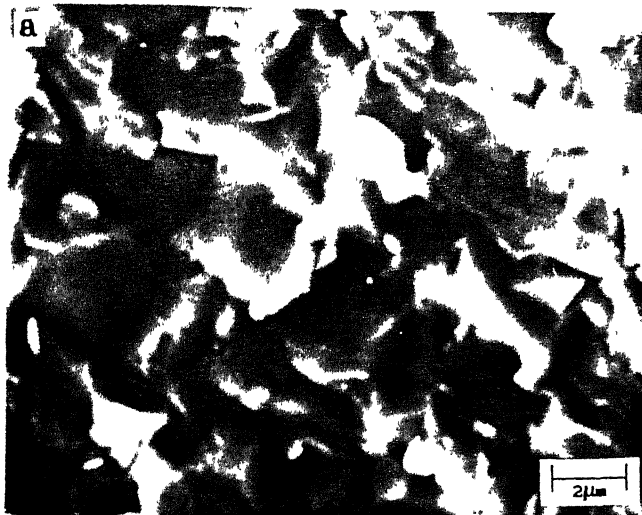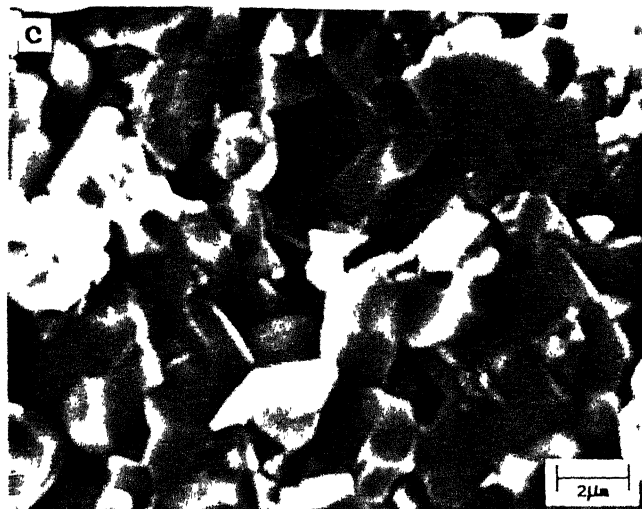
i) ZrO$_2$ additive

a) 5 vol%   b) 15 vol%   c) 25 vol%

contd.

ii) ZrO_2-MgO additive

a)   5 vol%   b)   15 vol%   c)   25 vol%
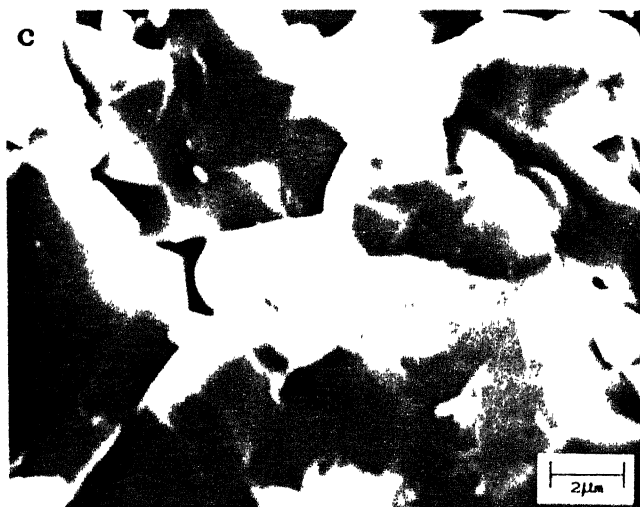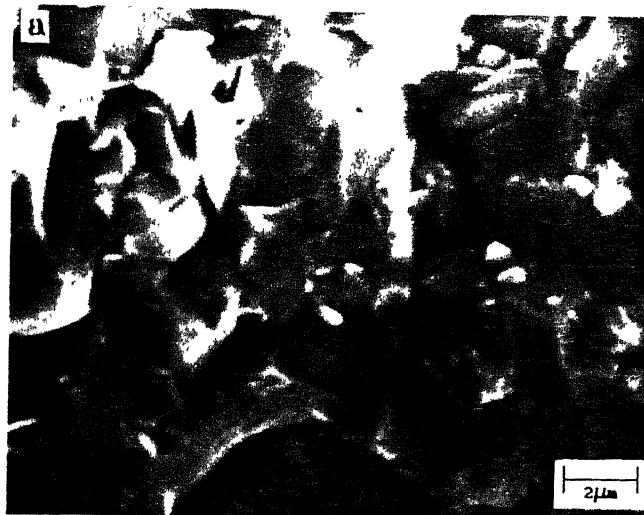
iii) ZrO$_2$-MgO-Y$_2$O$_3$ additive

a)   5 vol%   b)   15 vol%   c)   25 vol%

Fig.3.31 SEM   Fractographs   of   MP-40   Mullite   Based
         Composites, Sintered at 1700°C
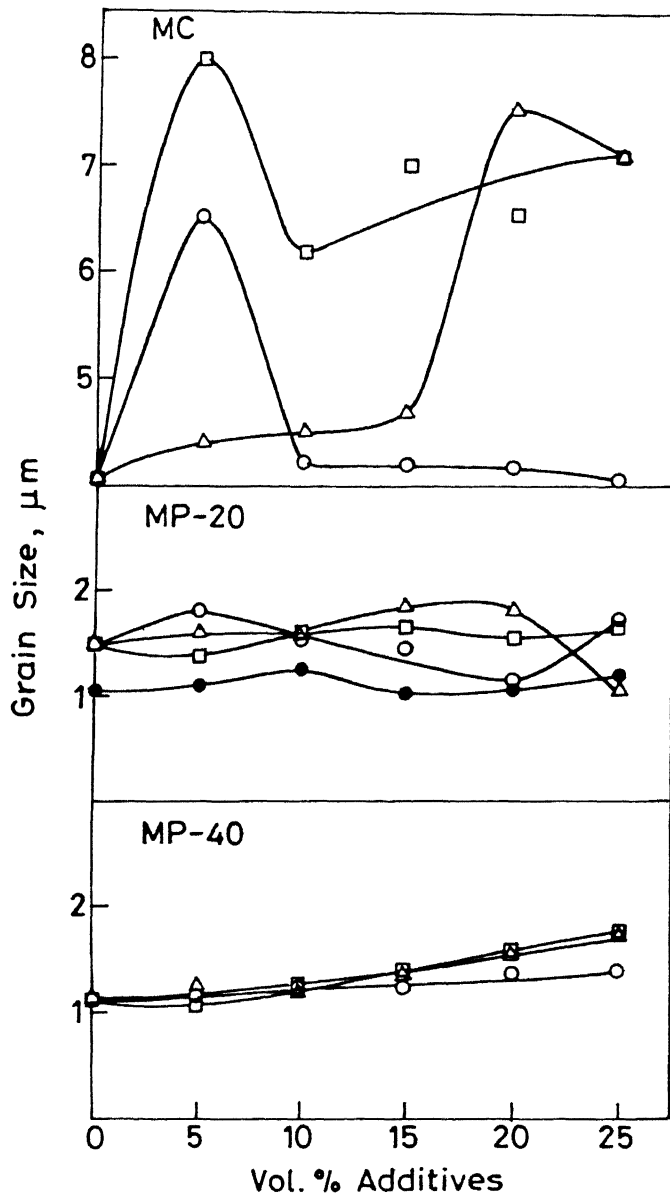
Fig. 3.32 Variation of mullite grain size in MC, MP-20 and MP-40 mullite base composites.

● Mullite-ZrO₂ (sintered at 1600°C)
○ Mullite-ZrO₂ (sintered at 1650°C)
△ Mullite-ZrO₂-MgO (sintered at 1650°C)
□ Mullite-ZrO₂-MgO-Y₂O₃ (sintered at 1650°C)
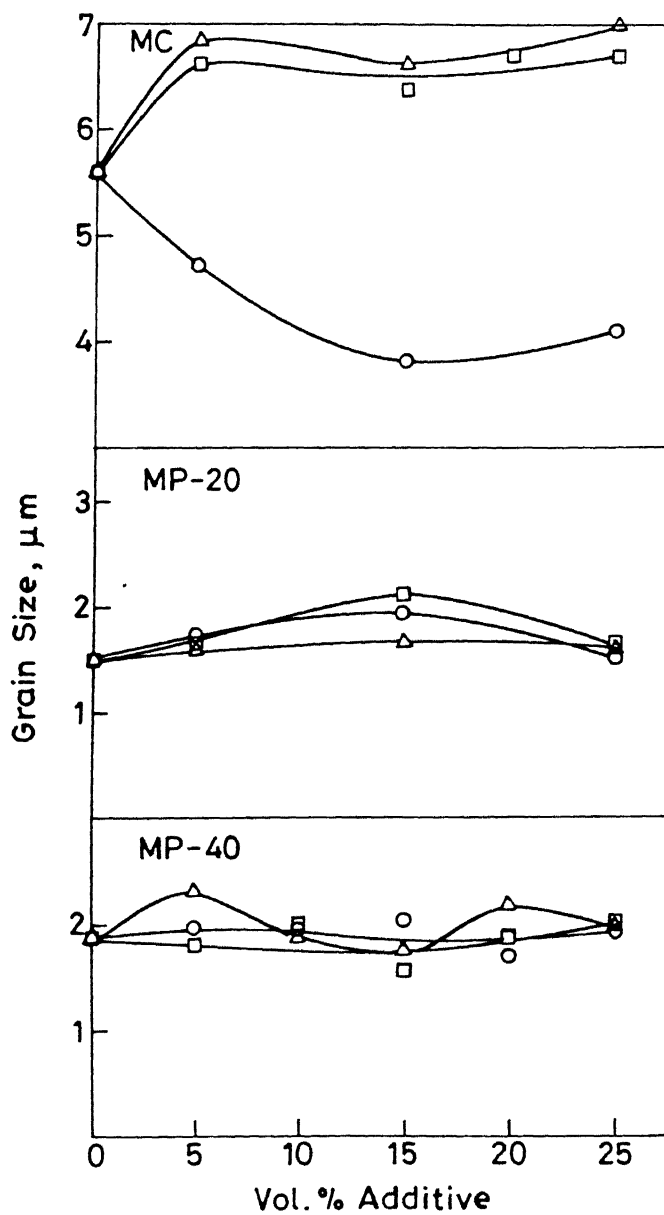
Fig.3.33 Variation of mullite grain size in MC, MP-20
and MP-40 mullite based composites
sintered at 1700°C.
  o Mullite–ZrO_2
  △ Mullite–ZrO_2–MgO
  □ Mullite–ZrO_2–MgO–Y_2O_3
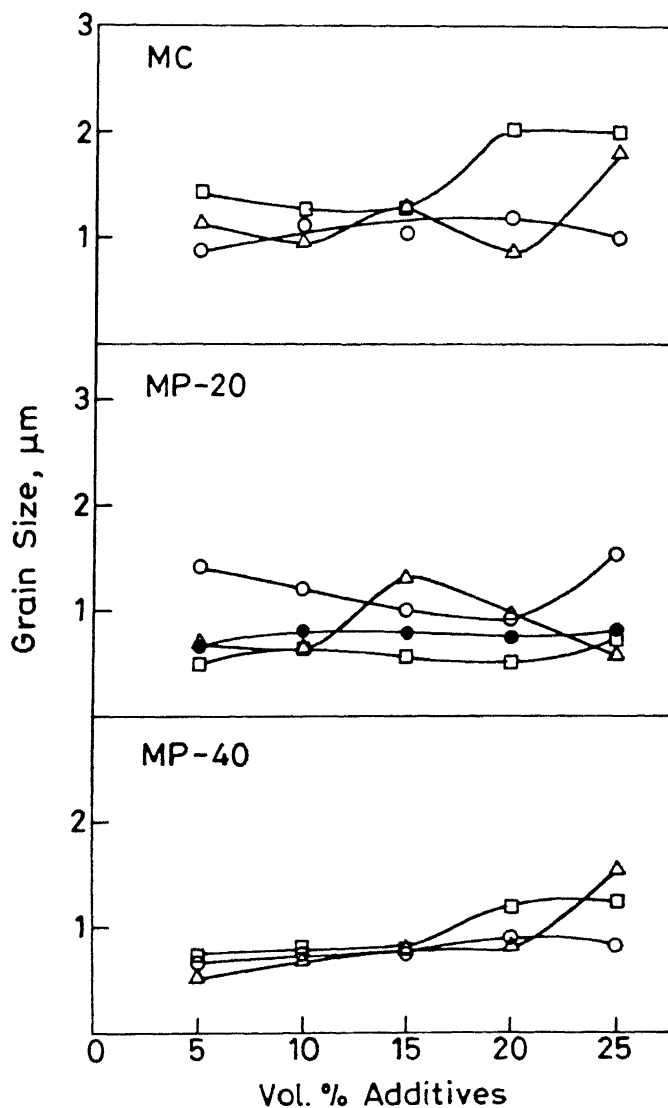
Fig. 3.34 Variation of ZrO₂ grain size in MC, MP-20
and MP-40 mullite based composites.

● Mullite – ZrO₂ (sintered at 1600°C)
○ Mullite – ZrO₂ (sintered at 1650°C)
△ Mullite – ZrO₂ – MgO (sintered at 1650°C)
□ Mullite – ZrO₂ – MgO – Y₂O₃ (sintered at 1650°C)

size remains almost same with the increase in vol% additives at either sintering temperature with the exception for MP-40 based composites, sintered at 1650°C where grain size increases with the increase in vol% additives (Fig 3.32, 3.33). Like MC based composites, increase in sintering temperature increases the mullite grain size. ZrO_2 particle size also increases with the increase in vol% additives in the composites (Fig. 3.34). The scattering in the result is ±3.00 μm for fused mullite grains and ± 0.67 μm for sol- gel mullite grains. It is ± 0.77 μm and ±0.43 μm for ZrO_2 particles in fused and sol-gel based composites respectively.

III 4.5   X-ray Diffraction Analysis

From the X-ray diffraction analysis (Fig 3.35, 3.36, 3.37) it is clear that fractional tetragonal ZrO_2 (f_t) decreases with the increase in vol% additive irrespective of the type of mullite powders with the exception for MP-20 based composites, sintered at 1650°C, where f_t for MgO and MgO-Y_2O_3 stabilized ZrO_2 containing composites show a minimum at a particular composition. f_t also decreases with increase in sintering temperature. Among all the composites, MgO-Y_2O_3 stabilized ZrO_2 containing composites show highest values and straight ZrO_2 containing ones show lowest values at either sintering temperature with the exception for MC based composites, sintered at 1700°C where MgO stabilized ZrO_2 containing composites show highest f_t values. However no cubic ZrO_2 is detected in any of the composites.
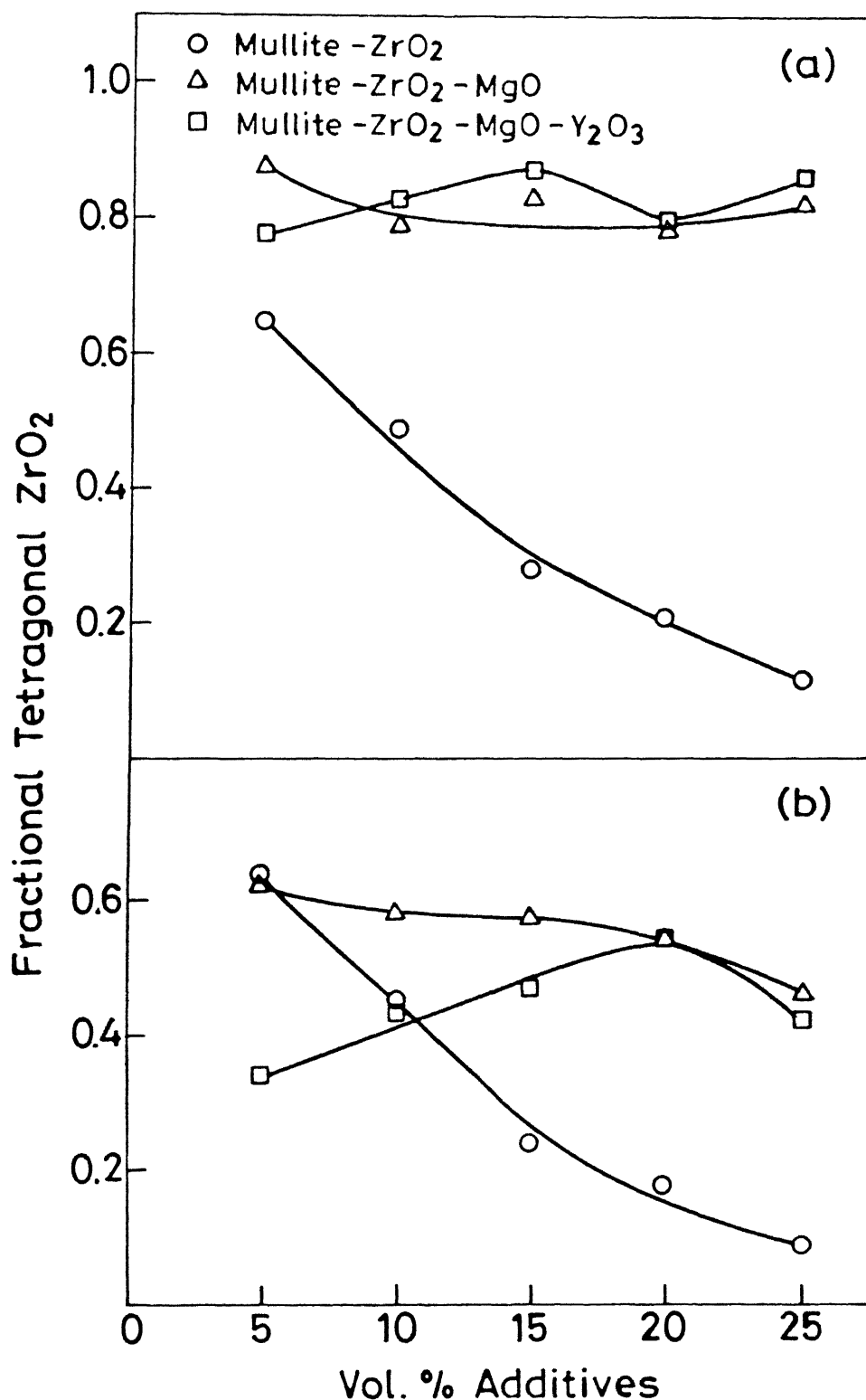
Fig. 3.35 Variation of fractional tetragonal ZrO_2 in MC mullite based composites (a) sint. temp. 1650°C, (b) sint. temp. 1700°C.
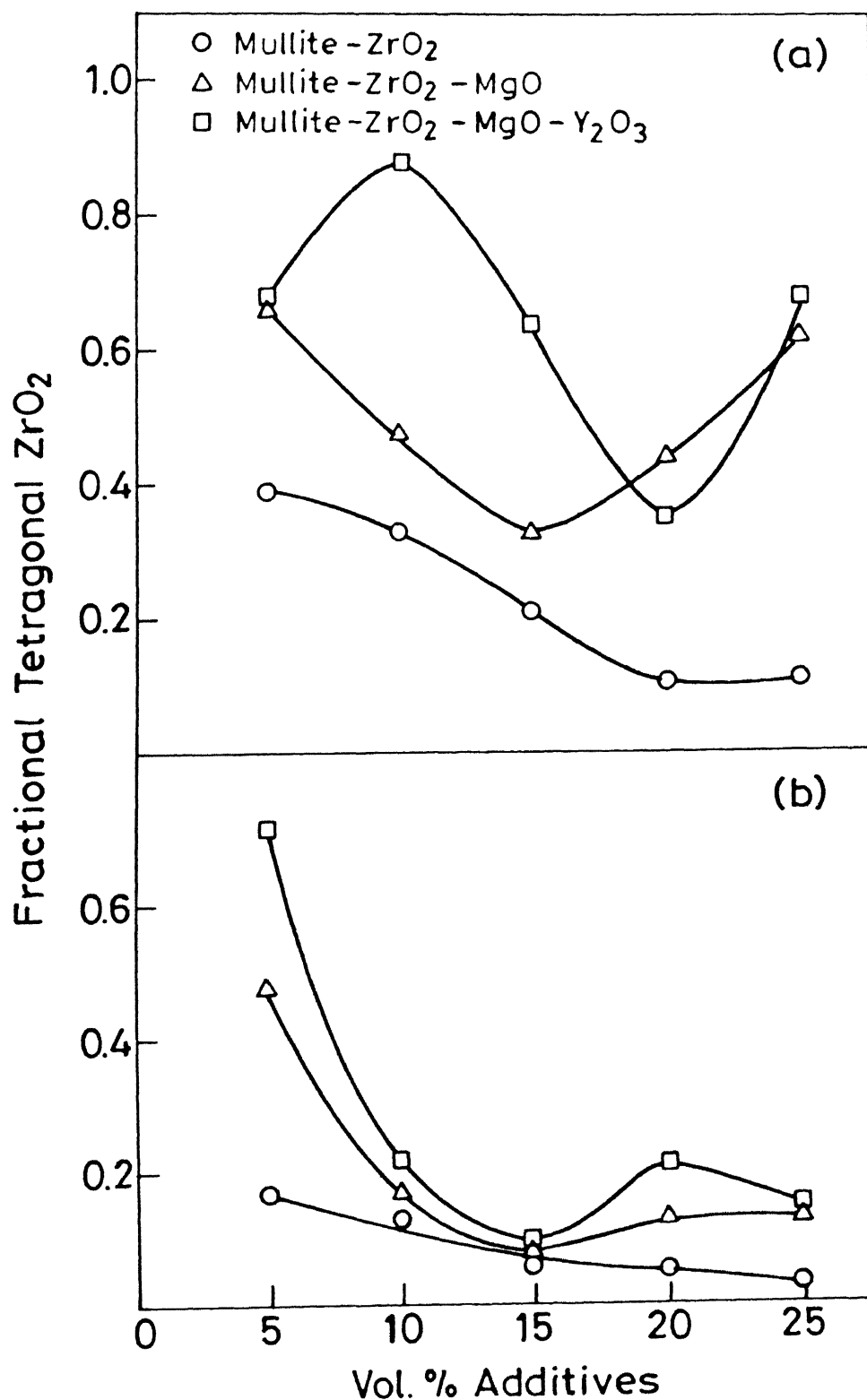
Fig. 3.36 Variation of fractional tetragonal ZrO_2 in
MP-20 mullite based composites
(a) sint. temp. 1650°C (b) sint. temp. 1700°C
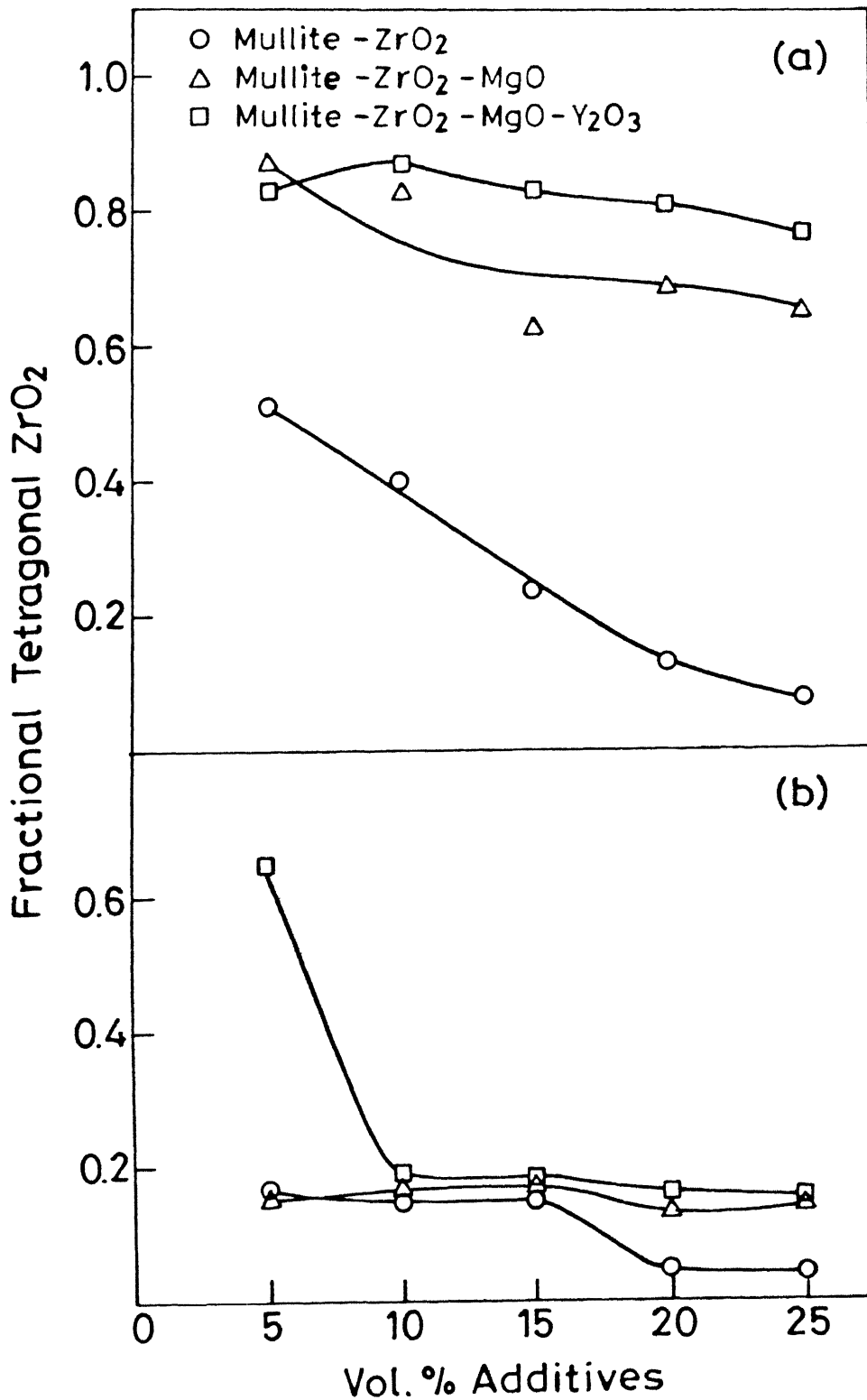
Fig. 3.37 Variation of fractional tetragonal ZrO₂ in MP-40 mullite based composites (a) sint. temp. 1650°C. (b) sint. temp. 1700°C.

III 4.6   Dielectric Constant

Dielectric constant values (k′) for all the composites significantly increase with the increase in vol% additive at either sintering temperature (Fig. 3.38, 3.39, 3.40). The higher sintering temperature (1700°C) always show higher k′ values than the 1650°C sintering.   The absolute values for MP-40 based sintered composites are higher than for either MC or MP-20 based ones.   Straight ZrO_2 containing composites always show highest k′ values irrespective of the type of mullite powders at either sintering temperature, while the MgO stabilized ZrO_2 containing ones show lowest k′ values.

III 4.7   Thermal Shock Resistance

Thermal shock resistance (ΔT) values for all the composites increase with the increase in sintering temperature from 1650°C to 1700°C with some scattering in the results(Fig. 3.41, 3.42, 3.43). In terms of absolute values MP-20 based composites sintered at 1700°C show highest ΔT values among all the composites.
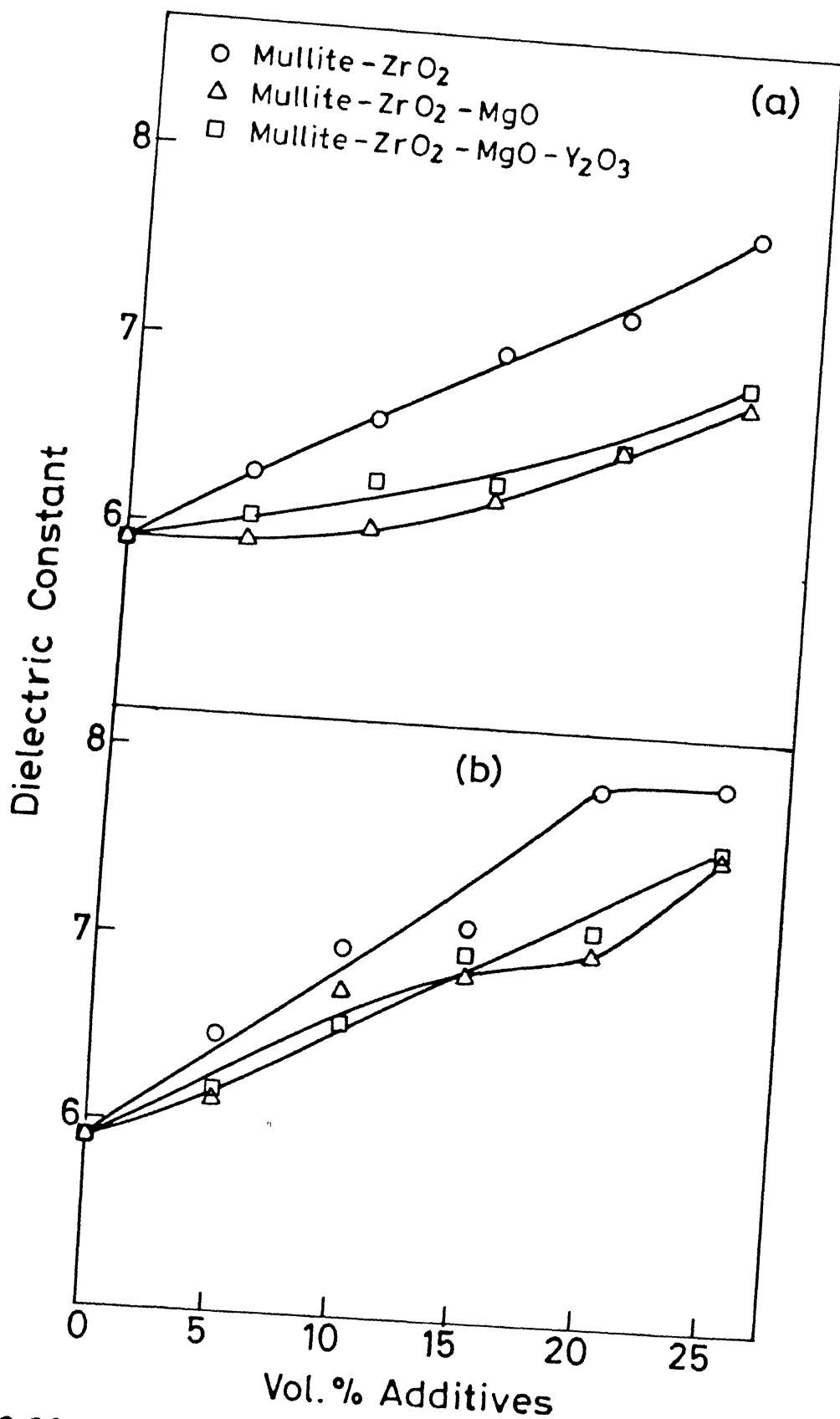
Fig. 3.38 Variation of dielectric constant of MC mullite based composites (a) sint. temp. 1650°C, (b) sint. temp. 1700°C.
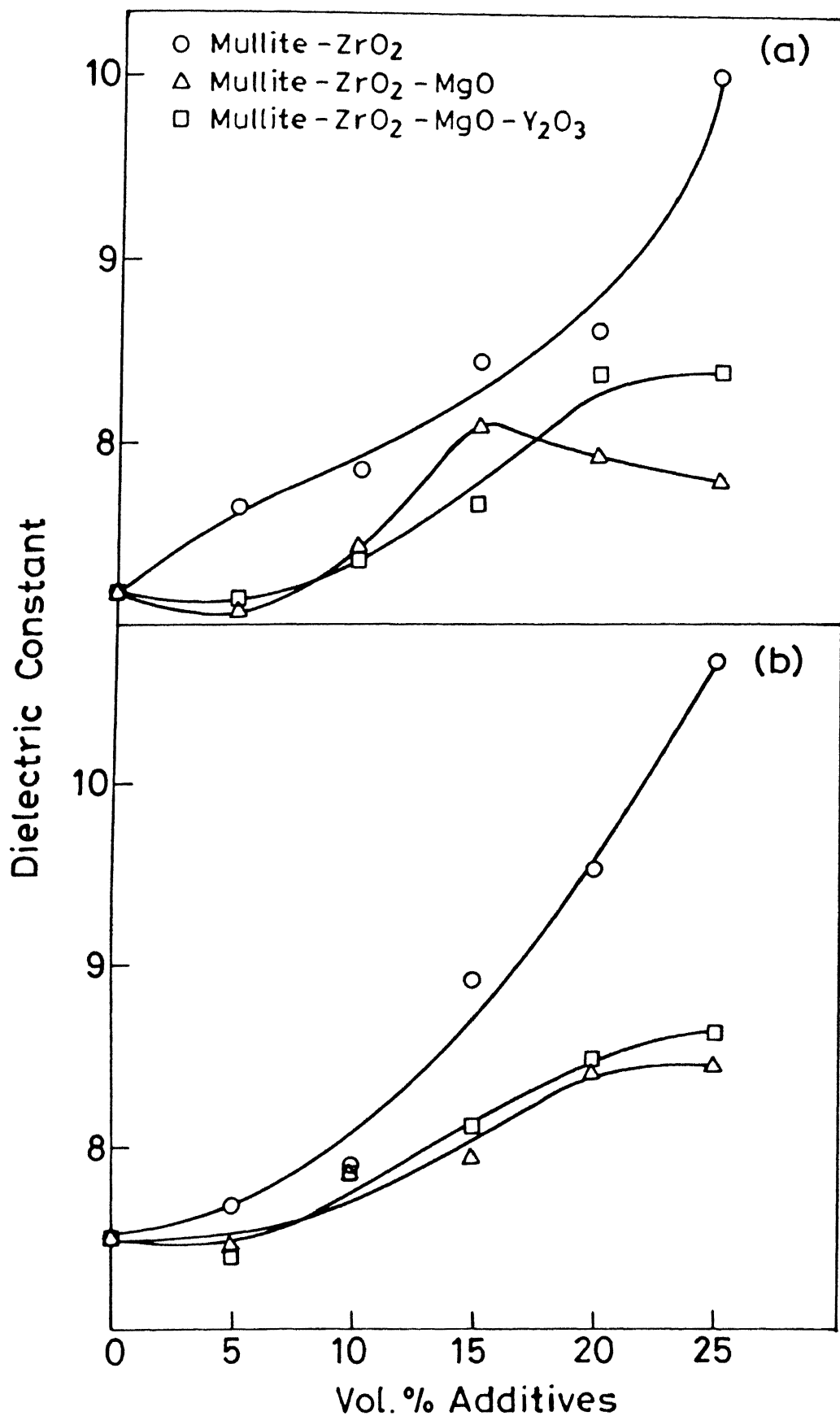
Fig. 3.39 Variation of dielectric constant of MP-20
mullite based composites
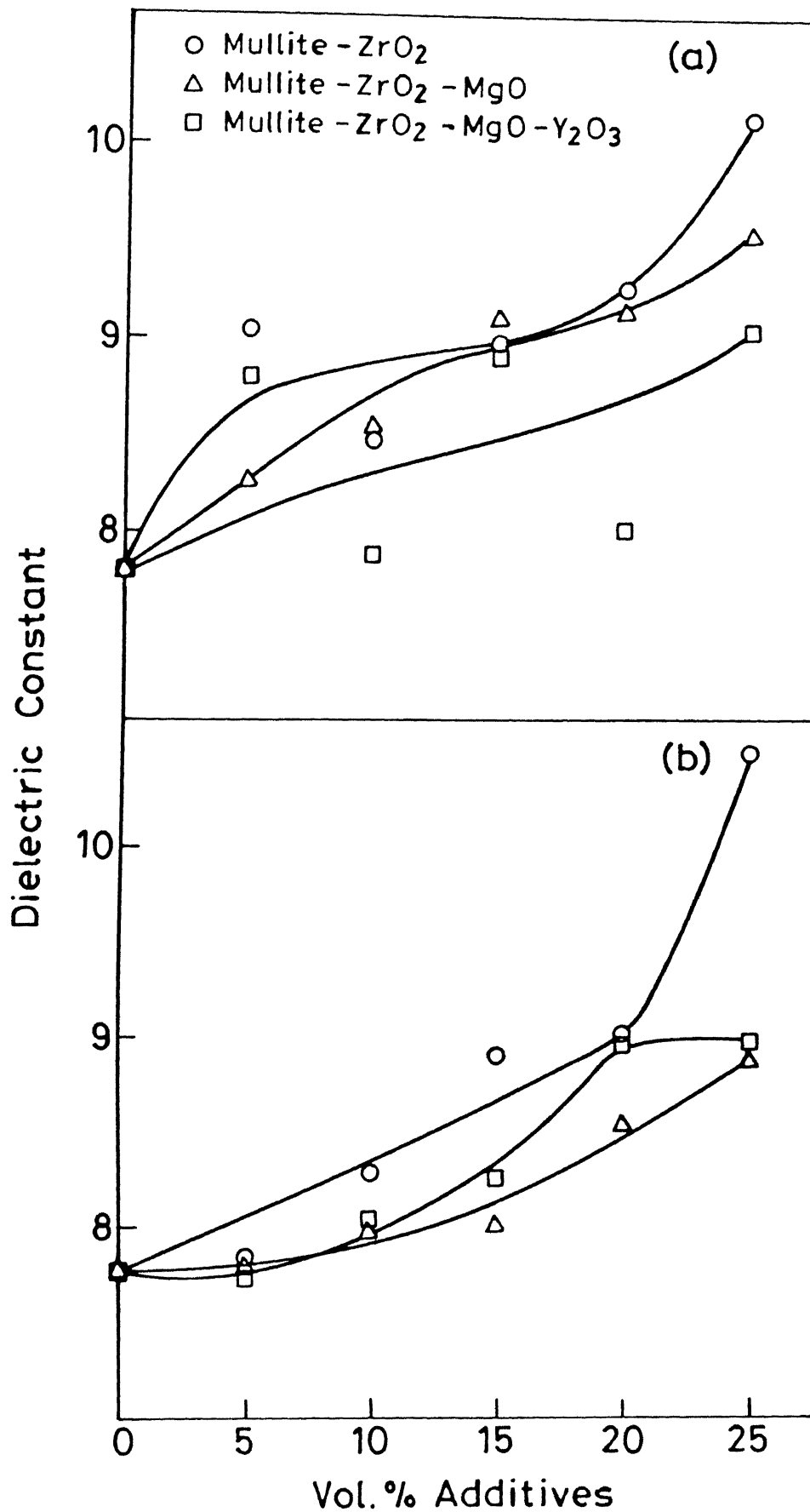
Fig.3.40 Variation of dielectric constant of MP-40
mullite based composites
(a) sint. temp. 1650°C. (b) sint. temp. 1700°C.
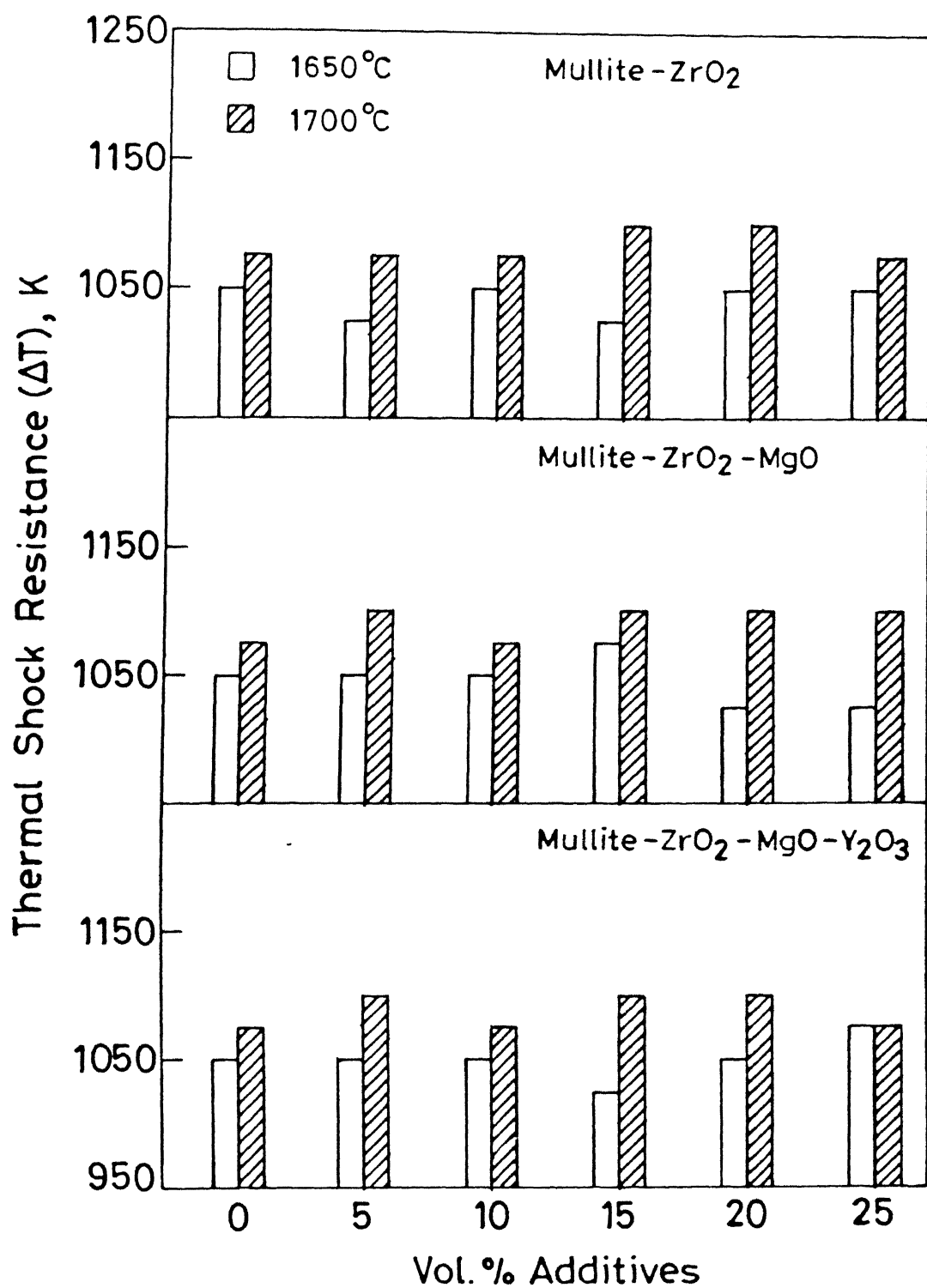
Fig. 3.41 Variation of thermal shock resistance of MC mullite based composites.
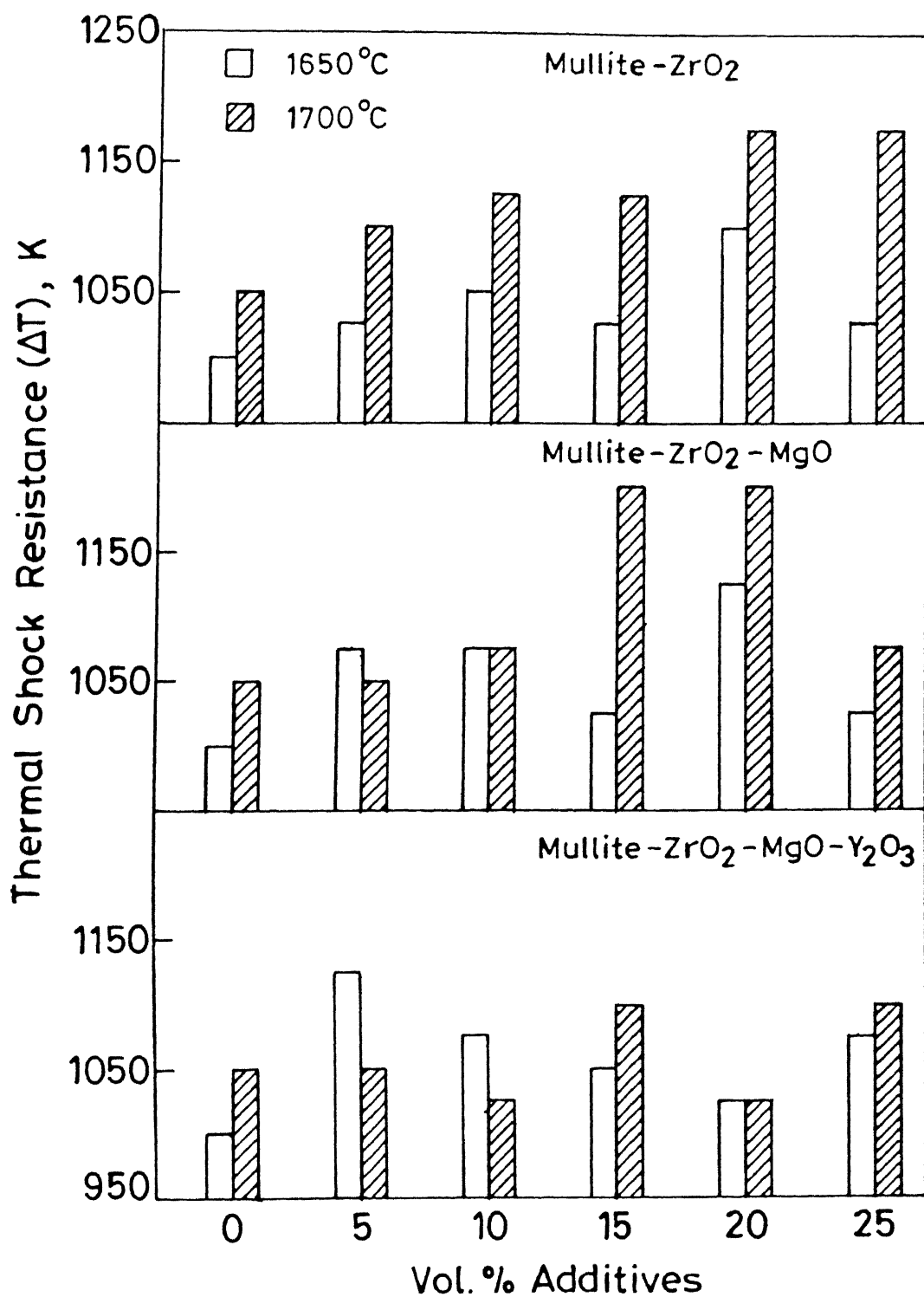
Fig. 3.42 Variation of thermal shock resistance of MP-20 mullite based composites.
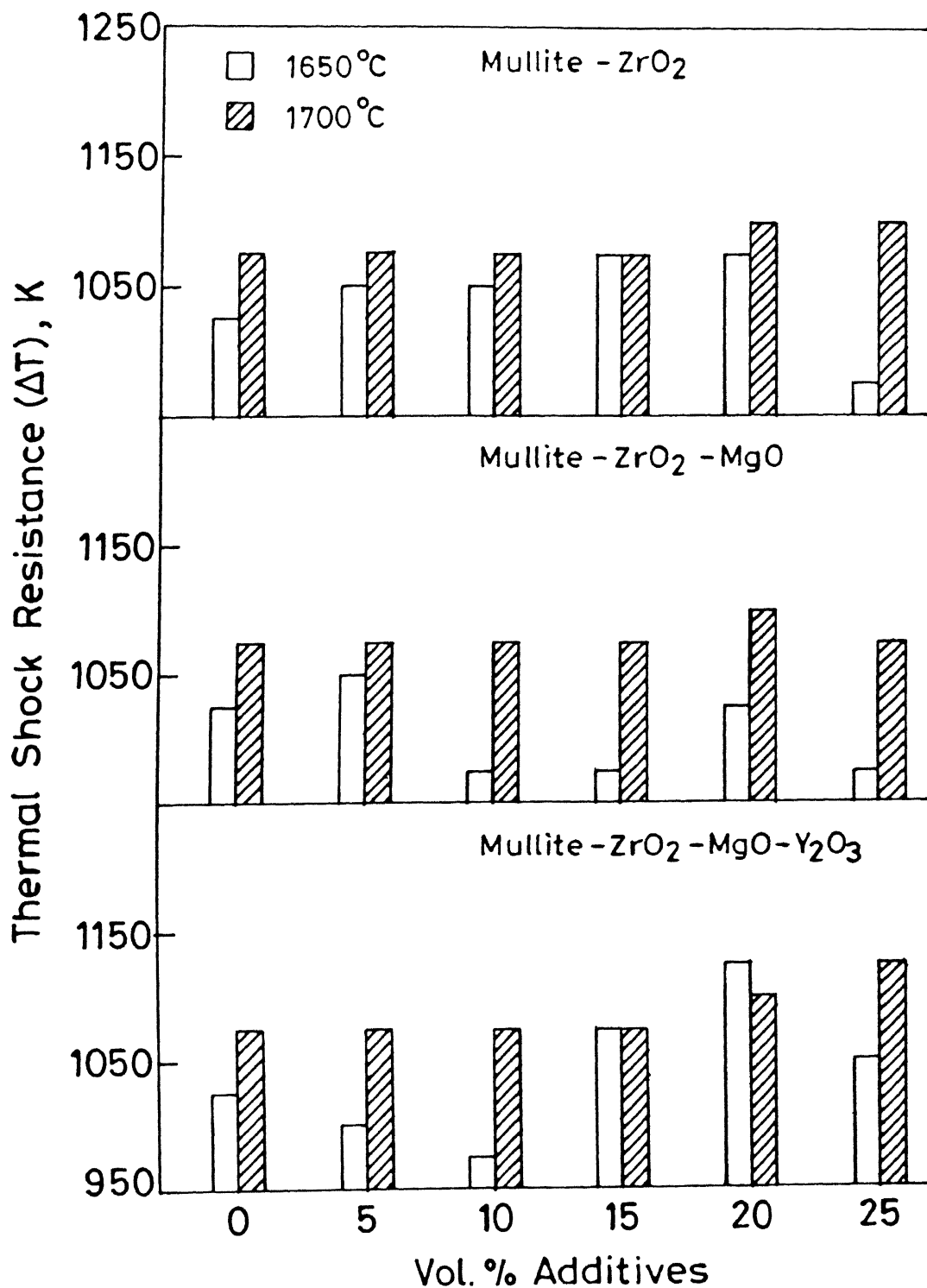
Fig. 3.43 Variation of thermal shock resistance of MP-40 mullite based composites.

CHAPTER IV

DISCUSSION

IV. 1   SINTERED MULLITES

Mullite ($3Al_2O_3 \cdot 2SiO_2$) is a solid solution of Al_2O_3 and SiO_2 containing 71.8% Al_2O_3 and 28.2% SiO_2. The solid solution ranges from $3Al_2O_3 \cdot 2SiO_2$ to $2Al_2O_3 \cdot SiO_2$ and melts incongruently at $1828°C$. Sintering and mechanical properties of mullite are very much dependent on its composition. The presence of impurities affects the sintering behaviour of this ceramic.

Sintering of mullite occurs mainly through solid-state sintering, where the driving force for densification is the lowering of the surface free energy by the elimination of solid-vapour interfaces. This usually takes place with the coincidental formation of new but lower-energy solid-solid interfaces. On a microscopic scale, the material transport is affected by the change in the free energy across a curved surface. If the particle size is small, these effects may be of a substantial magnitude. That is why finer particles sinter more rapidly than the coarser ones. On the other hand presence of small amount of impurities such as alkalies, Fe_2O_3, TiO_2, etc. which are often present in the starting mullite powder may lead to the formation of liquid phase during sintering. The amount and viscosity of this liquid phase are important for liquid phase sintering. Iron oxide and alkali impurities are known to have detrimental effects on the final products. They show tendency to demullitization at higher temperatures ($1700°C$) [7].

Higher sinter porosity (26%) of MC mullite than either MP-20 or MP-40 mullite (Table 3.1) reveals lower sinterability of fused

mullite (MC) over the sol-gel ones. This is due to the relatively larger particle size and as well as higher Al_2O_3 content of MC mullite as compared to MP-20 or MP-40 mullite (Section II.1.1). This is in accordance with the findings of Sacks and Pask [8], who reported lower sinterability for higher Al_2O_3 containing mullite than for the lower Al_2O_3 containing one. Present findings confirm that the sinterability increases with the increase in sintering temperature from 1650 to 1700°C, with the exception for MC mullite where sintered density remains same at either sintering temperature (Table 3.1). This may be attributed to the grain coarsening (Table 3.1, Fig. 3.3a) at higher sintering temperature, 1700°C.The stoichiometric mullite (MP-20) shows higher densification at lower sintering temperature (1650°C) than the MP-40 mullite due to its relatively lower particle size and lower Al_2O_3 content. However, the presence of lowest sintered porosity of MP-40 mullite after 1700°C sintering is not very clear. This may be due to the presence of TiO_2 impurity in MP-40 mullite which reacts with equal amount of excess Al_2O_3 to from Al_2TiO_5 [34] Al_2TiO_5 forms an eutectic at 1705-1715°C with TiO_2 [84]. In the present investigation, there a likelihood to form transient liquid phase during sintering (1700°C) leading to higher densification than MP-20 mullite which does not contain any TiO_2.

Literatures [4,5,79] have confirmed the existence of interlocked needle shaped mullite grains in presence of some extraneous liquid phase. However, Mazdiyasni [1] reported such type of grain morphology even in the absence of liquid phase. Elongated grains of MC mullite (Fig. 3.1a) observed in the present investigation may be attributed to the presence of liquid phase

during sintering because of the relatively high impurity content (2%). Unlike MC mullite MP-20 and MP-40 mullites show equiaxed microstructures (Fig. 3.1), confirming solid-state sintering.

Increase in transverse rupture strength (TRS) and fracture toughness with the increase in sintering temperature in all types of investigated mullites is due to the attainment of higher sintered density at higher sintering temperature with the exception for MC mullite (Table 3.1), where sintered porosity remains same. In absolute magnitude MP-20 mullite gives highest TRS and K_{IC} values among all the types of mullites investigated due to its smallest starting particle size. Lowest values for MC mullite is because of its largest starting particle size (Section II.1.1) and highest sintered porosity (Table 3.1) among all types of mullites investigated. A relatively higher TRS and K_{IC} values after 1700°C sintering without any associated change in sintered porosity in case of MC mullite may be attributed to more homogeneous resultant structure.

Dielectric constant (k') values obtained in the present investigation show a direct correlation with the sintered density, such that an increase in sintered density enhances the dielectric constant (Table 3.1). In absolute values the k' is lowest for MC mullite, because of its highest sintered porosity. Unlike MC mullite, k' values for either MP-20 or MP-40 mullite increase with the increase in sintering temperature. This is in accordance with the findings of Perry [4]. Al_2O_3 has higher k' values (8.6 – 10.55) than either SiO_2 (3.78) or pure mullite (6.60). MP-40 mullite, therefore, shows higher k' values than MP-20 mullite. MC mullite also contains higher Al_2O_3 than either MP-20 or MP-40

mullites, but lower sintered density is the main barrier in achieving higher k' values.

The increase in thermal shock resistance with the increase in sintering temperature may be attributed to the increase in sintered density. Alumina is known to have relatively lower thermal expansion coefficient ($7.2-8.6 \times 10^{-6}$/K) than SiO_2 ($12.3 - 21.0 \times 10^{-6}$/K). Thermal shock resistance (ΔT) of higher Al_2O_3 containing mullite i.e. MP-40, therefore, shows higher values than for MP-20. In case of MC mullite, although containing higher Al_2O_3 than MP-40, a lower sintered density appears to be responsible for the lower ΔT values.

IV.2 SINTERED MULLITE-ZrO_2 COMPOSITES THROUGH DIFFERENT ROUTES

The sintered properties of mullite – ZrO_2 composites prepared from fused (MC)/sol-gel (MP-20) mullite, and reaction sintering route (RSMZ) are discussed in this section. The properties of such composites are given in Table 3.2. Coming to the densification of mullite – ZrO_2 composites, occurring through solid-state sintering, it is found that the densification at any sintering temperature increases in the order of MC → RSMZ → MP-20. All the starting powders used for preparing the composites contain some impurities such as CaO, Na_2O, K_2O, Fe_2O_3, etc. The presence of small amount of liquid phase, during sintering originated because of such impurities, therefore, cannot be ruled out [79] as discussed in section IV.1. The lowest densification of MC mullite based composite may be due to the relatively larger particle size [Section II.1.1] of the precursor material. As the starting particle size of MP-20 mullite based composites is lowest [Section

II.1.1] among others, its based composites naturally densify to the maximum level. In case of RSMZ route densification starts before decomposition of zircon occurs [22]. Later on zircon dissociates into ZrO_2 and SiO_2 leading to dedensification. SiO_2, so formed traverses to the nearest Al_2O_3 particle to form mullite [22] leading to redensification. At the relatively lower sintering temperature, i.e. 1650°C, newly formed mullite grains, therefore, do not get sufficiently densified (Table 3.2).

As regards, mechanical properties, the role of fractional tetragonal ZrO_2 is found to be an important factor. It is well known that the tetragonal ZrO_2 (t - ZrO_2) helps to toughen the ceramics by its martensitic transformation to monoclinic ZrO_2 (m-ZrO_2) [80]. ZrO_2 particles greater than a critical size (1μm) are known to lead to a spontaneous transformation of tetragonal to the monoclinic structure [81] during post-sintering cooling. Decrease in tetragonal ZrO_2 fraction of all the composites with the increase in sintering temperature (Table 3.2) irrespective of the processing routes may be due to the aforesaid feature of the probability of increase in ZrO_2 particle size. Such a decrease (Table 3.2) manifests in lowering in the mechanical properties of the composites. Other factors like densification, microstructural homogeneity, etc. also play their roles in controlling the mechanical properties of the composites.

It is seen from the present results (Table 3.2) that transverse rupture strength (TRS) values of the composites increase in the order of RSMZ → MC → MP-20. In MC mullite based composite the increase in TRS after 1700°C sintering can be attributed to a more homogeneous microstructure (Fig. 3.6 and

The increase in fracture toughness (K_{IC}) with the increase in sintering temperature can be predominantly attributed to the microcrack toughening mechanism. Spontaneous transformation of t-ZrO_2 to m-ZrO_2 during post sintering cooling and release of strain caused by the coefficient of thermal expansion mismatch between mullite (5.7×10^{-6}/K) and ZrO_2 ($8.0 - 10.6 \times 10^{-6}$/K) are responsible for microcracking [27].

Microcracking in ceramic systems has a beneficial effect on fracture toughness with the result the K_{IC} of the composites increases with the increase in sintering temperature. The existence of a mullite - ZrO_2 solid-solution region at the matrix particle interface as observed by Osendi et al. [29] is also to be taken into account, which would increase K_{IC} values. They reported a significant solid solution formation of mullite in ZrO_2 which was measured by energy dispersive X-ray spectroscopy using transmission electron microscopy. Since the solid solution region is assumed to be a dissipation energy region it avoids the crack propagation and, hence, leading to higher toughness (Table 3.2) of the composites. A comparison of the literature data [66,67] for the reaction sintered route of similar powder characters as ours shows that K_{IC} values obtained presently (Table 3.2) is higher (2.52 MPa.m$^{1/2}$); although our sintered samples were more porous (21% porosity).

Coming to the dielectric constant (k'), it can be explained that the highest k' values for MP-20 mullite based composites among all types is due to the fine grain size of mullite matrix and the lower sintered porosity (Table 3.2). An increase in sintering temperature in case of any preparation route invariably

raises the k' values because of better densification. In case of MC mullite based composites, the increase in k' values with increased sintering temperature is mainly due to the better homogeneous microstructure (Fig. 3.6, 3.7) than due to any change in the sintered porosity.

It is evident from the results (Table 3.2) that the change in preparation route has little effect on thermal shock resistance. The increase in thermal shock resistance for MP-20 and RSMZ based composites with the increase in sintering temperature is attributed to higher densification of the composites. In the case of MC mullite based composites, although the sintered porosity is constant with the change in the sintering temperature, the formation of mullite-ZrO_2 solid-solution at the grain boundary at higher sintering temperature appears to arrest the crack propagation during thermal shock.

Unlike MC mullite (fused) based composites, fused mullite-38 vol% ZrO_2 composite shows inferior sintered properties (Table 3.3) because of its larger particle size of the starting prealloyed powder.

IV.3   EFFECTS OF ZrO_2 OR ITS MODIFIED FORMS' ADDITION ON SINTERED PROPERTIES OF MULLITES

Sintering behaviour of mullite ZrO_2 composites containing varying volume fractions of additives prepared from fused (MC) or sol-gel (MP-20 and MP-40) mullite powders, and their properties with respect to temperature are discussed in this section. The role of stabilizing oxides (MgO and Y_2O_3) in ZrO_2, on sintering of composites is also discussed.

IV. 3. 1   Densification Behaviour

Mullite - ZrO_2 composites mainly densify through solid-state sintering. The ZrO_2 powders in the present investigation contain 0.25 to 0.37% oxide impurities such as Na_2O, K_2O, Fe_2O_3, etc. (Section II.1). Mullite powders also contain some impurities which are highest (2%) in the case of MC mullite. Small amount of liquid phase formation, as a result of these impurities, during sintering, therefore, is enevitable [79]. The decrease in sintered porosity for MC mullite (Fig. 3.13) with the increase in vol% additive as well as sintering temperature confirms the increased sinterability of the composites. This sinterability increases in the order of ZrO_2 → ZrO_2-MgO → ZrO_2-MgO-Y_2O_3 addition. ZrO_2 additives retard the grain growth of mullite (Fig. 3.32, 3.33 top) and promotes densification, which supports the findings of Prochazka et al. [82]. Leriche [63] showed that unlike straight ZrO_2 containing composites, MgO modified ZrO_2 containing ones exhibit the presence of intergranular glassy phase which favours the grain growth of mullite matrix. Ismail et al. [5] also reported the mullite grain growth in the presence of liquid phase. Such a feature in the present study in presence of MgO and MgO-Y_2O_3 modified ZrO_2 may be due to the aforesaid reason. The present findings also confirm the enhanced sinterability of MgO and MgO-Y_2O_3 containing composites (Fig. 3.13) as compared to straight ZrO_2 containing ones possibly due to the presence of intergranular liquid phase. A unique feature in this type of composites is the elongated nature of mullite grains as evidenced in Fig. 3.23, 3.26, 3.27. This may be because of higher amount of oxide impurities (2%) in MC mullite powders than in either MP-20

or MP-40 mullite. Furthermore, the decrease in the total sintered porosity with the increase in vol% additive may be due to the filling up of large voids of mullite grains by the relatively small particle size additive powders.

Coming to the composites prepared from MP-20 mullite, enhanced densification due to formation of liquid phase is not so prominent as in case of MC mullite based composites, because of the less amount of impurities in such mullites. As a result no regular trend of increase in densification with increase in vol% additive (Fig. 3.14) is observed. In case of composites sintered at 1650°C enhanced densification is observed upto 10 vol% additive (Fig. 3.14). Higher amount of additives lead to coarsening of ZrO_2 particles (Fig. 3.24) causing poor densification. This may be due to the decreased ZrO_2-ZrO_2 interparticle spacing and the increased chances of ZrO_2 particles touching each other, leading to particle growth [83]. In case of MgO/Y_2O_3 modified ZrO_2 containing composites, unlike straight ZrO_2 containing ones the matrix grains at higher vol% additives are elongated (l/d = 2.8), which may be due to the possibility of enhanced liquid phase during sintering [5,63]. However, increased sintering temperature (1700°C) shows adverse effect on sinterability (Fig. 3.14) which may be associated to the grain growth of both mullite and ZrO_2 particles (Fig. 3.32-3.34).

MP-40 mullite based composites sintered at 1650°C,like MC based ones show increased densification with the increase in vol% additive. This is because of the enhanced densification as stated earlier. The enhancement of densification with addition of MgO/Y_2O_3 modified ZrO_2 in the composites supports the findings of

Yuan et al. [32] and Leriche [63]. Higher amounts of densification for MgO-Y$_2$O$_3$ modified composites is due to the combined effect of MgO and Y$_2$O$_3$ in enhancing the sinterability. An increase in the sintering temperature has not much effect on sinterability (Fig. 3.15) which may be due to the coarsening of mullite grains as well as ZrO$_2$ particles (Fig. 3.32-3.34).

In conclusion sol-gel mullite based composites densify better than fused mullite based ones, because of smaller starting particle size of the former powders.

IV.3.2   Mechanical Properties

In influencing the mechanical properties of mullite-ZrO$_2$ composites, the fractional tetragonal ZrO$_2$ (t-ZrO$_2$) plays an important factor. Under the effect of stress tetragonal-ZrO$_2$ transforms into monoclinic form leading to increase in mechanical properties [80]. This has been discussed in detail in section IV.2. The decrease in t-ZrO$_2$ with the increase in vol% additive, (Fig. 3.35-3.37) leads to a spontaneous transformation of t-ZrO$_2$ to m-ZrO$_2$ [81] during post sintering cooling because of its increased particle size above a critical value. In the present investigation such sizes of ZrO$_2$ particles (>1 μm) are observed (Fig. 3.26-3.31). At higher sintering temperature (1700°C) the decreasing trend of t-ZrO$_2$ with increasing vol% additives is more pronounced than at 1650°C sintering, because of higher chances of ZrO$_2$ particle coarsening above the critical level. Other than the critical ZrO$_2$ particle size factor, stabilizing agents viz. MgO and Y$_2$O$_3$ help in retaining t-ZrO$_2$ after post sintering cooling [80]. As a result, in MgO/Y$_2$O$_3$ modified ZrO$_2$ containing composites higher fraction of t-ZrO$_2$ is observed than in the

straight ZrO_2 containing ones (Fig. 3.35 - 3.37). Highest amount of fractional tetragonal phase in $MgO-Y_2O_3$ modified ZrO_2 containing composites, irrespective of the types of mullite powders at either sintering temperature, is due to the combined stabilizing effect of both the oxides i.e. MgO and Y_2O_3.

Coming to the transverse rupture strength of the composites, the marginal increase in TRS in case of MC mullite based composites (Fig. 3.16) at either sintering temperature appears to be dictated predominantly by the enhanced densification as otherwise one normally expects a fall in strength with decrease in t-ZrO_2 fraction. Increased sintering temperature (1700°C), obviously leads to the higher values of TRS owing to the higher densification (Fig. 3.13). The varying roles of MgO and Y_2O_3 in modifying ZrO_2 is not clearly reflected in the property, probably due to the fact that powder characters of modified ZrO_2 are different than that of unmodified ZrO_2 (Section II.1).

Apart from the strengthening due to the dispersioids, the increase in TRS of MP-20 based composites with the initial increase in vol% additive (Fig. 3.17, 3.18) may be attributed to the associated stress-induced transformable t-ZrO_2 in the composites [27]. At a still higher vol% additives (beyond the maximum in the plot), the size of ZrO_2 particles in the sintered composites increases (Fig. 3.29), because of the increased chances of their coarsening [83]. Coarsening of ZrO_2 particles above a critical level [81] and extensive microcracking [27] as discussed in section IV.2 result in reduced transverse rupture strength. An increase in the sintering temperature from 1650°C to 1700°C increases the TRS values because of the increased densification,

albeit with some scatter.

MP-40 mullite based composites sintered at 1700°C show identical trend similar to MP-20 based ones and hence same type of arguments are also applicable here. The increase in TRS values with the increase in vol% additive for the composites sintered at 1650°C is mainly linked to the increased sinterability of the composites (Fig. 3.15).

In absolute magnitude, the TRS values are lowest in MC mullite based composites due to its largest matrix grain size and % total porosity. Again owing to the lower starting particle size, MP-20 mullite based composites show higher values of TRS than MP-40 based ones. Even a slight change in the composition of stoichiometric mullite (Al_2O_3/SiO_2 = 1.5) powder (MP-20) to alumina rich side i.e., MP-40 mullite (Al_2O_3/SiO_2 = 1.51) shows a specific trend of increased TRS in the order of $ZrO_2 \rightarrow ZrO_2$-MgO $\rightarrow ZrO_2$-MgO-Y_2O_3 additives at either sintering temperature. This confirms the increased stabilizing effect of MgO and MgO-Y_2O_3 (Fig. 3.37) in ZrO_2, which supports the findings of Yuan et al. [32] and Leriche [63].

It is well known in mullite matrix systems that fracture toughness (K_{IC}) is not dependent on their grain size, but is controlled by the size and structure of ZrO_2 particles within the matrix [27]. Three types of toughening mechanisms would have contributed to the increase in fracture toughness. They are microcrack toughening caused by spontaneous transformation of ZrO_2 from tetragonal to monoclinic during post sintering cooling, crack deflection and stress induced transformation toughening of metastable t-ZrO_2. Microcracking and crack deflection being the

most predominant factors in K_{IC}, the toughness of all the composites increases with the increase in vol% additive irrespective of the type of matrix powders (Fig. 3.20 - 3.22). The existence of a mullite-ZrO_2 solid solution region as observed by Osendi et al. [29] at the matrix/ZrO_2 interface, discussed in section IV-2, would also increase the K_{IC} values. In the present investigation, the chemical analysis results of ZrO_2 near the mullite grain boundaries (Table 3.4) qualitatively infers the existence of interdiffusivity of ZrO_2 in mullite and vice versa leading to the formation of solid solution. Higher K_{IC} values for MgO and MgO-Y_2O_3 modified ZrO_2 containing composites than for straight ZrO_2 containing ones (MP-20 and MP-40 mullites) (Fig. 3.21, 3.22) may be attributed to the crosslinked microstructure of mullite matrix [63] apart from the effect of transformable t-ZrO_2. This has also been noticed to some extent in the present investigation (Fig. 3.28-3.31).

IV.3.3 Dielectric Constant

Coming to dielectric constant (k'), the increasing trend is due to combined effect of ZrO_2 content having high dielectric constant of 12 (in contrast to pure mullite, k' = 6.6) and the enhanced densification. This is true for all types of presently selected mullite powders. In the case, where densification does not increase with vol% additives, the increase in dielectric constant can be attributed to the high dielectric constant of the additives themselves. Because of this, composites sintered at 1700°C exhibit increase in dielectric constant (Fig. 3.40 bottom) despite lower densification (Fig. 3.15 bottom). The lowest k' values for MC mullite based composites are due to highest sintered

orosities (Fig. 3.13) and largest starting matrix particle size.
ince dielectric constant of Al_2O_3 (8.60-10.55) is higher than
hat of pure mullite (6.60), composite containing an excess
lumina possesses higher dielectric constant. This is the reason
hy MP-40 based composites have higher dielectric constants than
P-20 based ones. MC mullite also contains higher Al_2O_3 than
P-40 one, but lower sintered porosities of this type of composite
s the main barrier to achieve higher k' values [4] apart from the
atrix grain size effect.

V.3.4   Thermal Shock Resistance

Thermal shock resulting due to inhomogeneous temperature
istribution throughout the body, results into generation of
trains and stresses which may cause cracking and failure. In
eneral, cracking will be initiated when the maximum tensile
hermal stress in the material reaches the fracture stress as
easured under conditions appropriate to the thermal shock in
erms of temperature, environment, starting stress and duration of
tress.

In ZrO_2 containing composites, it has been stated [85] that
iicrocracks produced during the phase transformation of tetragonal
;rO$_2$ to monoclinic during thermal cycling interacts with the local
;tress field of the transforming particles and hence could be
irrested. Hasselman [86] suggested that such microcracks would
iropagate quasistatically in response to thermal stresses. In
ither words, if there is a sufficient density of microcracks, they
iropagate in a stable fashion so that rather than a sudden
reduction in strength, thermal shock would lead to only a gradual
reduction in strength.

In the present investigation, the variation of thermal shock esistance is little influenced by the type of matrix and additive owders at either sintering temperatures (Fig. 3.41--3.43). This ay be due to the microcracks formed owing to the thermal xpansion coefficient mismatch between mullite (5.7×10^{-6}/K) and artially stabilized ZrO_2 ($8.0-10.6 \times 10^{-6}$/K). In general an mproved thermal shock resistance of composites, sintered at igher temperature is attributed to better sinterability.

CHAPTER V

CONCLUSIONS

From the investigations, carried out in the present study ollowing conclusions can be drawn:

.   Sinterability of electrofused mullite is lower than that of sol-gel mullites. Extraneous liquid phase leads to the elongated nature of mullite grains.

.   Transverse rupture strength and fracture toughness of mullites increase with increase in sintering temperature. Stoichiometric sol-gel mullite gives highest mechanical properties.

.   Dielectric constant of mullites has a direct relation with sintered density, such that an increase in sintered density increases the dielectric constant. Higher Al_2O_3 containing mullites give higher dielectric constant.

.   Higher Al_2O_3 containing mullites exhibit higher thermal shock resistance such that it increases in the order of MP-20 → MP-40 → MC mullites.

5. Full reaction sintering of mullite-(25 vol%) ZrO_2 composite occours at 1700°C with homogenized microstructure. However, sintered properties of this composite is not better than sol-gel mullite based composite containing equal volume fraction of ZrO_2.

6. Fused mullite- (38 vol%) ZrO_2 prealloyed composite shows inferior sintered properties as compared to fused MC mullite based composite. This is related to the larger particle size of the former powder.

7. Mullite-ZrO_2 composites mainly sinter through solid-state sintering mechanism. Some extraneous liquid phase due to the presence of oxide impurities, however, leads to enhanced densification being more pronounced in fused mullite based composites. MgO/Y_2O_3 modified ZrO_2 containing composites sinter better than unmodified ZrO_2 containing ones.

8. MgO containing mullite-ZrO_2 composites exhibit interlocked grain structure of mullite phase, which is not so in case of straight ZrO_2 addition. Mullite grain size increases with the increase in vol% additive and sintering temperature.

9. Retention of tetragonal ZrO_2 after sintering decreases with the increase in vol% additive and sintering temperature. The relative content of this phase increases in the order of ZrO_2 → ZrO_2-MgO → ZrO_2-MgO-Y_2O_3 additives in the composites.

10. Transverse rupture strength (TRS) of fused mullite-ZrO_2 composites increase marginally with the increase in vol% additives and sintering temperature. Sol-gel mullite based composites show maxima in TRS variation, which appears at different compositions for different additives with the exception for MP-40 mullite based one, sintered at $1650^{\circ}C$. MP-20 mullite based composites show highest TRS values.

11. Fracture toughness (K_{IC}) of mullite ZrO_2 composites increases with the increase in vol% additives. Microcrack toughening appears to be the main toughening mechanisms of such composites. Highest K_{IC} values are obtained for MP-20 mullite based composites.

2. Fracture mode for mullite-ZrO_2 composites is mainly intergranular in nature.

3. Dielectric constant (k′) exhibits a direct relation with the sintered density of mullite-ZrO_2 composites irrespective of the type of mullite powders, such that the values increase with the increase in sintered density. Lower grain size and higher Al_2O_3 containing mullite matrix composites show higher values of dielectric constant.

4. Different types of mullite and ZrO_2 powders appear to show little effect on thermal shock resistance. A higher sintering temperature (1700°C) does have a positive role in increasing the thermal shock resistance of the composites.

REFERENCES

- K. S. Mazdiyasni and L. M. Brown, "Synthesis and Mechanical Properties of Stoichiometric Aluminium Silicate (Mullite)", J. Am. Cer. Soc., 55(11), 1972, 548-52.

- H. Adkins, "Selective Activation of Alumina for Decarboxylation or for Dehydration", J. Am. Chem. Soc., 44, 1922, 2175-86.

- D. C. Bradley, R. C. Mehrotra and W. Wardlaw, "Structural Chemistry of the Alkoxides: III", J. Chem. Soc., London, 1952, 5020-23.

- G. S. Perry, "Microwave Dielectric Properties of Mullite", Trans. Brit. Cer. Soc., 72, 1973, 279-283.

- M.G.M.U. Ismail, Z. Nakai, H. Ohira and S. Somiya, "Preparation and Characterization of Mullite Containing Materials", Ceramic Transactions, 1(3), 1988. 1108-1114.

- B. L. Metcalfe and J.H. Sant, "The Synthesis, Microstructure and Physical Properties of High Purity Mullite", Trans. Brit. Cer. Soc., 74(6), 1975., 193-201.

- P. Reynen and M. Faizullah, "Sintering of Mullite", in "Sintering and New Developments", ed. M. M. Ristic, Elesevier, North Holland Inc., 1979, p. 178-94.

- M.D. Sacks and J.A. Pask, "Sintering of Mullite Containing Materials : I, Effects of Composition", J. Am. Cer. Soc., 65(2), 1982, 65-70.

- J.S. Moya, C.J. Cerna and J.E. Iglesias, "On the Formation of Mullite from Kandites", J. Mat. Sc., 20, 1985, 32-36.

0. J. Ma Rincon and G. Thomas, "Microstructural Study of Sintered Mullite Obtained from Premullite", J. Am. Cer. Soc., 69(2), 1986, C29-C31.

1. M. D. Sacks and J. A. Pask, "Sintering of Mullite Containing Materials : II, Effect of Agglomeration", J. Am. Cer. Soc., 65(2), 1982, 70-77.

2. M.G.M.U. Ismail, Z. Nakai, K. Minegishi, "Synthesis of Mullite Powder and its Characteristics", Int. J. High Tech. Cer., 2, 1986, 123-134.

3. M.G.M.U. Ismail, Z. Nakai and S. Somia, "Microstructure and Mechanical Properties of Mullite Prepared by the Sol-Gel Method", J. Am. Cer. Soc., 20 (1), 1987, C7-C8.

14. T.I. Mah and K. S. Mazdiyasni, "Mechanical Properties of Mullite", J. Am. Cer. Soc., 66(10), 1983, 699-703.

15. R. A. Penty, D. P. H. Hasselman and R. M. Spriggs, "Young's Modulus of High-Density Polycrystalline Mullite", J. Am. Cer. Soc. 55(3), 1972, 169-70.

16. P. A. Lessing, R. S. Gordon and K. S. Mazdiyasni, "Creep of Polycrystalline Mullite", J. Am. Cer. Soc., 58(3-4), 1975, 149.

17. P. C. Dokko and J. A. Pask, "High Temperature Mechanical Properties of Mullite Under Compression", J. Am., Cer. Soc., 60(3-4), 1977, 150-55.

18. N. Claussen and J. Jahn, "Mechanical Properties of Sintered, In Situ-Reacted Mullite-Zirconia Composites", J. Am. Cer. Soc., 63(3-4), 1980, 228-29.

19. P. Boch and J. P. Giry, "Preparation and Properties of Reaction - Sintered Mullite-ZrO_2 Ceramics", Mat. Sc. Engg., 71, 1985, 39-48.

20. C.B. De La. Lastra, C. Leblud, A. Leriche, F. Chambier and M. R. Anseau, "K_{IC} Calculations for Some Mullite-Zirconia Composites Prepared by Reaction Sintering", J. Mat. Sc. Lett., 4, 1985, 1099-1101.

21. P. Boch and J. P. Giry, "Preparation of Zirconia-Mullite Ceramics by Reaction Sintering", in "High Tech. Ceramics", ed. P. Vincenzini, Elsevier Science Publishers B.V., Amsterdam, 1987, 851-59.

22. J. V. Emiliano and A.M. Segadaes, "Reaction-Sintered Mullite-Zirconia Composites : Mechanism and Properties", in "Zirconia - 88: Advances in Zirconia Science and Technology", ed. S. Meriani and C. Palmonari, Elsevier Applied Science, Barking, 1988, 51 - 65.

23. M. Holmstrom, T. Chartier and P. Boch, "Reaction-Sintered ZrO_2 - Mullite Composites" in "Ceramic Materials Research-I", ed. R.J. Brook, E-MRS, North Holland, Amsterdam, 1989, 105-109.

24. J. S. Moya and M. I. Osendi, "Effect of ZrO_2 (ss) in Mullite on the Sintering and Mechanical Properties of Mullite /ZrO_2 composites", J. Mat. Sc. Lett., 2, 1983, 599-601.

25. Qi-Ming Yuan, Jia-Qi Tan and Jheng-Guo Jin, "Preparation and Properties of Zirconia - Toughened Mullite Ceramics", J. Am. Cer. Soc., 69(3), 1986, 265-67.

26. R. McPherson, "Preparation of Mullite-Zirconia Composites from Glass Powder", J. Am. Cer. Soc. 69(3), 1986, 297-98.

27. M.G.M.U. Ismail, Z. Nakai and S. Somia, "Properties of Zirconia-Toughened Mullite Synthesized by the Sol-Gel Method", in "Advances in Ceramics, Vol. 24 : Science and Technology of Zirconia III", The American Ceramic Society, Westerville, 1988, 119-25.

28. E.Di Ripo and M. R. Anseau, "Solid State Reactions in the ZrO_2-SiO_2-α Al_2O_3 System", J. Mat. Sc., 15, 1980, 114-18.

9. M.I. Osendi, P. Miranzo and J. S. Moya, "Solid-Solution Effects on the Fracture Toughness of Mullite-ZrO_2 Composites", J. Mat. Sc. Lett., 4, 1985, 1026-28.

0. D. Lewis, R. P. Ingel, W.J. McDonoughs and R. W. Rice, "Microstructure and Thermomechanical Properties in Alumina-and Mullite-Boron-Nitride Particulate Ceramic-Ceramic Composites", in "Ceramic Engineering and Science Proceedings", 2(7-8), 1981, 719-27.

1. G. Orange, G. Fantozzi, F. Chambier, C. Leblud, M. R. Anseau and A. Lerichie, "High Temperature Mechanical Properties of Reaction-Sintered Mullite/Zirconia and Mullite/Alumina /Zirconia Composites", J. Mat. Sc., 20, 1985, 2533-40.

2. Qi-Ming Yuan, Jia-Qi Tan, Ji-Yao Shen, Xuan-Hui Zhu and Zheng-Fang Yang, "Processing and Microstructure of Mullite - Zirconia Composites Prepared from Sol-Gel Powders", J. Am. Cer. Soc., 69(3), 1986, 268-69.

3. P. Pena, M. A. Rodriguez, J. S. Moya and S. De Aza, "Zirconia-Mullite-Alumina Composites Obtained by Reaction Sintering in the Presence of Calcium Oxide", in "High Tech Ceramics", ed. P. Vincenzini, Elsevier Science Publishers B. V., Amsterdam, 1987, 861-70.

4. M.F. Melo and J. S. Moya, "Ageing Effect on Microstructural and Mechanical Properties of Mullite-ZrO_2-TiO_2 composites", in "Zirconia-88 : Advances in Zirconia Science and Technology", ed. S. Meriani and C. Palmonari, Elsevier Applied Science, Barking, 1988, 67-79.

5. A. Leriche, M. Vivey and F. Chambier, "Preparation of Mullite-Zirconia Ceramics by Reaction Sintering Study of their Thermomechanical Properties", in "Technical Ceramics", ed. H. Nosbusch and I. V. Mitchell, Elsevier Sc. Pub. Ltd., Barking, 1988, 215-21.

6. A. Leriche, P. Descamps and F. Chambier, "High Temperature Mechanical Behaviour of Mullite Zirconia Composites Obtained by Reaction Sintering", in "Zirconia - 88 : Advances in Zirconia Science and Technology", ed. S. Meriani and C. Palmonari, Elsevier Applied Science, Barking, 1988, 137-51.

37. M. F. Melo and M. O. Figueiredo, "Behaviour of Titanium in Mullite-Zirconia Composites", in "Ceramic Materials Research-I", ed. R. J. Brook, E-MRS, North Holland, Amsterdam, 1989, 61-68.

38. J. S. Moya, P. Miranzo and M. I. Osendi, "Influence of additives on the Microstructural Development of Mullite-ZrO_2 and Alumina-ZrO_2", in "Ceramic Materials Research-I", ed. R. J. Brook, E-MRS, North Holland, Amsterdam, 1989, 139-44.

39. M. J. Hoffmann, H. Liu and G. Petzow, "Processing and Mechanical Properties of SiC whisker Reinforced Mullite ($-ZrO_2$)-Composites", in "Metal and Ceramic Matrix Composites : Processing, Modelling and Mechanical Behaviour", ed. R. B. Bhagat, A. H. Clauer, P. Kumar and A. M. Ritter, TMS, Warrendale, 1990, 177-84.

40. H. Suzuki, H. Morimitsu and H. Saito, "Sintering Behaviour of Alkoxy-Derived Mullite Compacts", in "Sintering '87, Vol. 1", ed. S. Somiya, M. Shimada, M. Yoshimura and R. Watanabe, Elsevier Applied Science, Barking, 1987, 120-26.

41. B E. Yoldas, "Mullite Formation from Aluminium and Silicon Alkoxides", in "Ceramic Transaction Vol.6 : Mullite and Mullite Matrix Composites",ed. S. Somiya, B. F. Davis and J. A. Pask, The American Ceramic Society, Inc., Westerville, 1990, 255-62

42. H. Suzuki, H. Saito, Y. Tomokiyo and Y. Suyama, "Processing of Ultrafine Mullite Powder through Alkoxide Route, in "Ceramic Transactions, Vol. 6 : Mullite and Mullite Matrix Composites", ed. S. Somiya, R. F. Davis, J. A. Pask, The American Ceramic Society, Inc., Westerville, 1990, 263-74

43. S. Mitachi, M. Matsuzawa, K. Kaneko, S. Kanzaki and Y. Tabata, "Characterization of SiO_2-Al_2O_3 Powders Prepared from Metal Alkoxides", in "Ceramic Transaction Vol.6 : Mullite and Mullite Matrix Composites ", ed. S. Somiya, R. F. Davis and J. A. Pask, The American Ceramic Society, Inc., Westerville, 1990, 275-86.

44. S. Somiya, M. Yoshimura, M Suzuki and T. Yamaguchi, "Mullite powder from Hydrothermal Processing", in "Ceramic Transactions, Vol. 6 : Mullite and Mullite Matrix Composites", ed. S. Somiya, R. F. Davis and J. A. Pask, The American Ceramic Society, Inc. Westerville, 1990, 287-310.

45. L. Man and W. Xitang, "Investigation on Mullite Prepared from Refined Bauxite" in "Ceramic Transactions, Vol. 6: Mullite and Mullite Matrix Composites", ed. S. Somiya, R. F. Davis and J. A. Pask, The American Ceramic Society Inc. Westerville, 1990, 457-62.

46. M. Mizuno, "Microstructure, Microchemistry and Flexural Strength of Mullite Ceramics", J. Am. Cer. Soc., 74(12), 1991, 3012-22.

47. D. J. Lewis, "Technique for Producing Mullite and Other Mixed-Oxide Systems", J. Am. Cer. Soc., 74 (10), 1991, 2410-13.

48. N. Ushifusa and M. J. Cima, "Aqueous Processing of Mullite-Containing Green Sheets", J. Am. Cer. Soc., 74 (10),1991, 2443-47.

49. S. Komarneni and R. Roy, "Mullite Derived from Diphasic Nanocomposite Gels", in "Ceramic Transactions, Vol. 6: Mullite and Mullite Matrix Composites", ed. S. Somiya, R. F. Davis and J. A. Pask, The American Ceramic Society, Inc. Westerville, 1990, 209-220.

50. J. C. Huling and G. L. Messing, "Surface Chemistry Effects on Homogeneity and Crystallization of Colloidal Mullite Sol-Gels" in "Ceramic Transactions, Vol. 6: Mullite and Mullite Matrix Composites", ed. S. Somiya, R. F. Davis and J. A. Pask, The American Ceramic Society, Inc., Westerville, 1990, 221-30.

51. M.G.M.U. Ismail, Z. Nakai and S. Somiya "Sintering of Mullite Prepared by Sol-Gel Method", in "Ceramic Transactions, Vol. 6 : Mullite and Mullite Matrix Composites" ed. S. Somiya, R. F. Davis and J. A. Pask, The American Ceramic Society, Inc., Westerville, 1990, 231-42.

52. S. Sundaresan and I. A. Aksay, "Mullitization of Diphasic Aluminosilicate Gel", J. Am. Cer. Soc., 74 (10), 1991, 2388-92.

53. D. X. Li and W. J. Thomson, "Mullite Formation from Nonstoichiometric Diphasic Precursor", J. Am. Cer. Soc., 74(10), 1991, 2382-87.

54. A. P. Hynes and R. H. Doremus, "High-Temperature Compressive Creep of Polycrystalline Mullite", J. Am. Cer. Soc., 74(10), 1991, 2469-75.

55. E. A. Richards, C.J. Goodbrake and G. Sowman, "Reaction and Microstructure Development in Mullite Fibers", J. Am. Cer. Soc., 74(10), 1991, 2404-09.

56. J. A. Pask and A. P. Tomsia, "Formation of Mullite from Sol-Gel Mixtures and Kaolinite", J. Am. Cer. Soc., 74(10), 1991, 2367-73.

57. P. Boch, T. Chartier and P. D. D. Rodrigo, "High-Purity Mullite Ceramics by Reaction Sintering" in "Ceramic Transactions, Vol. 6: Mullite and Mullite Matrix Composites", ed. S. Somiya, R. F. Davis and J. A. Pask, The American Ceramic Society, Inc., Westerville, 1990, 353-374.

58. S. Wu and N. Claussen, "Fabrication and Properties of Low-Shrinkage Reaction-Bonded Mullite", J. Am. Cer. Soc., 74 (10), 1991, 2460-63.

59. K. S. Mazdiyasni, "Preparation and Characterization of Mullite Powders from Alkoxides and other Chemical Routes", in "Ceramic Transactions,, Vol. 6: Mullite and Mullite Matrix Composites", ed. S. Somiya, R. F. Davis and J. A. Pask, The American Ceramic Society, Inc., Westerville, 1990, 243-53.

60. P. Boch and J. P. Giry, "Zirconia-Toughened Mullite Ceramics - The Role of Zirconia Dissociation", in "Ceramic Transactions, Vol. 6 : Mullite and Mullite Matrix Composites", ed. S. Somiya, R. F. Davis and J. A. Pask, The American Ceramic Society, Inc., Westerville, 1990, 473-94.

61. P. Boch and T. Chartier, "Tape Casting and Properties of Mullite and Zirconia-Mullite Ceramics", J. Am. Cer. Soc., 74(10), 1991, 2448-52.

62. M. Yoshimura, T. Noma, Y. Hanaue and S. Somiya, "Zirconia Dispersed Mullite Ceramics Through Hot-Pressing of Amorphous ZrO_2-SiO_2-Al_2O_3 Obtained by Rapid Quenching", in "Materials Research Society, Vol. 78 : Advanced Structural Ceramics", ed. P. F. Becher, M. V. Swain and S. Somiya, MRS, Pittsburgh, Pennsylvania, 1987, 165-72.

63. A. Leriche, "Mechanical Properties and Microstructures of Mullite Zirconia Composites", in "Ceramic Transactions, Vol. 6 : Mullite and Mullite Matrix Composites", ed. S. Somiya, R. F. Davis and J. A. Pask, The American Ceramic Society, Inc., Westerville, 1990, 541-52.

64. J. S. Moya and P. Miranzo, "Influence of Processing Method on Microstructural and Mechanical properties of R. S. Mullite/ZrO_2 Composites", in "High Tech Ceramics", ed. P. Vincenzini, Elsevier Science Publishers B.V., Amsterdam, 1987, 1317-24.

65. P. Descamps, S. Sakaguchi, M. Poorteman and F. Cambier, "High-Temperature Characterization of Reaction-Sintered Mullite-Zirconia Composites", J. Am. Cer. Soc., 74(10), 1991, 2476-81.

66. K. Das, B. Mukherjee and G. Banerjee, "Mechanical Properties and Microstructural Character of Isopressed Reaction Sintered Mullite-Zirconia Composites", Trans. Ind. Cer. Soc., 52(2), 1993, 47-50.

67. K. Das, B. Mukherjee and G. Banerjee, "Preparation and Characterization of Reaction Sintered Zirconia-Mullite Composites", Trans. Ind. Cer. Soc., 52(4), 1993, 135-38.

68. S. Shiga, H. Tsunatori, M.G.M.U. Ismail and K. Katayama, "Synthesis and Sintering of MgO Doped Mullite/ZrO_2 Composite Powder Using the Sol-Gel Method", J. Cer. Soc. Jpn., 100(2), 1992, 128-33.

69. J. S. Moya, "Reaction Sintering of Mullite-ZrO_2 and Mullite-ZrO_2-SiC Ceramics", in "Ceramic Transactions, Vol. 6: Mullite and Mullite Matrix Composites", ed. S. Somiya, R. F. Davis and J. A. Pask, The American Ceramic Society, Inc., Westerville, 1990, 495-508.

70. M. N. Rahaman and D-Y. Jeng, "Sintering of Mullite and Mullite Matrix Composites" in "Ceramic Transactions : Sintering of Advanced Ceramics", ed. C. A. Handwerker and J. E. Blendell, The American Ceramic Society Inc., Westerville, 1989, 753-66.

71. T. N. Tiegs, P. F. Becher, and P. Angelini, "Microstructures and Properties of SiC whisker Reinforced Mullite Composites", in "Ceramic Transactions, Vol. 6: Mullite and Mullite Matrix Composites", ed. S. Somiya, R. F. Davis and J. A. Pask, The American Ceramic Society, Inc., Westerville, 1990, 463-72.

72. R. Ruh, K. S. Mazdiyasni and A. Zangvil, "Mullite-SiC-Whisker-Reinforced Ceramic Composites : Characterization and Properties", in "Fiber Reinforced Ceramic Composites : Materials, Processing and Technology", ed. K. S. Mazdiyasni, Noyes Publications, New York, 1990, 328-41.

73. H. Takada, A. Nakahira, H. Ohnishi, S. Ueda and K. Niihara, "Improvement of Mechanical Properties of Natural Mullite / SiC Nanocomposites", J. Jpn. Soc. Powd. and Powd. Met., 38(3), 1991, 36-39.

74. C. Nischik, M. M. Seibold, N.A. Travilzky and N. Claussen, "Effect of Processing on Mechanical Properties of Platelet-Reinforced Mullite Composites", J. Am. Cer. Soc. 74(10), 1991, 2464-68.

75. M. D. Sacks, N. Bozkurt and G. W. Scheiffele, "Fabrication of Mullite and Mullite-Matrix Composites by Transient Viscous Sintering of Composite Powders", J. Am. Cer. Soc., 74(10), 1991, 2428-37. Also in "Ceramic Transactions Vol. 19: Advanced Ceramic Materials", ed. M. D. Sacks, The American Ceramic Society, Inc., Westerville, 1991, 111-23.

76. D. R. Larson, J. A. Coppola and D.P.H. Hasselman, "Fracture Toughness and Spalling Behaviour of High-Al_2O_3 Refractories", J. Am. Cer. Soc. 57(10), 1974, 417-21.

77. S. Tomono, K. Tokumoto and A. Tanaka, "Thermal Shock Resistance of Cemented Carbides", Nippon Tungsten Review, Vol. 22, 1989, 13-27.

78. J-J. Shyu, Y-C. Chen, "Zirconia-Mullite Ceramics Made from Composite Particles Coated with Amorphous Phase : I. Effect of Zirconia Addition", J. Mat. Res. 10(1), 1995 (in press).

79. R. F. Davis and J. A. Pask, 'Mullite' in "High Temperature Oxides Part - IV", ed. A. M. Alper, Academic Press, New York, 1971, 37-75.

80. D.J. Green, R.H.J. Hannink and M.V. Swain, in "Transformation Toughening of Ceramics", CRC Press, Inc., Boca Raton, Florida, 1989, 17-55.

81. R. Warren and V. K. Sarin, in "Ceramic Matrix composites", ed. R. Warren, Blackie and Son Ltd., Glasgow, 1992, 153.

82. S. Prochazka, J. S. Wallace and N. Claussen, "Microstructure of Sintered Mullite-Zirconia Composites", J. Am. Cer. Soc., 66, 1983, C-125.

83. J. S. Wallace, N. Claussen, M. Rühle and G. Petzow, "Development of Phases in In-Situ-Reacted Mullite-ZrO_2 Composites" in "Surfaces and Interfaces in Ceramic and Ceramic-Metal Systems: "Materials Science Research, Vol. 14", ed. J. A. Pask and A. G. Evans, Plenum, New York, 1981, 155.

84. E. M. Levin, H. F. McMurdie and F. P. Hall, in "Phase Diagrams for Ceramists", ed. M. K. Reser and H. Insley, The American Ceramic Society, Columbus, Ohio, 1956, 64.

85. R. C. Garvie and P. S. Nicholson, "Structure and Mechanical Properties of Partially Stabilized Zirconia in the CaO-ZrO_2 system", J. Am. Cer. Soc., 55, 1972, 152.

86. D. P. H. Hasselman, "Unified Theory of Thermal Shock Resistance of Ceramic Materials", J. Am. Cer. Soc., 52, 1969, 600.